Distribution Agreement

In presenting this thesis or dissertation as a partial fulfillment of the requirements for an advanced degree from Emory University, I hereby grant to Emory University and its agents the non-exclusive license to archive, make accessible, and display my thesis or dissertation in whole or in part in all forms of media, now or hereafter known, including display on the world wide web. I understand that I may select some access restrictions as part of the online submission of this thesis or dissertation. I retain all ownership rights to the copyright of the thesis or dissertation. I also retain the right to use in future works (such as articles or books) all or part of this thesis or dissertation.

_____ _____

Mary Bushman Date

Within-host competition and evolution of drug resistance in *Plasmodium falciparum*

By

Mary Bushman
Doctor of Philosophy

Graduate Division of Biological and Biomedical Science
Population Biology, Ecology and Evolution

_____
Jacobus de Roode
Advisor

_____
Venkatachalam Udhayakumar
Advisor

_____
Rustom Antia
Committee Member

_____
Tracey Lamb
Committee Member

_____
Bruce Levin
Committee Member

_____
Lance Waller
Committee Member

Accepted:

_____
Lisa A. Tedesco, Ph.D.
Dean of the James T. Laney School of Graduate Studies

_____
Date

Within-host competition and evolution of drug resistance in *Plasmodium falciparum*

By

Mary Bushman
B.A. Carleton College, 2011

Advisor: Jacobus de Roode, Ph.D.
Advisor: Venkatachalam Udhayakumar, Ph.D.

An abstract of a dissertation submitted to the Faculty of the
James T. Laney School of Graduate Studies of Emory University
in partial fulfillment of the requirements for the degree of
Doctor of Philosophy
Graduate Division of Biological and Biomedical Science
Population Biology, Ecology and Evolution
2017

Abstract

Within-host competition and evolution of drug resistance in *Plasmodium falciparum*

by Mary Bushman

The focus of this dissertation is the role of within-host competition in the evolution of drug resistance in the malaria parasite *Plasmodium falciparum*. In high-transmission settings, such as those in sub-Saharan Africa, most *P. falciparum* infections contain multiple genetically distinct strains. If drug-sensitive and drug-resistant strains both exist in a population, then mixed-strain infections may contain both, with the potential for competition between sensitive and resistant parasites. Previous studies have found evidence for such competition in a rodent malaria parasite, and mathematical models have suggested that within-host competition could have a significant effect on the rate at which resistance evolves. However, evidence for within-host competition in *P. falciparum* is scarce, and theoretical models have generated conflicting predictions regarding the impact of within-host competition on the spread of resistance. I used samples from naturally occurring (human) infections to look for empirical evidence of within-host competition in *P. falciparum*. In samples from Angola, Ghana, and Tanzania, I used a molecular marker of chloroquine resistance to quantify sensitive and resistant parasites, and found strong empirical support for within-host competition in *P. falciparum*. In addition, I used deep sequencing of samples from a longitudinal study in Kenya to test for so-called "competitive release" – an expansion of drug-resistant parasites in the host following the removal of drug-sensitive parasites by antimalarial drug treatment, and a potentially important facilitator of the spread of resistance. The preliminary results from this ongoing study are consistent with competitive release of resistant parasites. Finally, I used a nested model – a model of within-host infection dynamics embedded into a second model of transmission between humans and mosquitoes – to explore the impact of within-host competition on the spread of resistance under a variety of conditions. The results suggest that within-host competition serves to inhibit the emergence of resistance in high-transmission settings; however, once resistance is established in the population, its spread in high-transmission settings may be paradoxically accelerated by competitive release. These results are consistent with, and advance our understanding of, global patterns of drug resistance evolution in *P. falciparum*.

Within-host competition and evolution of drug resistance in *Plasmodium falciparum*

By

Mary Bushman
B.A. Carleton College, 2011

Advisor: Jacobus de Roode, Ph.D.
Advisor: Venkatachalam Udhayakumar, Ph.D.

A dissertation submitted to the Faculty of the
James T. Laney School of Graduate Studies of Emory University
in partial fulfillment of the requirements for the degree of
Doctor of Philosophy
Graduate Division of Biological and Biomedical Science
Population Biology, Ecology and Evolution
2017

Acknowledgements

A simultaneously great and not-so-great thing about my dissertation research was that it was highly interdisciplinary. I lived with one foot in the world of ecology and evolution, and another in the world of malaria and public health, and since I only have two feet, I guess it was one of my hands in the world of mathematical modeling, like intellectual Twister. It was exhilarating, scientifically powerful, and a lot of fun, but it was also isolating at times, with my project sitting on its own little interdisciplinary island way offshore.

That makes it all the more amazing that people went to such lengths to support this research, even when it was peripheral to their own work. My advisors, Jaap de Roode and Venkatachalam Udhayakumar (Kumar), contributed their time, knowledge, and resources to this work, even though it was outside the core focus of each of their labs. Their unwavering support, especially when the going got rough, was invaluable and I will forever be in their debt.

I am similarly indebted to Rustom Antia, who took me under his wing for no reason I can discern other than scientific curiosity and pure goodwill. His expertise in mathematical modeling, and more importantly, his habit of calling people out on their bullshit have vastly improved the quality of the work presented here, especially the mathematical model.

My thanks also go out to the other members of my committee: Bruce Levin, who taught me how to combine empirical studies and mathematical models to attack a problem; Lance Waller, who despite being the chair of Emory's biostatistics department somehow seemed to have time to personally deal with my statistical

quandaries, and Tracey Lamb, who continued to make time for my research even after taking a job opportunity in Utah.

I cannot thank enough the members of Kumar's lab who made my PhD so much easier – and more fun – with their help in and out of the lab. Lindsay Morton, Dragan Ljolje, Julia Kelley, Eldin Talundzic, Naomi Lucchi, Ira Goldman, Mara Karell, and many others were invaluable for the assistance they gave, and all of them were brilliant, cheerful, and kind every single day.

I am lucky to have made some great friends during my PhD, including my CDC coworkers, Lindsay and Dragan; the fellow members of my PBEE cohort, especially Zach Lynch and Carolyn Ayers; fellow PBEE members Mari Peterson and Nate Jacobs, and several others. They've helped me celebrate the good things, made me forget about the bad things, and generally brought a lot of fun and light into my life.

Despite being several hundred miles away in Madison, WI, my parents and sisters (Ellen, Wade, Emily and Norah) have been a source of constant support, encouragement, and most importantly, amusement. They make me whole and I love them with all my heart.

Finally, and most importantly, there is Paul Dunbar, whose patience and support have never wavered in the last five years. He makes me laugh, keeps me sane, reminds me to do human things like eat and sleep, and indulges my odd and quirky ways. He has always treated my work as important simply because it is important to me. My love and thanks to him know no bounds.

Table of Contents

Chapter 6: Appendix

Chapter 1: Introduction

1.1 Overview

Malaria is a vector-borne disease caused by microscopic parasites of the genus *Plasmodium*. Five such species cause malaria in humans: *P. falciparum*, *P. vivax, P. malariae, P. ovale,* and *P. knowlesi.* Infections range from asymptomatic to fatal (with most falling somewhere in the middle) and can manifest in a variety of ways, from fever and chills to hemolytic anemia to seizures and coma. Severe illness and death are almost always caused by *P. falciparum*, and are most likely in young children who lack protective immunity. Of an estimated 429,000 deaths from malaria in 2015, 99% were caused by *P. falciparum* and approximately 70% occurred in children under the age of five [1].

Fortunately, malaria is easily treated with a course of antimalarial drugs. The first of these was quinine, which reigned until it was supplanted by a wave of synthetic antimalarial drugs in the first half of the twentieth century [2]. The most important of these synthetic drugs, chloroquine, was deployed on a massive scale in the 1950s. However, by the 1960s, parasites in Southeast Asia and South America had developed chloroquine resistance (i.e., the ability to withstand chloroquine treatment, resulting in failure to cure the infection) [3]. Over the next few decades, chloroquine resistance spread to virtually every corner of the malaria-endemic world. Sulfadoxine-pyrimethamine, the prevailing substitute for chloroquine, was also rapidly undermined by resistance [3], although it remains slightly more

effective than chloroquine in many areas [4]. Artemisinin-based combination therapies (ACTs), which are now the standard treatment for *falciparum* malaria in most countries, are in danger of widespread failure, with resistance to artemisinin and piperaquine entrenched and spreading in Southeast Asia (piperaquine is the 'partner drug' to artemisinin for one of two ACTs used in the region) [5]. At present, there are no effective drugs lined up to replace ACTs if they, too, fall to resistance. It is therefore imperative to develop additional strategies to combat the spread of drug resistance, and a promising path to such developments may be through a deeper understanding of the factors that facilitate (or inhibit) the evolution of resistance.

Molecular markers of drug resistance – meaning mutations either associated with or responsible for a drug-resistant phenotype - have yielded a wealth of information on the evolutionary origins of resistance. These "markers" are typically point mutations in genes encoding proteins that interact with the drug in some way – such as mutations in the *PfCRT* gene that contribute to efflux of chloroquine from its site of action (the digestive vacuole), or mutations in the *dhps* and *dhfr* genes, which alter the enzymatic targets of sulfadoxine and pyrimethamine, respectively [6, 7]. The relationship between molecular markers and resistant phenotypes is typically identified by associations between genetic polymorphisms and treatment failure, but can be confirmed by testing the phenotypic effects of particular mutations *in vitro,* as has been done for chloroquine resistance mutations in *PfCRT* [8, 9].

Molecular markers have allowed the origins and spread of drug resistance in *P. falciparum* to be characterized in detail; and yet there is relatively little understanding of the fact that resistance consistently emerges in some settings and not others. In particular, although sub-Saharan Africa accounts for roughly 90% of the global burden of malaria, drug resistance has seldom evolved locally within Africa. Rather, resistance has arisen numerous times in low-transmission settings outside Africa, most often in Southeast Asia and South America [10]. In at least two cases (those of resistance to chloroquine and pyrimethamine, respectively), drug-resistant parasites were carried to Africa from Southeast Asia, after which the imported drug-resistant alleles swept across the African continent via gene flow. In general, drug resistance has been years to decades slower to appear in Africa than in other parts of the world.

The tendency for drug resistance to emerge in low-transmission settings is an unsolved puzzle. The high-transmission settings of sub-Saharan Africa account for most of the world's malaria infections [1], and therefore offer no shortage of opportunity for drug resistance mutations to occur. Indeed, such mutations must occur fairly frequently, but fail to spread through the population. It can therefore be inferred that low-transmission settings are more conducive to the sustained transmission of drug-resistant parasites from host to host, which must occur for drug resistance to become established in the population. There are at least three hypotheses as to why this should be the case.

The first hypothesis stems from the fact that recombination in *P. falciparum* increases with transmission intensity [11]. As a result, if multiple mutations are

required for drug resistance, these mutations will be continually separated by recombination in high-transmission settings. However, resistance to chloroquine, which exemplifies the pattern of emergence in low-transmission settings, is encoded primarily by mutations in codons 72-76 of the *PfCRT* gene [10], and recombination between such closely linked sites is negligible. Therefore, while recombination may frequently separate unlinked mutations (such as the SP resistance mutations in *dhps* and *dhfr*, which are on different chromosomes [12, 13]), it cannot fully explain the delayed appearance of resistance in high-transmission settings.

The second hypothesis is that, because immunity to *P. falciparum* is acquired gradually, residents of low-transmission areas will have little or no protective immunity because of limited exposure to the parasite. Therefore, according to this hypothesis, infections in low-transmission settings will almost always be symptomatic, while many are asymptomatic in high-transmission areas. As a result, a higher percentage of infections will be treated with antimalarial drugs in low-transmission settings, resulting in stronger selection for resistance [14]. Contrary to this thinking, a 2013 meta-analysis by Lindblade et al. [15] found only a weak correlation between transmission intensity and the fraction of infections that were symptomatic, with a majority of infections found to be asymptomatic in both high- and low-transmission settings, suggesting that levels of antimalarial drug use could actually be similar across of range of transmission intensities. In addition, until 2010, the World Health Organization recommended a policy of "presumptive treatment" in high-transmission settings, in which fever in children under age 5 was assumed to be caused by malaria and treated with antimalarial drugs [16, 17]. Thus,

until recently, the strength of selection for resistance in high-transmission settings was probably somewhat greater than would be expected based solely on the frequency of asymptomatic infections. It is therefore difficult to estimate the relative strength of selection for resistance in different transmission settings without empirical data on the amount of antimalarial drug use in each.

The last hypothesis is that within-host competition between drug-sensitive and drug-resistant *P. falciparum* serves to inhibit the transmission of drug-resistant parasites in high-transmission settings, making it harder for resistance to spread. There is a positive correlation between transmission intensity and the average multiplicity of infection (number of parasite strains or clones per host) [18], which means that as transmission intensity increases, drug-resistant parasites will more frequently be found in mixed-strain infections with drug-sensitive parasites. Experiments in mice have shown within-host competition between drug-sensitive and drug-resistant strains of the rodent malaria parasite *Plasmodium chabaudi*, and demonstrated that such competition can inhibit transmission of resistant parasites [19]. Furthermore, mathematical models indicate that such competition can, in theory, have a significant impact on the spread of resistance [20-22].

Although within-host competition has been demonstrated in rodent malaria, whether similar competition occurs in *P. falciparum* has remained an open question. The infection dynamics of *P. chabaudi* in laboratory mice are very different from those of *P. falciparum* in humans; for instance, parasitemia in the rodent model can be several times higher than levels observed in humans, suggesting that parasites in humans might be limited by different factors than parasites in mice.

In addition, the predictions made by mathematical models may be heavily influenced by a few key assumptions, most of which lack empirical support. For example, Klein et al. [22] assume a fitness cost of resistance that only manifests in mixed-strain infections, which effectively ensures that the spread of resistance will be hindered in high-transmissions settings. On the other hand, papers by Hastings and D'Alessandro [20, 21] assume that resistance will be encoded by at least two unlinked loci, and their conclusions therefore incorporate the combined effects of recombination and within-host competition. No published models exist which examine the effects of within-host competition in isolation, let alone take into account the complexities of within-host dynamics and transmission in mixed-strain infections – complexities which may have important implications for the fate of a newly emerged drug-resistant strain in an established parasite population.

Therefore, two major questions remain with regard to within-host competition and the evolution of drug resistance. First: does within-host competition between drug-sensitive and drug-resistant parasites occur in *Plasmodium falciparum*? Second: what effect does within-host competition have on the evolution of drug resistance, and how does this depend on factors such as fitness costs of resistance and levels of antimalarial drug use? Can within-host competition alone explain the observed relationship between transmission intensity and the emergence of drug resistance in *P. falciparum*?

These questions are the subject of this dissertation. Chapters 2 and 3 are devoted to empirical studies which examine evidence for within-host competition and related phenomena in *Plasmodium falciparum*, while Chapter 4 presents a

mathematical model which is used to dissect the complex relationship between transmission intensity and the evolution of drug resistance. Finally, Chapter 5 provides perspective by summarizing the work presented here, highlighting unresolved questions and suggesting avenues for further investigation. A brief introduction to the specific subjects examined in Chapters 2, 3, and 4 follows.

1.2 Within-host competition in *Plasmodium falciparum*

Competition is a simple but widely misunderstood concept. It is often assumed to require some asymmetry between the competitors - a "winner" and a "loser." However, in ecological terms, competition simply means an interaction between two populations that is beneficial to neither and detrimental to one or both. If the niches of two populations overlap – whether partially or completely – then the growth of one or both of them will be reduced when the two populations try to occupy the same environment, and this reduction in growth is the negative effect that defines competition. Applied to the specific case of within-host competition between malaria parasites: if two distinct populations (for the sake of brevity, we will call them *strains*) compete within the host, then the growth of one or both strains should be impaired relative to that achieved in the absence of competitors.

In a rodent model, controlled experiments can be used to test for within-host competition between parasite strains. Experiments by de Roode et al. showed that mice infected with three strains of *Plasmodium chabaudi* produced approximately

the same total number of parasites as mice infected with any of the three strains individually, suggesting that the coinfecting strains were in competition for a shared niche [23]. Additional experiments added nuance to this picture, demonstrating that the degree of competitive suppression was dependent on the specific strains involved, the number of parasites of each strain introduced, whether one of the strains was introduced first, and even the host genotype [24-27].

A rigorous demonstration of within-host competition in *Plasmodium falciparum* would require controlled experiments in which some people were infected with one strain, others with a different strain, and still others with both strains together; such experiments are neither safe nor ethical to perform in humans. A decent approximation is to obtain "snapshots" of infections via observational studies of humans living in malaria-endemic areas, and measure the parasite densities of two different strains in both single- and mixed-strain infections. If competition occurs in *P. falciparum*, the average parasite density of one or both strains should be reduced in mixed-strain infections compared to single-strain infections. A study taking this approach is presented in detail in Chapter 2.

1.3 Competitive release of drug-resistant parasites following treatment

In the *Plasmodium chabaudi* model system, within-host competition between drug-sensitive and drug-resistant parasites is alleviated when drug-sensitive parasites are removed by antimalarial drugs. In the sudden absence of competitive suppression, the drug-resistant parasites expand; this expansion is known in the

literature as “competitive release” [11]. The expansion is what distinguishes competitive release from mere selection: selection deals only with relative fitness, while competitive release is defined by an increase in both relative and absolute fitness. The expansion of the resistant parasite population is also what makes competitive release potentially important in terms of public health, because it magnifies the benefit of antimalarial treatment to drug-resistant parasites (Fig. 1.1)

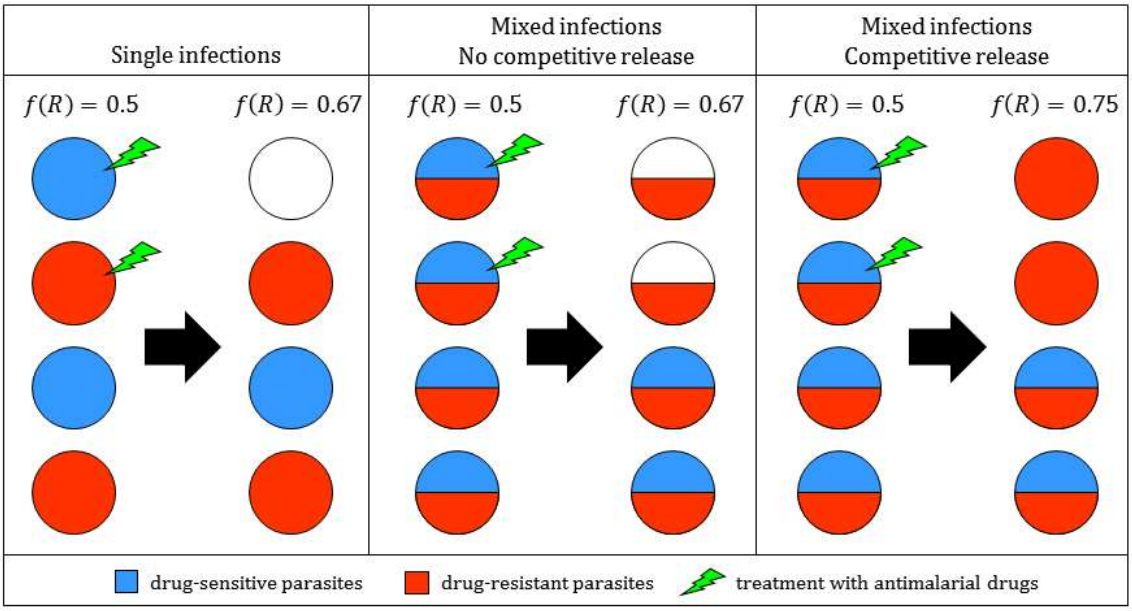

Figure 1.1 Effect of competitive release on the frequency of resistance in a parasite population. Schematics are shown for three populations, one comprised of single infections (each host carries sensitive or resistant parasites) and two comprised of mixed infections (each host carries both sensitive and resistant parasites in equal proportions). Assuming that all infections harbor equal numbers of parasites, the initial frequency of resistance (denoted $f(R)$ in the figure) is 0.5 in all three populations. Half of the hosts in each population are then treated with antimalarial drugs, after which the frequency of resistance increases in all three populations. In the first population, the final frequency of resistance is 0.67, as it is in the second population, where drug-sensitive parasites are cleared by

treatment but resistant parasites do not expand (no competitive release). In the third population, however, resistant parasites undergo competitive release where the sensitive parasites have been removed, with the result that the final frequency of resistance is 0.75. In this case, competitive release amplifies the benefit that drug-resistant parasites experience as a result of antimalarial drug use.

Both verbal arguments and mathematical models have been made to suggest that competitive release could cause drug resistance to spread faster in high-transmission settings [12][13][28]. Clearly, this runs counter to empirical observations; however, it is possible that the evolution in high-transmission settings might be slowed by competitive suppression of resistant parasites *and* accelerated by competitive release, and that the balance between these two processes determines the actual rate at which resistance spreads. Therefore, we might expect resistance to evolve more slowly in high-transmission settings when rates of antimalarial drug use are relatively low (probably the status quo, given the high frequency of asymptomatic infections) but more rapidly when treatment rates are high. Thus, competitive release, if it occurs in *P. falciparum*, might cause interventions involving mass drug administration (MDA) to backfire in high-transmission settings, causing a massive increase in the frequency of resistance with smaller-than expected reductions in the burden of disease.

Once again, to unequivocally demonstrate competitive release in *P. falciparum* would require experiments that are not feasible in humans. Expansion of resistant parasites following treatment may be observed by comparing pre- and post-treatment samples from hosts infected with both sensitive and resistant

parasites; a study taking this approach is described in Chapter 3. The downside of this method is the lack of proper controls; since treated infections will often have been symptomatic at the time of sampling, while untreated infections will generally have been asymptomatic, the two groups are not perfectly equivalent. However, evidence for within-host competition in *P. falciparum* will reinforce evidence for competitive release, and vice versa.

1.4 Transmission intensity, within-host dynamics, and the evolution of drug resistance

As described above, there is an observed correlation between transmission intensity and the rate of evolution of drug resistance in *P. falciparum*; however, the underlying mechanism(s) are still unclear. Although recombination can effectively be ruled out as the driving force, at least two potential explanations remain: immunity-driven differences in the strength of selection and within-host competition between drug-sensitive and drug-resistant parasites. The former is difficult to evaluate in the absence of empirical data on levels of antimalarial drug use in different transmission settings, while the importance of the latter is unknown in part because its effects have not been clearly delineated.

The relationship between transmission intensity and the evolution of drug resistance is a complicated one. The fate of drug-resistant parasites is determined by their transmission success, which is governed by within-host dynamics; within-host dynamics, in turn, interact with several other factors. Figure 1.2 summarizes

the interactions of the relevant factors, but the key point is that these effects are interdependent and hard to disentangle. A model which accurately captures the effects of transmission intensity on the spread of drug resistance must include these factors, as well as their essential interactions; these interactions can then be altered or weakened to examine the effect on the relationship between transmission intensity and the spread of drug resistance. A model along these lines is the subject of Chapter 4.

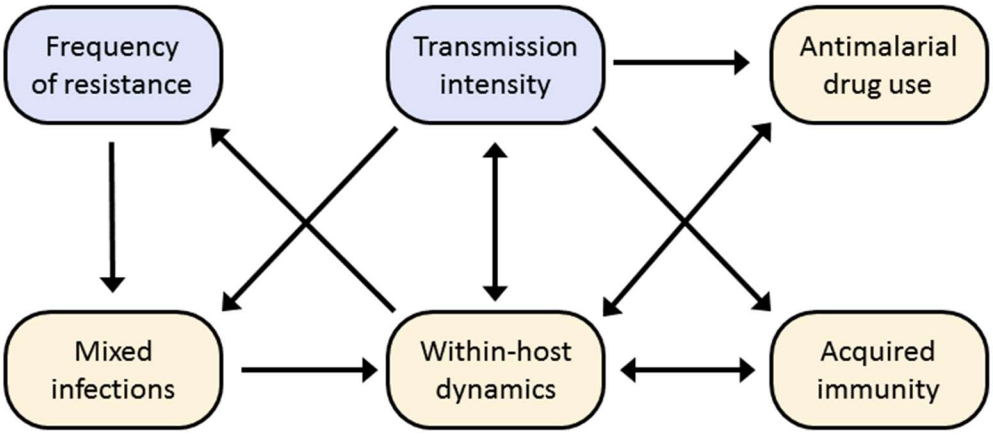

Figure 1.2 Schematic representation of the relationships between transmission intensity and drug resistance (blue) and the various factors that link them (yellow). In this context, mixed infections refer to those with both drug-sensitive and drug-resistant parasites, and frequency of resistance refers to the proportion of parasites (or infections) that are resistant to antimalarial drugs.

A challenging but fascinating aspect of this particular puzzle is that it involves feedbacks between population dynamics on two different scales: within-host and between-host. Most models deal with only one or the other (infection

dynamics or epidemiological dynamics); those that include both [29] have not allowed for feedbacks in both directions. The model described in Chapter 4 is a "nested model" which not only describes both within- and between-host dynamics for a population of hosts, but allows for bidirectional feedbacks between scales. It is, to the best of my knowledge, unusual if not unique in this regard [30].

Chapter 2: Within-host competition in *Plasmodium falciparum*

2.1 Introduction

The global spread of drug-resistant pathogens is a major threat to the control of infectious disease [31]. The malaria parasite *Plasmodium falciparum* has developed resistance to every type of antimalarial drug available. Resistance to former first-line therapies chloroquine and sulfadoxine-pyrimethamine originated in low-transmission settings in Asia and South America [32, 33] and then spread via gene flow, ultimately invading most of sub-Saharan Africa. If artemisinin resistance, which recently appeared in Southeast Asia [34, 35], continues to follow the same pattern, the world may soon find itself without reliable antimalarial drugs.

One potentially crucial, but frequently overlooked, determinant of the evolution of resistance is the occurrence of coinfections, in which different pathogens or different strains of a pathogen infect the same host [36, 37]. In the case of *Plasmodium falciparum*, mixed-strain infections are very common, especially in high-transmission areas where infectious mosquito bites occur frequently [18, 38]. Within-host competition between strains may result in competitive suppression of drug-resistant parasites [19, 23]; theoretical models suggest that this could have dramatic consequences for the evolution of drug resistance [39].

On the one hand, within-host suppression of resistant strains (in untreated infections) could impede the spread of resistance, especially in high-transmission areas where mixed-strain infections are common [20-22, 40]. On the other hand,

competitive suppression could be alleviated by treatment, which removes drug-sensitive competitors, leading to increased growth and transmission of resistant parasites – a phenomenon known as competitive release [19, 41-43]. This may have the opposite effect, accelerating the spread of drug resistance in high-transmission settings.

The best evidence to date for within-host competition and competitive release comes from mouse models of malaria. In the rodent malaria parasite *Plasmodium chabaudi*, mixed-strain infections exhibit intraspecific competition, in which growth of each strain is impaired by the others [23]. In this system, intrahost competition reduces the density and transmission of resistant parasites (competitive suppression) [19, 27, 44, 45] and removal of drug-sensitive strains with antimalarial drug therapy results in competitive release of resistant strains [19, 41, 42, 44, 45]. However, evidence for within-host competition and suppression of drug-resistant strains in *Plasmodium falciparum* remains lacking. Important discrepancies between *P. chabaudi* and *P. falciparum*, such as order-of-magnitude differences in parasite density [46], preclude generalization from the rodent model to human malaria. It is possible, for example, that *P. chabaudi* might be limited primarily by erythrocytes, resulting in competition, and *P. falciparum* by strain-specific immune responses [47], allowing strains to grow independently.

There is currently only indirect evidence to support within-host competition in *P. falciparum*: one study observed longitudinal infection dynamics consistent with competition between different *Plasmodium* species [48], while another study observed an effect of treatment on placental parasitemia consistent with

competitive release of resistant parasites [49]. Here, we describe a study of naturally acquired *P. falciparum* infections in which we sought to determine whether within-host competition occurs in mixed-strain infections and whether drug-resistant parasites suffer competitive suppression.

2.2 Methods

Focus on chloroquine resistance

We chose to focus on resistance to chloroquine, a largely retired antimalarial drug, for several reasons. The genetic basis of chloroquine resistance is straightforward and well-characterized [6], and chloroquine-resistant genotypes are present at intermediate frequencies in many parts of the world, making it possible to obtain sufficient numbers of mixed-genotype infections. In contrast, resistance to another older drug, sulfadoxine-pyrimethamine, can be complex (multiple mutations in two different genes, with varying degrees of resistance [50]), while resistance to modern artemisinin-based drugs is still quite rare. We expect findings related to within-host competition to be generalizable to other forms of resistance (see Discussion).

Sample collection and processing

Blood spots on filter papers were collected from children (ages 6-59 months in Ghana and Tanzania and 6-108 months in Angola) with symptomatic but uncomplicated microscopy-confirmed *Plasmodium falciparum* infection (Table A1,

Appendix, 6.1). All samples were obtained from children enrolled in antimalarial therapeutic efficacy studies conducted in accordance with the guidelines of the World Health Organization [51]. Samples used in this study were collected prior to treatment. Samples from Ghana were collected between 1999 and 2010; samples from Tanzania in 2011; and samples from Angola in 2013 [52]. Figure A1 (Appendix, 6.1) shows study locations and malaria prevalence. All available samples from these clinical efficacy studies were included; sample sizes were not pre-determined to ensure statistical power. Investigators were blinded to patient clinical data in both experimental and analytical phases of the study. Parents or guardians gave informed consent on behalf of enrolled children.

DNA was extracted from blood spots using QIAamp DNA Mini Kit (Qiagen) and eluted in 150 μl buffer AE. For samples from Ghana, each blood spot was excised entirely, cut up into pieces and used for DNA extraction. The average blood spot was about 1 cm in diameter (approximately 50 μl), but there was some variation in size and therefore in volume. This variation is expected to increase the variance in parasite density, but is not expected to result in bias because parasite density and *PfCRT* genotype should not influence the size of blood spots. For samples from Tanzania and Angola, a consistent amount of each blood spot was used for DNA extraction: for Tanzania, three triangles (3 mm each side) were cut out of each spot, while for Angola, three 3 mm hole punches were used. The pieces excised from each blood spot were pooled for DNA extraction. The different volumes used for DNA extraction (approximately 50 μL for Ghana, 8.3 μL for Tanzania, and 13 μL for Angola) were corrected for in calculating parasite densities.

Quantification of drug-sensitive and drug-resistant parasites

We measured parasite densities by using extracted DNA in a quantitative real-time PCR assay which amplified codons 72-76 of the *PfCRT* gene on chromosome 7 (Tables A2-A3, Appendix, 6.1). TaqMan® probes (Life Technologies) were designed to bind to two different genotypes, one encoding the amino acid sequence CVMNK, which is chloroquine-sensitive (abbreviated CQS), and the other encoding CVIET, which is chloroquine-resistant (abbreviated CQR). Previous studies have shown that these genotypes dominate most countries in Africa, including Ghana, Tanzania, and Angola [53-55]. Due to reports of a third genotype, SVMNT, circulating in Angola [56], samples from Angola were analyzed with a third probe designed to bind to SVMNT. Samples positive for SVMNT ($n = 13$) were excluded from analysis.

A full description of the methods for quantifying CQS and CQR can be found in the Appendix (6.1).

Neutral microsatellite genotyping and analysis

To examine within-host diversity beyond *PfCRT*, six microsatellites (Table A4, Appendix, 6.1) were genotyped for all samples from Angola. These microsatellites consist of tandem repeats of 1-6 bp and exhibit considerable polymorphism in repeat number. Each microsatellite was amplified by PCR (Tables A5-A6, Appendix, 6.1) and analyzed by fragment electrophoresis on a capillary sequencer (ABI 3130 xl Genetic Analyzer) to determine amplicon size(s). Sequence

data were read manually using GeneMapper (Life Technologies) by counting the number of distinct size variants of each microsatellite for each sample. MOI_{ms} (multiplicity of infection based on microsatellites) is defined as the maximum number of variants identified at any of the six microsatellites for a given sample and provides a lower bound on the number of strains in the sample.

Statistical analysis

All analyses were carried out in the statistical software R, version 3.1.2 [57]. Parasite densities were $\log_{10}$-transformed to meet the assumptions of normality of errors and homogeneity of variance. Unless noted otherwise, significance of fixed effect terms was determined by removal of the term followed by model comparison using the command *anova* [58].

(i) Prevalence of mixed-genotype infections

To determine whether allele frequencies and the prevalence of mixed-genotype infections varied by country, we used X^2 tests for equality of proportions. One X^2 test compared the frequencies of single-genotype (CQS-only and CQR-only) and mixed-genotype (CQS + CQR) infections between the three countries, while another test compared the frequencies of CQS-only and CQR-only infections between the countries.

(ii) Factors affecting total parasite densities

We carried out two analyses to identify factors affecting total parasite densities. In the first analysis, which included the samples from all three countries, we used a linear mixed effects model (using the function *lmer* in the R package *lme4*

[59]) to analyze the effects of infection type (single- vs. mixed-genotype) and country (Angola, Ghana, or Tanzania), as well as site within country (see Table A1, Appendix, 6.1 for study sites within each country). Infection type and country were modeled as fixed effects while site was modeled as a random effect.

The second analysis was restricted to samples from Angola, which were genotyped for microsatellite markers and for which patient age data were available. We analyzed the effects of age, infection genotype (CQS, CQR or CQS+CQR), and MOI_{ms} on overall parasite density. We began with a linear mixed effects model (using *lmer*) and included study site (Uige or Zaire) as a random effect; however, site did not explain significant variation in parasite density. We therefore analyzed the effects of age, infection genotype and MOI_{ms} (and their two- and three-way interactions) using a linear model. Finally, we analyzed the relationship between patient age and MOI_{ms} using a linear model, with patient age serving as the explanatory variable.

(iii) Within-host competition

If within-host competition occurs in mixed-genotype infections, then the density of an individual genotype should be reduced in mixed-genotype infections compared to single infections. We therefore analyzed differences in parasite densities of each genotype (CQS or CQR) between single- and mixed-genotype infections.

As above, we carried out two analyses. First, using a linear mixed effects model – again with *lmer* – we analyzed the effects of infection type (single vs. mixed), parasite genotype (CQS vs. CQR), country (Angola, Ghana or Tanzania) and

site within country (see Table A1, Appendix, 6.1) on parasite density. Again, site was treated as a random effect, while all other factors and their interactions were treated as fixed effects. The interaction between infection type, genotype and country was statistically significant; therefore, the significance of other terms could not be assessed by deletion and model comparison using *anova*. Instead, we re-ran the model using the *lme* function in the package *nlme* [60] to obtain approximate p-values for the remaining terms in the model.

The second analysis, which included patient age as an additional explanatory variable, was restricted to samples from Angola (the only samples for which age data were available). We started with a linear mixed effects model (using *lmer)*, which included infection type (single versus mixed), parasite genotype (CQS versus CQR), and patient age – plus all two- and three-way interactions - as fixed effects, while site (Uige or Zaire) was included as a random effect. Because site did not explain significant variation in parasite density, we excluded it from the model and analyzed the effects of infection type, parasite genotype and age and their interactions using a linear model instead.

Finally, to check the assumption that mixed-genotype infections contained more strains than single-genotype infections, we used a Mann-Whitney *U* test to compare MOI_{ms} between single- and mixed-genotype infections from Angola (the only samples for which MOI_{ms} data were available).

(iv) Fitness cost of resistance in mixed-genotype infections

A null model was developed to calculate the expected proportion CQR in mixed-genotype infections in the absence of a fitness cost of resistance. This model

was based on population-level CQS and CQR allele frequencies and information about within-host strain diversity; a second version incorporated estimates of fitness costs of resistance based on *PfCRT* qPCR results (a full description of the model can be found in the Appendix (6.1)). For each country, a one-sample, two-sided *t*-test was used to determine whether the observed proportions of CQR in mixed-genotype infections (logit-transformed to correct for non-normality) differed from the expected values.

(v) Temporal dynamics of resistance in Ghana

Patient samples from Ghana were collected between 1999 and 2010, while chloroquine was retired in favor of artemisinin-based therapies in early 2005. The prevalence of the CQR genotype in Ghana over time was analyzed using a generalized linear mixed effects model with binomial errors (using the function *glmer* in the R package *lme4*). In this model, the frequency of CQR was modeled as a bivariate variable in which the numbers of CQR-positive and CQR-negative samples for each location and time point were column-bound (using the R command *cbind*). Time was included as a continuous fixed effect, and site (Hohoe, Navrongo, Sunyani or Yendi) as a random effect. We also included data point (each measurement of CQR prevalence for a given site and time point being one data point) as a random effect to account for overdispersion of the data [61].

2.3 Results

Using quantitative real-time PCR, we were able to accurately determine the density of chloroquine-sensitive (CQS) and chloroquine-resistant (CQR) *P. falciparum* in patient samples. Infections with either CQS or CQR were classified as single-genotype and infections with both were classified as mixed-genotype.

Variation in PfCRT genotype frequencies

The three countries differed significantly in the relative frequencies of the CQS and CQR alleles ($X^2_2 = 326.97$, $p < 0.0001$), but not in the relative frequencies of single-genotype and mixed-genotype infections ($X^2_2 = 2.89$, $p = 0.24$) (Fig. A1, Table A7, Appendix, 6.1).

Infection genotype frequencies (CQS, CQR, and CQS+CQR) did not vary significantly between the sites in Angola ($X^2_2 = 4.452$, $p = 0.108$). There was significant variation among the sites in Ghana ($X^2_6 = 20.5$, $p = 0.002$); however, this was likely the result of different sampling schedules for the various sites, combined with longitudinal change in the frequency of CQR. Restricting to years in which all sites were sampled, variation between sites was not significant (Fisher's Exact Test, $p = 0.061$).

Overall parasite densities in single- and mixed-genotype infections

The total parasite density of mixed-genotype infections was roughly the same as, or lower than, that of single-genotype infections (Fig. 2.1). The linear mixed

effects model that included data from all three countries showed a significant interaction between infection type (single- versus mixed-genotype) and country ($X^2_2 = 7.33$, $p = 0.026$), indicating that while overall parasite densities did not differ between single- and mixed-genotype infections in Angola or Ghana, in Tanzania, the overall density of mixed infections was slightly lower than that of single infections (Fig. 2.1). These observations are consistent with a model in which different strains occupy the same niche within a host, resulting in competition.

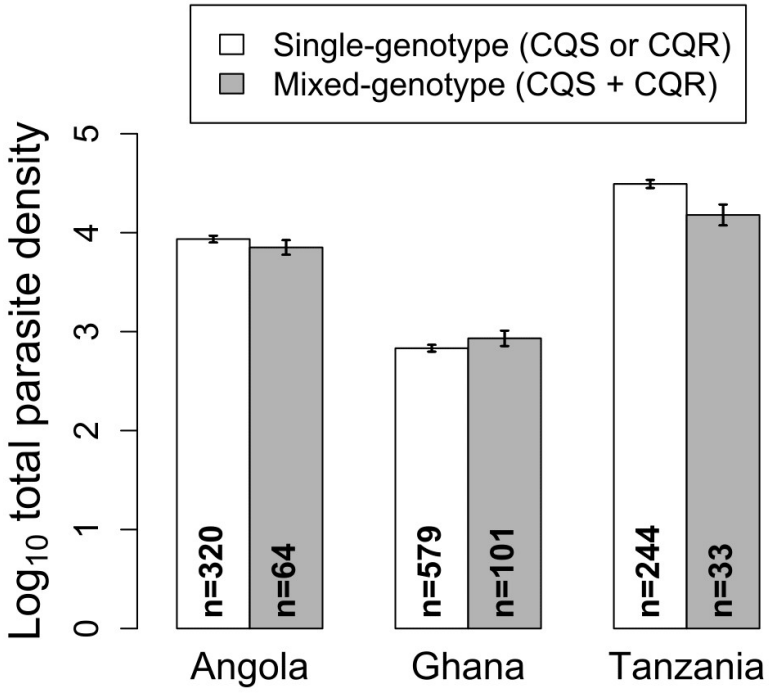

Figure 2.1. Total parasite densities of single- and mixed-genotype infections. Mean $\log_{10}$ parasite density of single-genotype infections (those with only CQS or only CQR; white bars) vs. mean $\log_{10}$ total density of mixed-genotype infections (those with both CQS and CQR; gray bars), stratified by country. Sample sizes for each group are shown inside bars. Error bars: $\pm$S.E.M.

We also genotyped the samples from Angola at six neutral microsatellite loci to obtain an independent estimate of the number of strains per sample, MOI_{ms}. Among these samples, CQS+CQR mixed infections were indeed more diverse than single-genotype infections (mean $MOI_{ms} = 2.38$ and 1.54, respectively; Mann-Whitney U test, $p < 0.0001$).

In the linear model restricted to data from Angola, we analyzed the effects of MOI_{ms}, patient age, and infection genotype (CQS, CQR, or CQS+CQR) on total parasite density. The effect of MOI_{ms} was not significant ($F_{1,379} = 3.78$, $p = 0.053$; Fig. 2.2a), indicating that total parasite density does not increase with the number of strains in a host (indeed, the trend was toward decreasing overall parasite density with increasing MOI_{ms}). However, overall parasite density was negatively associated with patient age ($F_{1,380} = 10.37$, $p = 0.001$, Fig. 2.2b), and was significantly affected by infection genotype ($F_{1,380} = 4.89$, $p = 0.008$, Fig. 2.2b), with CQS-only infections having higher total parasite densities than CQR-only or mixed-genotype (CQS+CQR) infections. None of the two- or three-way interaction terms in the model were significant ($p > 0.05$).

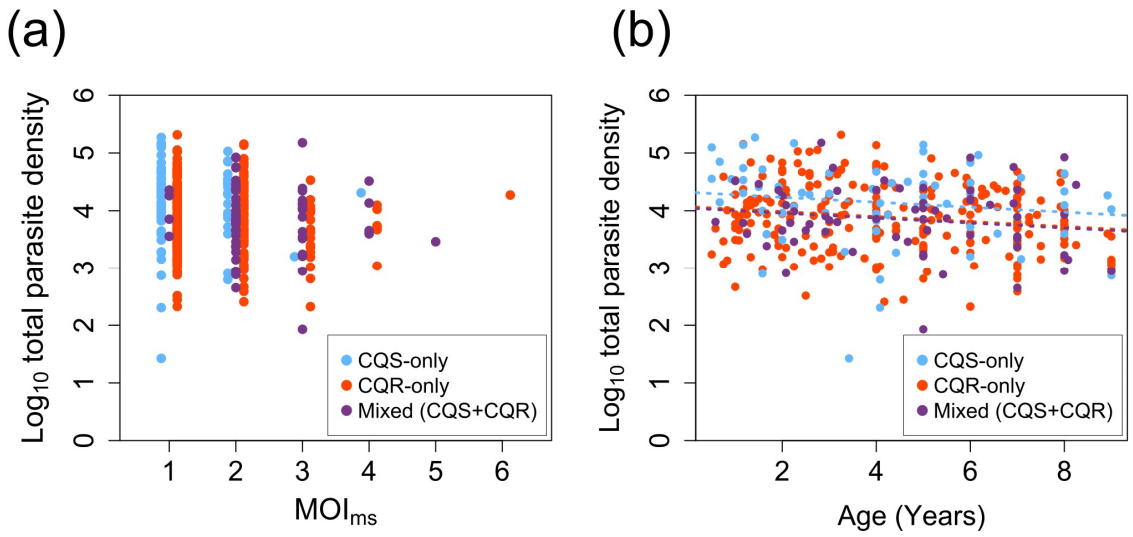

Figure 2.2. Effects of MOI_{ms} and host age on total parasite density. (a) Log_{10} parasite density vs. multiplicity of infection (number of strains per host, estimated by microsatellite genotyping) for samples from Angola (n=384). Points are colored to indicate *PfCRT* genotype composition of samples (CQS, blue; CQR, red; CQS+CQR, purple). (b) Log_{10} total parasite density vs. patient age for samples from Angola. Points are colored to indicate *PfCRT* genotype, as in panel (a). Dashed lines show linear regression for each genotype (same slope but different intercepts).

The lack of association between MOI_{ms} and overall parasite density –meaning that total parasite density does not increase with increasing numbers of strains - is also suggestive of within-host competition. An alternative explanation is that both MOI_{ms} and acquired immunity increase with exposure, such that, as more strains are acquired, immunity becomes more effective at reducing parasite density. As our linear model showed, total parasite density did decrease with age (a reasonable proxy for exposure); however, an additional linear model showed that MOI_{ms} was

not significantly associated with age ($F_{1,382} = 0.0061$, $p = 0.94$; Fig. A2, Appendix, 6.1); these results do not support the alternative explanation.

Within-host competition

Since mean total parasite density of mixed-genotype infections was less than or equal to that of single-genotype infections, it follows that each genotype should have lower density in mixed infections than in single infections. This is clearly supported by the data: for both CQS and CQR, mean parasite density in mixed-genotype infections was reduced by over 50% compared to single-genotype infections (Fig. 2.3). The linear mixed effects model that analyzed data from all three countries indicated a significant three-way interaction between infection type (single- vs. mixed-genotype), parasite genotype (CQS vs. CQR) and country ($X^2_2 = 6.18$, $p = 0.045$). This interaction is apparent in Figure 2.3: although both CQS and CQR strains had much lower density in mixed- than single-genotype infections (approximated p-value < 0.0001), and CQR generally had lower density than CQS in both single and mixed infections (approximated p-value < 0.0001), in Tanzania, CQR had similar density to CQS in single infections, but much lower density in mixed infections. This suggests that, in Tanzania, CQR parasites were competitively suppressed to a greater degree than in the other two countries, and to a larger extent than CQS.

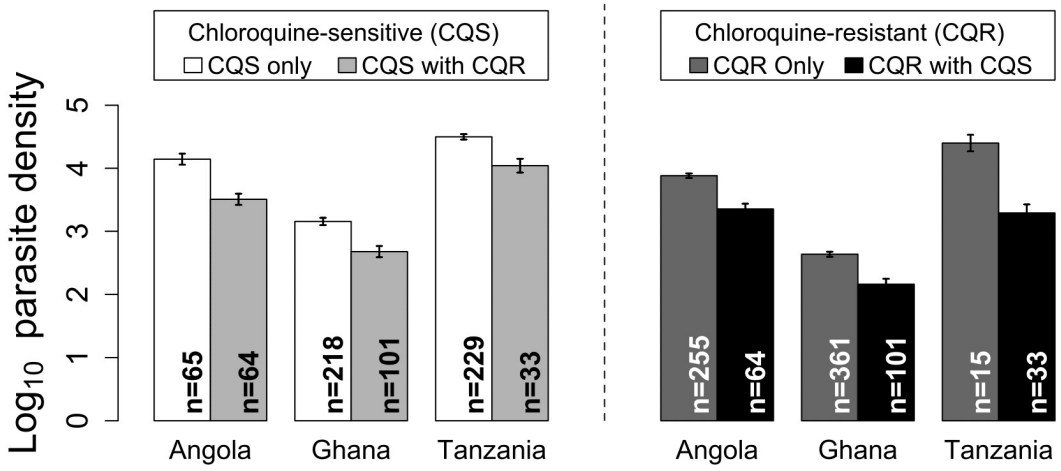

Figure 2.3. Densities of CQS and CQR parasites in single- and mixed-genotype infections. Mean $\log_{10}$ densities of chloroquine-sensitive (CQS, left half) and chloroquine-resistant (CQR, right half) parasites in single- and mixed-genotype infections, stratified by country. Numbers of samples in each group are shown inside the bars. Error bars: $\pm$ S.E.M.

We used a linear model to examine the effects of patient age, infection type (single vs. mixed), and genotype on parasite density in the samples from Angola (the only samples for which age data were available). This analysis showed that, although parasite density did decrease with age ($F_{1,444} = 11.3$, $p = 0.0009$), the significant effect of infection type was retained ($F_{1,444} = 65.8$, $p < 0.0001$), as was the effect of genotype ($F_{1,444} = 9.67$, $p = 0.002$). None of the two- or three- way interaction terms in the model were significant. Thus, irrespective of age, both parasite genotypes had lower densities in mixed-genotype infections than they did in single-genotype infections; CQS parasites also consistently had higher densities than CQR parasites.

Fitness cost of resistance in mixed-genotype infections

This study also provided an opportunity to explore the fitness of chloroquine-sensitive and -resistant parasites *in vivo*. Epidemiological evidence suggests that chloroquine resistance carries a fitness cost in the absence of chloroquine, but the underlying population dynamics are unknown [62]. As mentioned above, CQR parasites consistently had lower densities than CQS parasites. This suggests a fitness cost of chloroquine resistance which manifests as reduced parasite density.

Comparing parasite densities of two genotypes in mixed infections can be complicated by infections harboring multiple strains of a given genotype; in such cases, a one-to-one ratio of the two genotypes is no longer an adequate null hypothesis. We therefore compared the frequencies of CQS and CQR parasites in mixed-genotype infections against predictions from a null model which takes these complications into account (see Appendix (6.1)). At the within-host level, CQR was proportionally less abundant than predicted by the null model in all three countries (Fig. 2.4). In Tanzania, the average proportion CQR was even less than predicted by a modified null model incorporating the fitness differences observed in single infections ($p = 0.0008$; Fig. 2.4), suggesting that in some but not all cases, the fitness cost of resistance may be amplified by competition. This result is in agreement with the finding of a significant interaction effect of infection type, genotype and country on parasite density, which suggested disproportionate competitive suppression of CQR parasites in Tanzania.

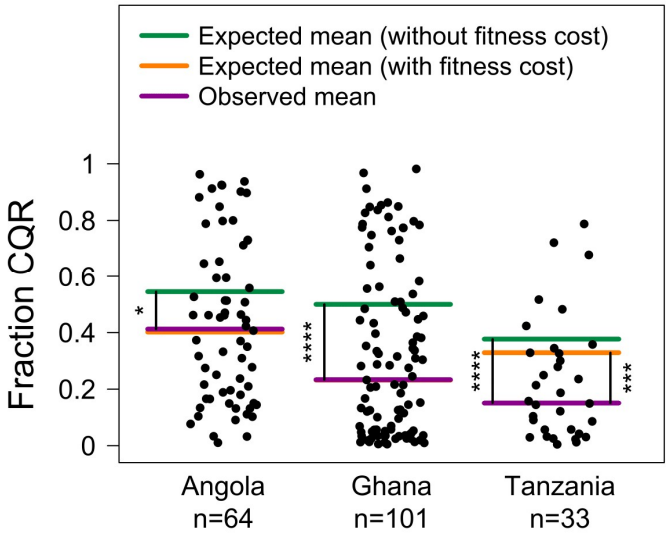

Figure 2.4. Proportions of chloroquine-resistant parasites in mixed-genotype infections. Fraction of all parasites in CQS+CQR mixed-genotype infections that were CQR (stratified by country). Sample sizes are given on the x-axis. For each country, the observed mean fraction CQR is shown in purple. Green lines indicate means predicted by a null model based on population-wide *PfCRT* allele frequencies and distributions of multiplicity of infection. Orange lines indicate means predicted by a similar null model incorporating fitness costs of resistance measured in single-genotype infections. (See Methods and Appendix (6.1) for full description of null models.) Black vertical lines indicate significant differences between observed and expected means; where these lines are absent, no significant differences were found. *$p < 0.05$; ***$p < 0.001$; ****$p < 0.0001$.

Temporal dynamics of resistance in Ghana

Samples from Ghana were collected between 1999 and 2010; chloroquine was the first-line treatment for uncomplicated malaria in Ghana until 2005, when it was retired in favor of artemisinin-based combination therapy. Following this change, the proportion of infections harboring CQR parasites rapidly decreased

throughout the country (Fig. 2.5, $X^2_1 = 10.6$, $p = 0.001$). This decline, along with similar declines observed elsewhere [63, 64], makes it clear that CQR parasites are selected against in the absence of chloroquine; our results suggest that the selective disadvantage is likely due, at least in part, by the fact that CQR parasites do not reach densities as high as those achieved by their CQS counterparts.

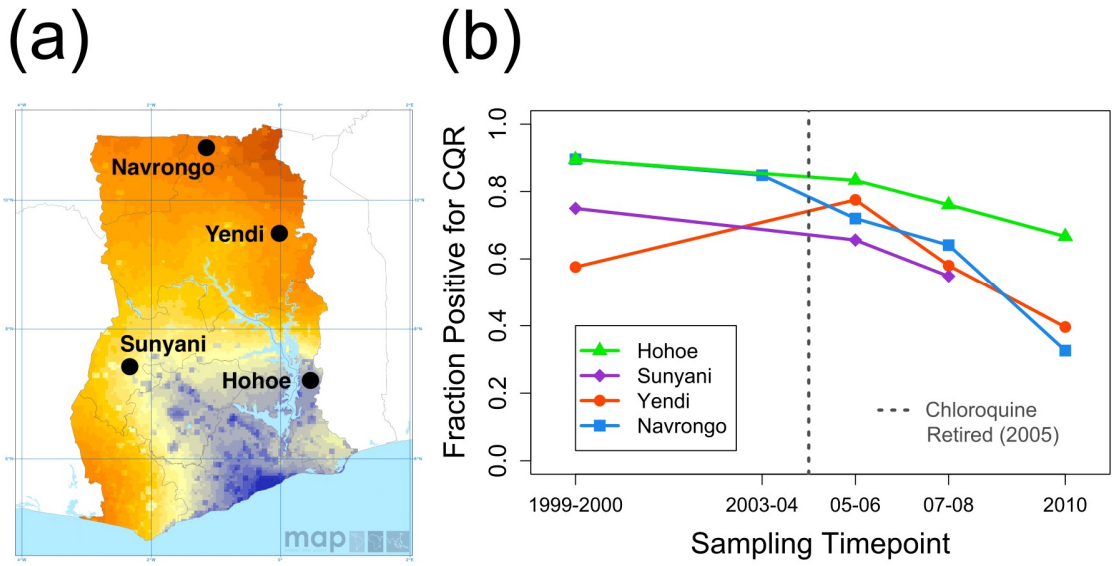

Figure 2.5. Longitudinal trends in prevalence of chloroquine-resistant allele (PfCRT $C_{72}V_{73}I_{74}E_{75}T_{76}$) at four sites in Ghana. (a) Sampling locations in Ghana; shading on map shows estimated transmission intensity (entomological inoculation rate) ranging from 0.1 (dark blue) to >100 (red) infective bites/person/year. Map modified from [65]. (b) Fraction of infections positive for CQR genotype, shown for each time point and location for which samples were available. Vertical dashed gray line shows the year (2005) that chloroquine was retired as a first-line treatment for malaria in Ghana.

2.4 Discussion

The findings presented here provide compelling evidence for within-host competition in *P. falciparum*. The observation that total parasite density is roughly constant with respect to the number of strains in a host suggests that different strains compete for a shared niche [18]. The mechanism responsible for competition is unknown, but possibilities include resource limitation, strain-transcending immunity, and direct interference between parasites [66-69].

The important corollary of within-host competition is the finding that, when hosts are coinfected with CQS and CQR parasites, the different genotypes are both competitively suppressed. Such competition is particularly important for drug-resistant parasites. Resistant parasites, when first emerging, are rare and therefore proportionally more likely than drug-sensitive strains to be found in mixed-genotype infections (meaning there will be few hosts with purely resistant infections, some with mixed-genotype infections, and many with purely drug-sensitive infections) [70]. Therefore, newly emerged resistant strains will suffer more competitive suppression overall than sensitive strains. In addition, antimalarial therapy, by clearing drug-sensitive parasites from mixed infections, may result in competitive release of resistant strains.

Competitive suppression likely inhibits transmission of resistant parasites to new hosts. Although our study did not examine transmission or transmission potential, previous studies have found parasite density to be positively correlated with gametocytemia (density of transmission stages) and infectivity to mosquitoes

[71, 72], and competitive suppression has also been shown to reduce gametocytemia and transmission success in *Plasmodium chabaudi* [19, 23, 44]. Therefore, in high-transmission settings, where mixed-strain infections occur frequently [18], within-host competition may impede the spread of resistance. This may help to explain the puzzling fact that resistance to antimalarial drugs emerges readily in low-transmission areas, but not in high-transmission settings [32, 33].

In addition to the findings related to within-host competition, we made several observations regarding the fitness of chloroquine-resistant parasites. CQR parasites were less abundant than their CQS counterparts in both single- and mixed-genotype infections, suggesting a fitness cost of resistance which manifests, at least in part, as impaired growth in the erythrocytic stage of infection. These findings help to explain the rapid decline of CQ resistance following the termination of chloroquine as a first-line drug in Ghana and elsewhere [63, 64]. Interestingly, we found only limited evidence in support of the idea that fitness costs of resistance will be amplified by competition, as has often been assumed (e.g. [22, 28]); evidence for disproportionate competitive suppression of resistant parasites was observed only in Tanzania. One possible explanation is that the fitness difference between CQS and CQR strains is larger in Tanzania due to the genetic background(s) of one or both genotypes (epistatic effects on the fitness cost of resistance) [73, 74].

Our findings relating to the fitness costs of resistance will help to develop appropriate models that can project the decline of resistance following retirement of a failing drug. Information on the fitness effects of resistance to various antimalarial drugs is likely to be extremely useful for prevention of multi-drug resistance, drug

cycling, and, potentially, strategies that exploit fitness costs to combat the spread of resistant strains [75]. We emphasize, however, that our observations regarding the fitness cost of resistance are specific to chloroquine. The existence, magnitude, and manifestation of fitness costs will depend on the drug. Our observation that CQR parasites are competitively suppressed, however, should readily generalize to other forms of resistance. This is because competitive suppression is not the result of fitness differences, but rather the inevitable result when two populations compete for a shared niche.

Within-host competition (and fitness costs, at least in the case of chloroquine) has likely played an important role in the evolution of resistance. In particular, competitive suppression may have slowed the spread of drug-resistant strains in sub-Saharan Africa, where intense transmission means that mixed-strain infections and therefore within-host competition are prevalent. It should be noted, however, that the effects of competition on resistant strains probably depend strongly on the amount of antimalarial drug use. Competitive suppression of resistant strains can only occur where drug-sensitive competitors are present, i.e. in untreated infections. Treatment may reverse suppression of resistant parasites by killing off the competitors, with the resistant strain not only surviving but expanding, increasing its transmission potential; this is known as competitive release [19]. The balance between competitive suppression and competitive release determines the rate at which resistance will spread. When relatively few infections are treated, as is probably the case in most settings due to high prevalence of asymptomatic infections [15], competitive suppression will dominate, inhibiting the

spread of resistance in high-transmission settings [22]. At higher rates of treatment, however, competitive release may have the opposite effect, causing resistance to spread more rapidly in a high-transmission setting than in a low-transmission area under similar drug pressure [20, 21, 40].

The risk of widespread competitive release suggests that broad application of antimalarial drugs, such as in mass drug administration, should be approached with caution in high-transmission settings, perhaps by employing aggressive transmission control measures in conjunction with mass drug administration in order to reduce opportunities for transmission of resistant strains. It has been suggested that competitive release of resistant parasites could be avoided by subcurative drug treatment that eliminates enough sensitive parasites to alleviate symptoms, but leaves enough to maintain competitive suppression of the resistant strain [28]. Such approaches have been demonstrated to work for the rodent malaria *Plasmodium chabaudi* [41, 44, 76], but whether they can be safely and effectively applied to *P. falciparum* in humans is an open question [36, 77, 78].

In summary, our findings support an important role for within-host competition in the evolution of drug resistance in *Plasmodium falciparum*. These findings will improve modeling and practical management of resistance to maximize the useful lifespan of existing antimalarial drugs.

Chapter 3: Competitive release of drug-resistant parasites following treatment

3.1 Introduction

In settings with intense malaria transmission, such as many areas in sub-Saharan Africa, frequent infectious mosquito bites coupled with high genetic diversity in the malaria parasite population result in most infections being comprised of multiple parasite strains or genotypes (termed mixed infections) [18]. As a result, when drug-sensitive and drug-resistant parasites are both circulating in a high-transmission setting, many infections will harbor both sensitive and resistant parasites [79]. Experiments with the rodent malaria parasite *Plasmodium chabaudi* have shown that infection with multiple parasite strains results in within-host competition [23, 27]; within-host competition between drug-sensitive and drug-resistant parasites was also recently observed for *P. falciparum* in humans.

In *Plasmodium chabaudi*, treatment of mixed (drug-sensitive + drug-resistant) infections with antimalarial drugs results in clearance of the drug-sensitive parasites and concomitant expansion of the drug-resistant parasites, which grow to fill the niche space previously occupied by the drug-sensitive population [19]. This expansion following the removal of competitors is known as 'competitive release' and is considered a potentially important factor in the evolution of drug resistance in malaria because it magnifies the selective advantage of drug resistance. In *P. chabaudi*, competitive release has been shown to increase

transmission of drug-resistant parasites to mosquitoes [41, 42] and it has been hypothesized that competitive release could accelerate the spread of drug resistance in high-transmission settings [20, 21, 80], where mixed infections are most common. It has also been suggested that the benefit of competitive release to drug-resistant parasites could be reduced by using less aggressive courses of antimalarial drug treatment than are currently recommended [28, 44, 76, 77].

However, there is very little empirical evidence for competitive release outside of rodent models. The best evidence for competitive release came from a study by Harrington et al. [49], who examined the effect of sulfadoxine-pyrimethamine intermittent preventive treatment in pregnancy (SP-IPTp) on parasitemia and frequency of SP-resistant alleles in blood from the placenta upon delivery. It was found that both the frequency of SP-resistant alleles and placental parasitemia were increased in women who had received SP-IPTp, which suggested competitive release and facilitation of SP-resistant parasites in the women who were treated. (Competitive facilitation, which has also been observed in *P. chabaudi* [41], refers to an effect in which the parasite density achieved by the resistant strain upon removal of competitors exceeds the density achieved when competitors are never present at all.) However, there are some significant limitations on these findings, including the specific focus on placental parasitemia and the measurement of parasitemia as the fraction of erythrocytes infected rather than the density of infected erythrocytes in the blood. However, the biggest limitation is that the observations were from a cross-sectional study. Competitive release is, by definition, a *change* in the density of resistant parasites following removal of drug-

sensitive competitors, and should therefore be evaluated using pre- and post-treatment samples from the same individuals.

Lack of clear evidence for (or against) competitive release in *P. falciparum* thus constitutes a major knowledge gap. We therefore undertook a study in which we analyzed the changes in drug-sensitive and drug-resistant parasite densities in children that were treated with antimalarial drugs, and compared these changes to those observed in children that did not receive antimalarial drugs, in order to determine whether treatment resulted in competitive release of drug-resistant parasites.

3.2 Methods

The samples used in this study were originally collected as part of the Asembo Bay Cohort Project (ABCP) in western Kenya from 1992 to 1999. The study has been described in detail elsewhere [81], but in brief: the Asembo Bay Cohort Project was a longitudinal study of malaria in a holoendemic setting (intense, year-round malaria transmission). The study followed young children for up to five years, with blood samples collected at least monthly, and malaria parasitemia – as determined by microscopy – in the presence of fever ($\geq$ 37.5°C) was treated with sulfadoxine-pyrimethamine. Blood samples were centrifuged to generate cell pellets, which were shipped on dry ice to the Centers for Disease Control and Prevention in Atlanta, GA and subsequently stored in liquid nitrogen.

For the purposes of this study, it was desirable to have several consecutive samples from an individual child in order to observe longitudinal changes in within-host parasite populations. An inventory of over 62,000 blood samples was searched to find sets of at least 5 consecutive samples with no more than 30 days between samples. Study records detailing use of antimalarial drugs and other medicines were used to filter out children that had been given chloroquine, amodiaquine, quinine, iron or folic acid, since any of these substances could potentially influence parasite dynamics. Sample sets were sorted into those with at least one instance of SP treatment and those without; a subset of the 'no treatment' sample sets, which were more numerous, was chosen to roughly match the age distribution of children that provided the 'treatment' sample sets.

Of 700 samples requested from the CDC inventory, 129 were no longer available, and of the 571 shipped from the storage facility, 40 were found to be in unusable condition (coagulated, dried, or insufficient sample). The remaining 531 samples were processed for further analysis. Depending on the available volume of each sample, either 40 μL or 10 μL was aliquoted and diluted in phosphate-buffered saline to a total volume of 200 μL. DNA was extracted with the QIAamp DNA Mini Kit from Qiagen (catalog no. 51306), using the 'spin' protocol for DNA purification from blood or body fluids. DNA was stored at 4°C.

Parasite quantification using PET-PCR

All samples were analyzed using PET-PCR (a species-specific real-time quantitative PCR) to determine *P. falciparum* parasite density in each sample [82].

Samples were run in triplicate using both *falciparum*-specific and genus-specific primers (tagged with different fluorescent dyes to allow multiplexing), and a standard curve was generated using serial dilutions of quantitated parasite DNA as described previously [79]. C_T values from PET-PCR were used in conjunction with the standard curve to estimate the parasite density of *P. falciparum* as well as the density of all *Plasmodium* genus parasites in each sample (the volume of each sample used for DNA extraction was corrected for when calculating parasite density for the original samples). However, it was found that the estimated density for *P. falciparum* was generally higher than that for all *Plasmodium*; thus, the data could not be used to exclude non-*falciparum* parasites. Instead, we simply used the estimates of *P. falciparum* parasite density for all subsequent analysis.

Targeted amplicon deep sequencing (TADS) of *dhps* and *dhfr*

PCR was used to amplify the genes *dhps* (dihydropteroate synthase) and *dhfr* (dihydrofolate reductase), which are involved in folate metabolism and which include markers of resistance to the antifolate drug combination sulfadoxine + pyrimethamine [83]. The master mix, primer sequences and thermal cycling protocol for PCR amplification are given in Tables A8-A10 in the Appendix. For each PCR reaction, amplification was verified for a subset of samples by gel electrophoresis.

PCR products were purified and normalized (standardized to a similar concentration across all samples) using the SequalPrep Normalization Plate Kit from ThermoFisher Scientific (catalog no. A10510-01). Normalized *dhps* and *dhfr*

amplicons for each sample were combined, fragmented using the Nextera XT DNA Sample Preparation Kit from Illumina (catalog no. FC-131-1096) and tagged with unique index primers using the Nextera XT Index kit, also from Illumina (catalog no. FC-131-1002). Fragmented and tagged ('tagmented') DNA libraries were purified using Agencourt AMPure XP magnetic beads from Beckman Coulter Genomics (part no. A63881) before being pooled for sequencing (between 90 and 270 samples were pooled for each sequencing run). Pooled libraries were analyzed to determine average DNA fragment size using the D5000 ScreenTape System from Agilent Technologies (catalog nos. G2940CA, 5067-4626, and 5067-4627) and DNA concentrations were determined using the Qubit 3 Fluorometer from Life Technologies (catalog nos. Q32853 and Q33216). Pooled libraries were then diluted to a concentration of either 4 nM or 2 nM, denatured and diluted to a final concentration of 10 pM, 'spiked' with 10 pM PhiX control library from Illumina (FC-110-3001) at a frequency of 5% and loaded using the MiSeq Reagent Kit v2 (catalog no. MS-102-2002) for sequencing using the MiSeq desktop sequencer from Illumina.

Targeted amplicon deep sequencing (TADS) was successfully completed for 381 samples. Raw sequence data were analyzed as described previously [84], with the following changes: a total of 31902838 reads were trimmed down to 27317608 with a minimum read length of 50 bp and Q20 quality score of 96.9%; and the threshold frequency for identification of non-WT variants was 10%. SNPs were called only using reads that mapped perfectly to the reference sequences (PFD0830w for *dhfr* and PF08_0095 for *dhps*). For each sample, a list of all polymorphisms observed in *dhps* and *dhfr* was generated, along with the

frequencies of these variants in the sample. We restricted our analysis to six polymorphisms that are strongly linked to SP resistance and which were found to be present at moderate to high frequency both in the samples analyzed and in previous work (Table 3.1) [83, 85]. Three polymorphisms in each gene were analyzed: N51I, C59R, and S108N for *dhfr*; and S436A, A437G, and K540E for *dhps*. (The reference strain, 3D7, has the 'mutant' genotype at *dhps* codon 437 – glycine instead of alanine – resulting in the calls for WT and mutant being reversed; the frequencies were corrected before analyzing the data.)

Statistical analysis

From 381 samples from 87 individuals, we identified 40 'treated' sample pairs (pre- and post-treatment samples no more than 30 days apart) and 258 'control' sample pairs (two samples no more than 30 days apart with no SP use in between). For all samples, measures of parasite density from PET-PCR and estimates of allele frequency from TADS were used to calculate the densities of parasites with drug-sensitive (WT) and drug-resistant (mutant, henceforth M) alleles at the six loci specified above. For each sample pair, if both WT and mutant alleles at a given locus were present in the first sample, then the relative changes in each allele in the second sample were calculated as follows:

$$\Delta_{WT} = \log_{10}\left(1 + \frac{D_{WT(2)} - D_{WT(1)}}{D_{WT(1)} + D_{M(1)}}\right)$$

$$\Delta_M = \log_{10}\left(1 + \frac{D_{M(2)} - D_{M(1)}}{D_{WT(1)} + D_{M(1)}}\right)$$

where $D_{WT(1)}$ and $D_{M(1)}$ are the densities of parasites with the WT and mutant alleles in the first sample, and $D_{WT(2)}$ and $D_{M(2)}$ are the same quantities for the second sample. A negative value of Δ_{WT} reflects a decrease in the density of WT parasites, whereas a positive value reflects an increase; the same is true of Δ_M. Plots of Δ_M vs. Δ_{WT} include dotted lines at $\Delta_M = 0$ and $\Delta_{WT} = 0$ in order to distinguish increases from decreases.

The question to be addressed was whether treatment with SP would cause a decrease in SP-sensitive parasites accompanied by an increase in SP-resistant parasites (competitive release). If this were the case, we would expect a negative correlation between Δ_{WT} (change in the WT allele density) and Δ_M (change in the mutant allele density) in treated sample pairs, but not necessarily in control sample pairs. (In the absence of antimalarial drugs, parasites may or may not be growing in a density-dependent manner; a most, a weaker negative correlation between Δ_{WT} and Δ_M would be predicted in control sample pairs, since density-dependence is likely to be weak, for example, in chronic infections with low parasite density).

A linear mixed-effects model was used to explore whether the relationship between Δ_{WT} and Δ_M differed between treated and control sample pairs. Using the function *lme* in the R package *nlme*, Δ_M was modeled as a function of Δ_{WT}, with SP treatment, allele, and time between samples included as fixed effects and patient (i.e., which child each sample pair was obtained from) as a random effect [60].

Higher-order interaction terms were removed from the model one at a time and each simplified model was compared to its predecessor using the command *anova*; when the minimal model was found, approximate *p*-values were found using *anova.*

Although sample interval (i.e. time between samples) was included as a continuous covariate in the linear mixed-effects model described above, we reduced this to a categorical variable in order to explore the effect of sampling interval on changes in parasite density. Sample pairs were sorted into two groups: those with intervals of 1-14 days, and those with intervals of 14-30 days. This resulted in a total of four groups of interest: treated and control sample pairs, each divided into pairs with intervals of $\leq$14 days and pairs with intervals of $>$14 days. Two-sided, two-sample *t*-tests were used to compare total parasite densities between groups (comparisons being restricted to the first sample from each sample pair) as well as within groups (comparing all first samples to all second samples for a given set of sample pairs). In the former case, unpaired *t*-tests were used, while paired *t*-tests were used for the latter.

3.3 Results

Targeted amplicon deep sequencing of *dhps* and *dhfr* was completed for 381 samples from 87 children. Among these samples, there were moderate to high frequencies of six known markers of resistance to sulfadoxine-pyrimethamine; these were the amino acid changes N51I, C59R, and S108N in *dhfr*; and S436A, A437G, and K540E in *dhps.* Other common mutations in these genes, including

A581G in *dhps* and I164L in *dhfr*, were observed rarely or not at all (see Table 3.1). These findings are consistent with other reports from the same region and time period [85]. The mutant alleles varied in their frequency within individual infections as well as at the population level (Figure 3.1).

Table 3.1 Numbers and percentages of samples carrying variants linked to SP resistance [83]. Polymorphisms used in subsequent analysis are indicated with asterisks.

Gene	Variant	Number of samples (%)
dhps	S436A*	84 (22.0%)
	A437G*	334 (87.7%)
	K540E*	191 (50.1%)
	A581G	0 (0%)
dhfr	C50R	0 (0%)
	N51I*	351 (92.1%)
	C59R*	283 (74.3%)
	S108N*	374 (98.2%)
	I164L	1 (0.3%)

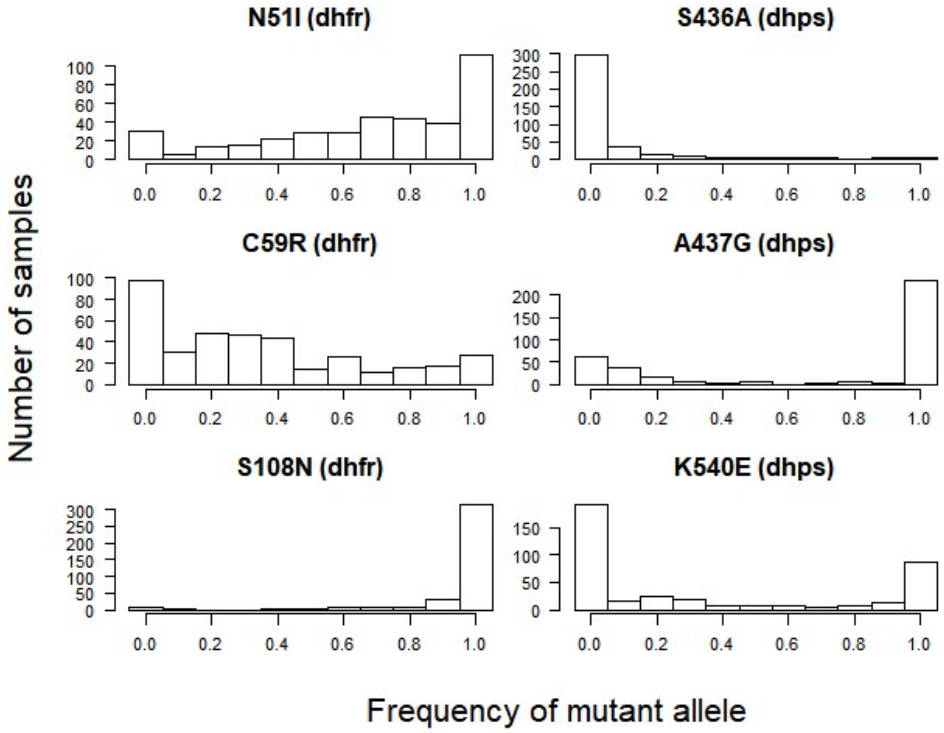

Figure 3.1 Within-host frequency distributions of mutant alleles for six known markers of resistance to sulfadoxine-pyrimethamine. All 381 samples are represented in each panel.

Out of 381 samples, we identified 298 pairs of consecutive samples obtained ≤30 days apart (these 298 pairs represented 337 different samples, meaning most samples appeared in two different pairs). 40 pairs consisted of samples that were obtained before and after treatment with sulfadoxine-pyrimethamine ('treated' sample pairs), and 258 pairs consisted of consecutive samples with no SP treatment in between ('control' sample pairs).

If competitive release of SP-resistant parasites occurred following treatment with SP, we would expect to see a decrease in the number of drug-sensitive parasites accompanied by an increase in the number of drug-resistant parasites. We

therefore examined the correlation between Δ_{WT} and Δ_M, which represent the relative changes in density of parasites with WT and mutant alleles at SP resistance loci (formulas for Δ_{WT} and Δ_M are given in the Methods). A linear mixed-effects model treating Δ_M as the response variable showed a significant interaction between Δ_{WT} and treatment with SP (approximated p-value $= 0.0015$), indicating that the relationship between Δ_{WT} and Δ_M was different for treated sample pairs than control pairs. As shown in Figure 3.2, there was a negative correlation between Δ_{WT} and Δ_M for treated sample pairs, but a positive correlation between the same variables in control sample pairs. Although there was a significant interaction between Δ_{WT} and locus (approximated p-value < 0.0001), the three-way interaction between Δ_{WT}, locus, and treatment was not significant; this indicates that the net relationship between Δ_{WT} and Δ_M varied between resistance loci (Figure 3.3), but that there was no evidence for allele-specific differences between control and treated sample pairs.

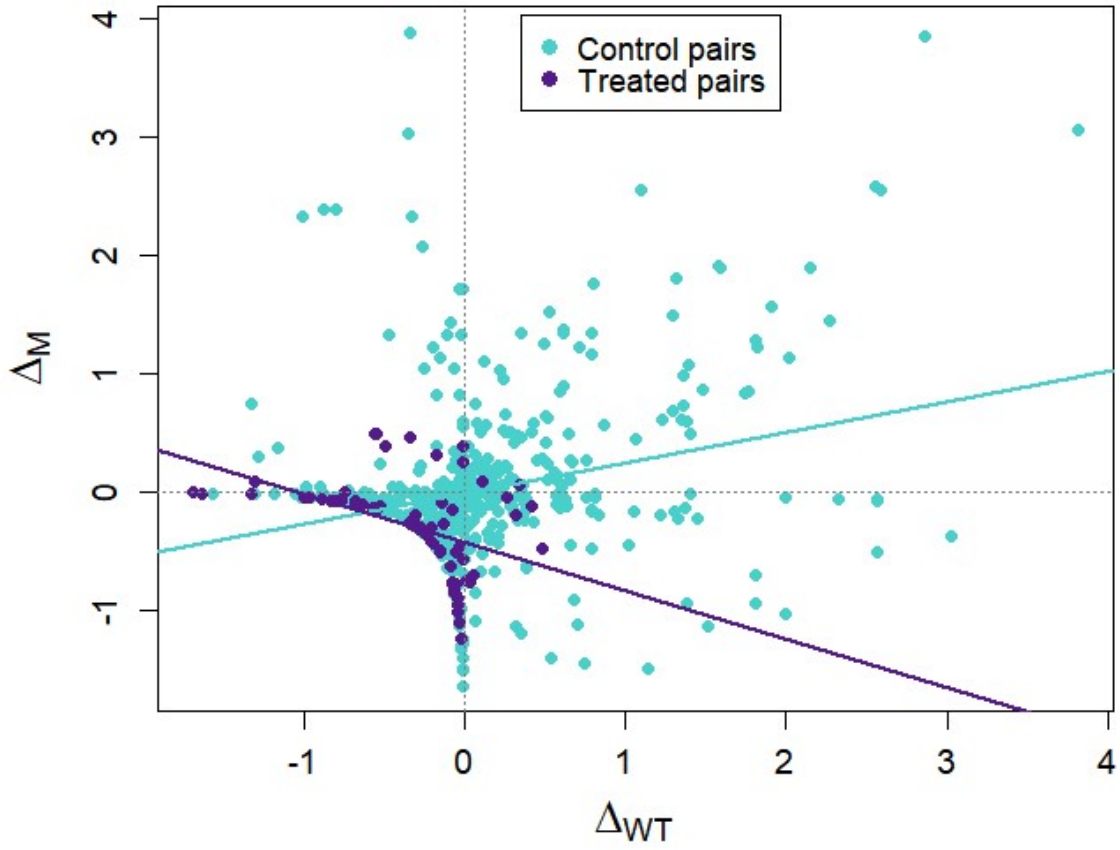

Figure 3.2 Relative changes in densities of mutant (drug-resistant) and WT (drug-sensitive) alleles in all 298 sample pairs. Each point is specific to a single locus (e.g. *dhfr* codon 51) for a single sample pair, but data is only shown for instances where mutant and WT alleles for a given locus were both present in the first sample of a pair. Data points and regression lines for control and treated sample pairs are shown in turquoise and purple, respectively.

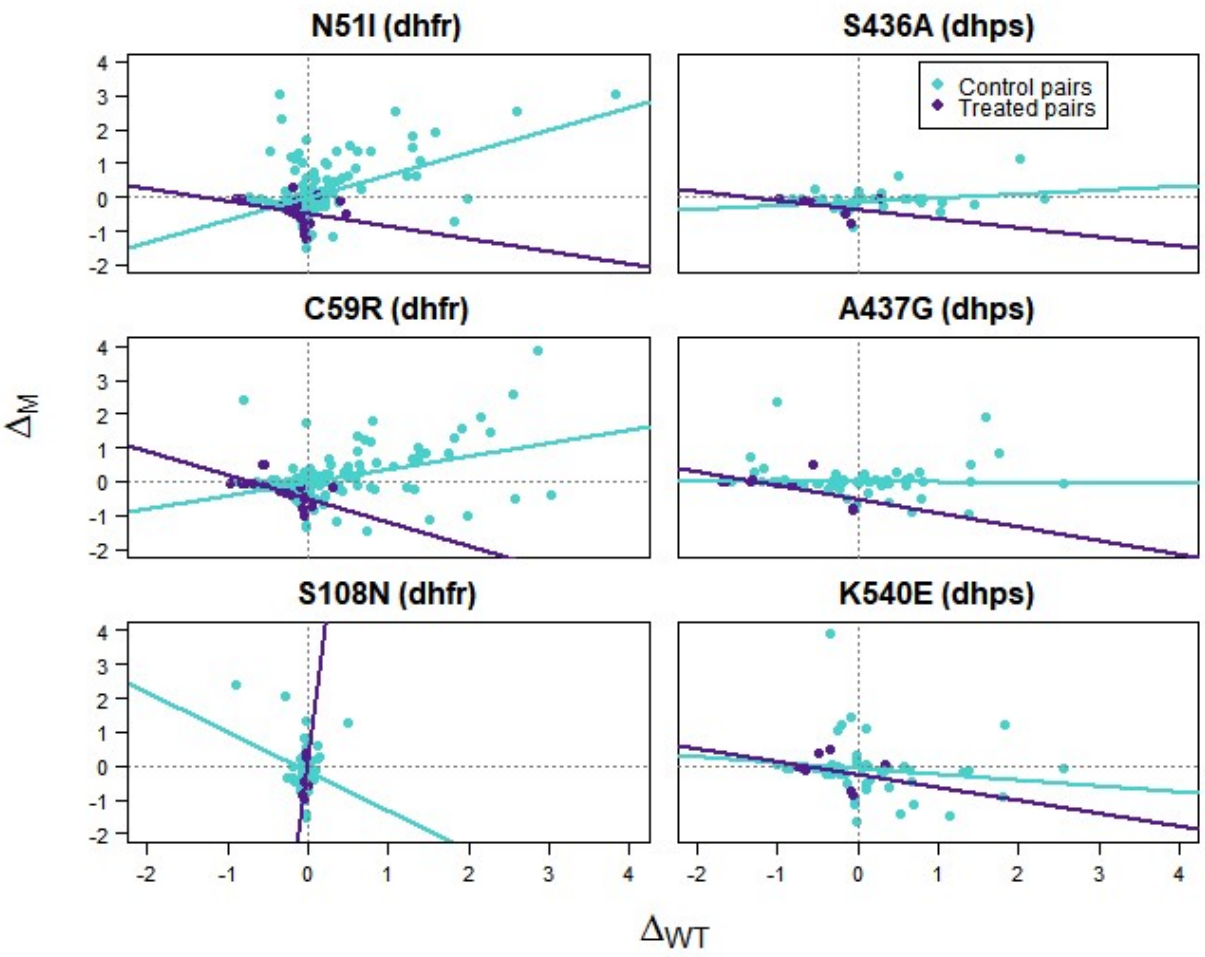

Figure 3.3 Relative changes in densities of mutant (drug-resistant) and WT (drug-sensitive) alleles for each individual resistance locus. Data points and regression lines are shown in turquoise and purple for control and treated sample pairs.

In order to determine whether the time between samples was a factor in the relationship between Δ_{WT} and Δ_M, we included sample interval as a fixed effect in the statistical model. If the effect of treatment on the correlation between Δ_{WT} and Δ_M (the negative correlation in treated sample pairs and positive correlation in control sample pairs) was influenced by the interval between samples, we would expect a significant three-way interaction between Δ_{WT}, sample interval, and

treatment, which was not found. There was a significant three-way interaction between Δ_{WT}, locus, and sample interval, indicating that there was an effect of sample interval on the relationship between Δ_{WT} and Δ_M, although this effect varied by locus. Figure 3.4 shows the correlations between Δ_{WT} and Δ_M for pairs of samples taken $\leq$14 days and >14 days apart. The same data shown separately for each resistance locus are in the Appendix (Figure A5).

As Figure 3.4(a) shows, in treated sample pairs with intervals of $\leq$14 days, both Δ_{WT} and Δ_M were generally negative, indicating a net decrease in both WT and mutant alleles. In contrast, a number of treated sample pairs with intervals >14 days showed increases in mutant alleles, WT alleles, or both (Figure 3.4(b)). This is reinforced by Figure 3.5, which shows that total parasite density was markedly decreased – by roughly two orders of magnitude on average – following treatment in treated sample pairs with intervals of $\leq$14 days (unpaired t-test, $p < 0.0001$), whereas there was a much smaller (but still significant) decrease in treated sample pairs separated by >14 days. Interestingly, the same trend held for control sample pairs, with a significant decrease in total parasite density in control pairs separated by $\leq$14 days, and no significant change in control pairs with intervals of >14 days.

It is important to note that patients were not randomized to treatment or control groups, but treated with SP on the basis of fever and parasitemia. Total parasite density was significantly greater in the first samples of treated sample pairs than the first samples of control pairs ($p = 0.002$, Figure 3.6), which is consistent with observed connections between parasite density and fever [86]. This may

contribute to the different relationships between Δ_{WT} and Δ_M observed in treated and control sample pairs, as discussed in more detail below.

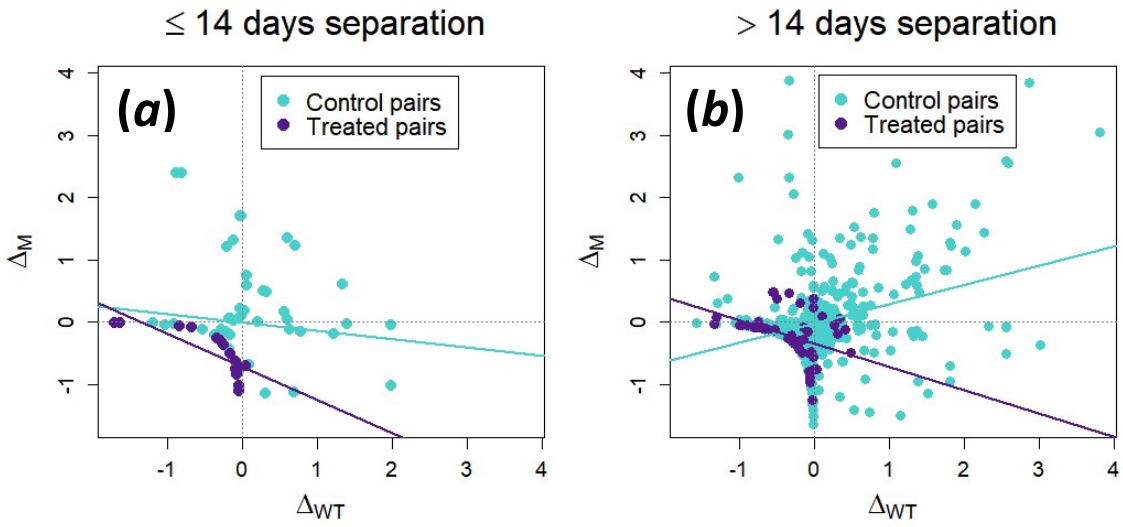

Figure 3.4 Relative changes in densities of mutant (resistant) and WT (sensitive) alleles for sample pairs separated by 1-14 days (*a*) and pairs separated by 15-30 days (*b*). Data points and regression lines for control and treated sample pairs are in turquoise and purple, respectively. Note that although regression lines are shown separately for control and treated sample pairs, the effect of sample interval on the relationship between Δ_{WT} and Δ_M did not depend on treatment.

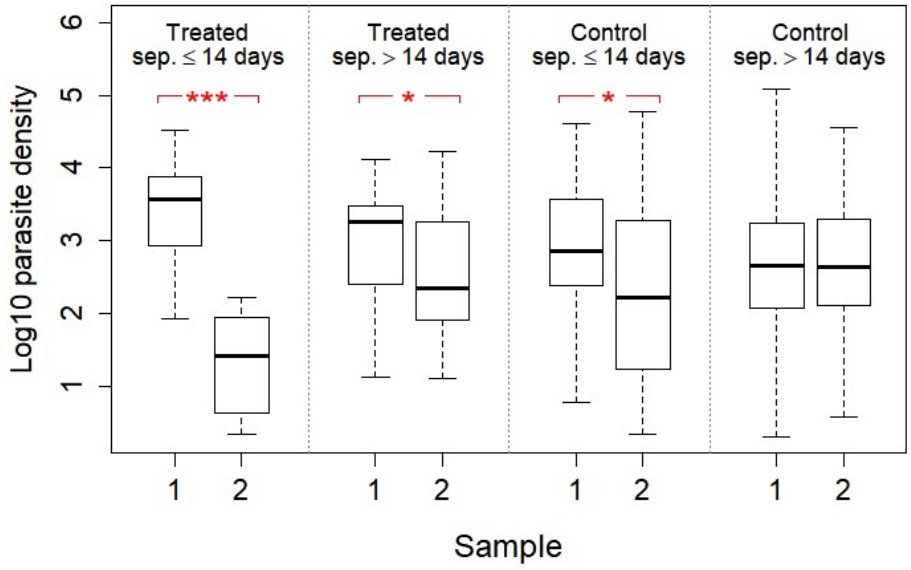

Figure 3.5 Log_{10} parasite density for first and second samples in four categories: treated pairs separated by ≤14 days, treated pairs separated by >14 days, control pairs separated by ≤14 days, and control pairs separated by >14 days. Whiskers show the full range of values. $*p < 0.05$; $***p < 0.001$.

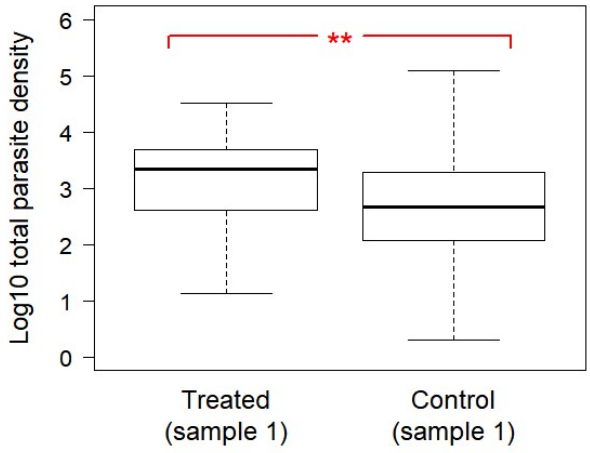

Figure 3.6 Log_{10} total parasite density of the first samples in treated sample pairs and control sample pairs. Whiskers show the full range of values. $**p < 0.01$.

3.4 Discussion

The results presented here support the hypothesis that treatment of mixed drug-sensitive and drug-resistant *P. falciparum* infections results in 'competitive release' of the resistant parasites. The hypothesis is supported by a negative correlation between changes in SP-sensitive and SP-resistant alleles following treatment with SP, whereas without treatment, changes in sensitive and resistant alleles were positive correlated (albeit extremely variable) (Fig. 3.2). Together with the fact that initial parasite densities were higher in treated than untreated infections, this suggests that parasite populations in hosts that received treatment may have been close to carrying capacity, such that resistant parasites could only grow if sensitive parasites were removed, and vice versa. In untreated infections, parasite densities were lower on average, and unlike in treated infections, it was common for sensitive and resistant parasites to increase simultaneously, which suggests that parasite populations may have been below carrying capacity in many untreated infections.

It is interesting to note that, in treated sample pairs with sample intervals of $\leq$14 days, the total parasite densities of post-treatment samples were, on average, reduced over one hundred-fold compared to pre-treatment samples; however, in treated pairs with intervals of >14 days, this difference was roughly 3.5-fold (Figure 3.5). As shown Fig. 3.4(a), treatment with SP often resulted in a decrease in both WT and mutant alleles, suggesting that even 'resistant' parasites were reduced by treatment; however, this is consistent with the nature of SP resistance, in which

individual mutations provide only partial resistance and the overall degree of resistance increases with the total number of mutations in *dhps* and *dhfr* [50]. The smaller difference in parasite density observed in treated sample pairs separated by >14 days suggests that parasite populations 'bounce back' following treatment with SP, and as seen in Fig. 3.4(b), in at least some cases this favors drug-resistant parasites. If such 'bounce back' does occur – which would need to be confirmed with time series data from individual infections – then any future studies of competitive release in *P. falciparum* should consider the possibility that 'resistant' parasites may still decline in response to treatment, and expansion might be observed only after the drug has been cleared from the patient's system.

There are at least two significant limitations to the inferences drawn from the data presented here. The first is that in the raw data from targeted amplicon deep sequencing, mutant alleles were only called if present at a frequency of >10%. This means that changes in abundance of mutant alleles could not be analyzed if the initial frequencies were below 10%. This limitation could be addressed to some extent by increasing the read depth and lowering the threshold for detection of mutant alleles. A second limitation is that, with the data obtained for this study, it was not possible to distinguish recrudescence from reinfection; doing so generally requires analysis of additional molecular markers, such as neutral microsatellites [87]. Our interpretation of the results presented here largely assumes that, for a given pair of samples, the WT and mutant parasite populations in the second sample are the same as in the first; however, in such a high-transmission setting, this was probably not always the case. However, the inverse relationship between changes in

drug-sensitive and drug-resistant alleles following treatment is an empirical one: a sensitive parasite's loss is a resistant parasite's gain – even if that resistant parasite is not the same one that was present before treatment.

The findings outlined here support the relevance of studies of within-host competition and competitive release in the rodent malaria parasite *Plasmodium chabaudi* to *P. falciparum*. Theoretical discussions of the impact(s) of competitive release on the spread of drug resistance have advanced over the last 15 to 20 years despite a paucity of evidence that competitive release occurs in *P. falciparum*. [19-21, 28, 41-44, 76, 77, 80, 88]. Thus, evidence for competitive release in *P. falciparum* malaria addresses a major gap in the literature on the subject and may advance the discussion of competitive release from theory to real-world impacts and interventions.

Chapter 4: Transmission intensity, within-host dynamics, and the evolution of drug resistance

4.1 Introduction

Drug resistance is a recurring threat to effective treatment and control of *Plasmodium falciparum* malaria. The appearance of chloroquine resistance in Africa during the 1970s and 1980s saw marked increases in malaria-related morbidity and mortality, especially in young children [89]. Sulfadoxine-pyrimethamine, which was widely introduced as a replacement for chloroquine, was similarly undermined by resistance soon after it was deployed. Artemisinin-based combination therapies (ACTs) – the current 'first-line' antimalarial drugs – appear to be failing in Southeast Asia [5], where resistance to artemisinin and partner drugs has been spreading despite ardent efforts to contain it. The arsenal of weapons against drug-resistant malaria is surprisingly limited; the strategy mostly revolves around preventing drug resistance mutations from occurring in the first place (hence the universal adoption of combination therapies).

Although *de novo* resistance mutations are a prerequisite for the evolution of drug resistance, they appear to account for a tiny fraction of drug-resistant *P. falciparum* infections, the vast majority of which result from person-to-person transmission of resistant parasites. This is supported by data showing that chloroquine-resistant parasites from every part of the world belong to just a handful of lineages, each stemming from a single *de novo* resistance mutation [32]. Similar

patterns have been found for resistance to sulfadoxine and pyrimethamine [33, 90, 91], and so far, the same appears to be true for artemisinin resistance [5]. Therefore, the dominant mechanism underlying the evolution of drug resistance in *P. falciparum* appears to be sustained transmission of drug-resistant parasites at the population level, rather than selection of *de novo* resistance mutations.

This should be kept in mind as we turn to an unsolved puzzle: the relationship between transmission intensity and the evolution of drug resistance in *Plasmodium falciparum*. Despite the fact that roughly 90% of all malaria infections occur in sub-Saharan Africa (where malaria transmission rates are generally high), drug-resistant parasites have consistently emerged earlier and more often in low-transmission settings outside of Africa, most frequently in Southeast Asia and South America. This, along with evidence that person-to-person transmission plays a key role in the evolution of resistance, suggests that low-transmission settings are more conducive to the sustained transmission of drug-resistant parasites than high-transmission settings.

There are at least three mechanisms that have been proposed to explain this pattern, which we will take up in turn. The first is recombination during sexual reproduction in the mosquito vector, which occurs when multiple parasite strains or genotypes are picked up by a single mosquito (during one or more blood meals). This happens more frequently in high-transmission settings because the prevalence of infection and the frequency of mixed-strain infections are both higher [18, 92]; as a result, the rate of recombination is generally greater in high-transmission settings [11]. If drug resistance is controlled by multiple loci – particularly if those loci are

unlinked – then recombination will tend to separate the individual mutations, reducing the probability that the next host will receive fully drug-resistant parasites; and this will happen more often in high-transmission settings due to higher rates of recombination [80, 93]. The problem with this otherwise elegant hypothesis is that chloroquine resistance, which exemplifies the pattern of delayed emergence in high-transmission settings, is governed by mutations in a narrow section of a single gene, providing limited opportunity for recombination [8, 32]. Thus, it seems doubtful that recombination is the primary mechanism delaying the evolution of drug resistance in high-transmission settings.

The second proposed mechanism, and perhaps the most widely believed, is that immunity affects the strength of selection in high-transmission settings. It is generally accepted that it takes years of frequent exposure to develop clinical immunity to malaria [94], and therefore residents of high-transmission areas (other than young children) will have considerable protection against symptomatic malaria, while people living in low-transmission settings will not. As a result, it is believed that malaria cases are frequently asymptomatic in high-transmission settings but generally symptomatic in low-transmission settings, and that levels of antimalarial drug use will accordingly be higher in low-transmission areas, resulting in stronger selection for resistance [14]. It turns out, however, that a majority of infections are asymptomatic even in low-transmission settings, and while there is a positive correlation between transmission intensity and the proportion of infections that are asymptomatic, it is relatively weak [15]. An additional factor that may have affected the spread of resistance in the past is that until 2010, the World Health

Organization recommended a policy of 'presumptive treatment' in high-transmission settings. Under this policy, any fever in a child under 5 years old was assumed to be caused by malaria and treated with antimalarial drugs. This policy almost certainly resulted in treatment of a significant number of asymptomatic malaria infections (which, in high-transmission settings, can account for a substantial fraction of the malaria burden even among young children [95]). The effect would have been to inflate overall levels of antimalarial drug use, though to what extent is not known. Thus, it is unclear how much antimalarial drug use and the strength of selection for resistance depend (or depended) on transmission intensity.

The third proposed mechanism, and the one that we will largely focus on, is that within-host competition between drug-sensitive and drug-resistant parasites affects the spread of resistance in high-transmission settings. There is a positive correlation between transmission intensity (the average number of infectious mosquito bites per day or per year) and the average multiplicity of infection (number of parasite strains or genotypes in a single host) [18]. As a result, in high-transmission settings, there is an increased likelihood of hosts being infected with both drug-sensitive and drug-resistant parasites contemporaneously. In a rodent model of malaria (*Plasmodium chabaudi*), it has been demonstrated that strains infecting the same host experience competition, meaning that the growth of one or both strains is reduced relative to that achieved in the absence of competitors [23]. More recent observations suggest that within-host competition – including competition between drug-sensitive and drug-resistant parasites – occurs in

Plasmodium falciparum, as well [79]. Some mathematical models have suggested that within-host competition between sensitive and resistant parasites could slow the spread of resistance in high-transmission settings [22, 29]; however, these findings hinge on the assumption that resistance carries a fitness cost, and that this cost is magnified by within-host competition. This assumption, which is based on findings from the *P. chabaudi* model [27] but lacks empirical support in *P. falciparum* [79], effectively guarantees that selection against resistance will be stronger in high-transmission settings. Thus, in these models, the effects of within-host competition on the spread of resistance are muddled by the effects of fitness differences between sensitive and resistant parasites; it is unclear from these models whether competition has any effect in its own right.

It has also been demonstrated in *Plasmodium chabaudi* that competition between drug-sensitive and drug-resistant parasites is reversed by treatment with antimalarial drugs; removal of drug-sensitive competitors allows the drug-resistant parasite population to expand in a phenomenon called 'competitive release' [19]. In *P. chabaudi*, competitive release has been shown to increase not only the asexual parasite density of the resistant strain, but also gametocyte density and transmission to mosquitoes [41, 42], indicating that the resistant strain experiences not just a survival advantage (relative fitness) but an increase in population size and transmission (absolute fitness). Mathematical models have shown that competitive release might accelerate the spread of resistance in high-transmission settings [20, 21] - obviously, reaching very different conclusions than the models described above – but it seems clear that this is not always the case, since the opposite

(delayed evolution of resistance in high-transmission settings) seems to be more common. One possibility is that the effects of competitive release might become important only with higher levels of antimalarial drug use than typically occur in endemic settings. If so, it is conceivable that higher rates of antimalarial drug treatment might flip the relationship between transmission intensity and evolution of resistance, such that resistance spreads most rapidly in high-transmission settings. This is a possibility worth investigating, since certain interventions, such as mass drug administration (MDA) and mass screening and treatment (MSAT) will transiently but significantly increase rates of antimalarial drug use at the population level.

As a whole, the existing literature has not reached a consensus regarding the effect(s) of within-host competition on the spread of resistance – in part, perhaps, because certain aspects of the problem have been overlooked, particularly the importance of within-host infection dynamics. Existing models have assumed essentially uniform behavior for all infections, other than differences in growth and/or transmission resulting from fitness costs [20-22, 29]. However, it is known that dynamics of infection vary, for instance, as a result of acquired immunity [94, 96], and that competition can affect different strains unequally depending on the order and timing of introduction [27], as well as the inoculum size for each strain [25]. All of these aspects have the potential to influence the fate of a newly emerged drug-resistant strain; for example, a resistant strain may have an advantage early on if it is not recognized by acquired immunity in the host population, but being rare

may also impose a competitive disadvantage if it frequently results in resistant parasites being introduced later or in smaller numbers than sensitive parasites. Within-host dynamics are the central link between transmission intensity and the spread of drug resistance (Figure 4.1); other relevant factors, including mixed-strain infections, antimalarial drug use, and acquired immunity, influence the spread of resistance only via within-host dynamics. These other factors, in turn, are not independent, but are influenced directly and indirectly by feedback loops that generally involve within-host dynamics (an example of such a feedback loop is the effect of within-host dynamics on the frequency of resistance in the parasite population, which in turn determines the frequency and composition of mixed-strain infections, which affect within-host dynamics). Thus, a model that does not include within-host dynamics, and allow these dynamics to respond to changing conditions, will likely fail to capture relationships that play an important part in the link between transmission intensity and the spread of resistance.

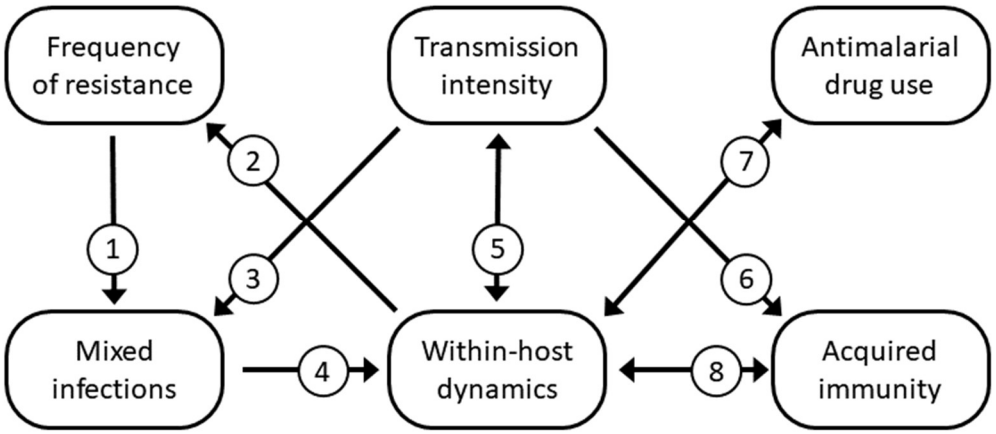

Figure 4.1 Within-host dynamics are the central link between transmission intensity and the frequency of drug resistance. Other factors, including mixed-strain infections, antimalarial drug use, and acquired immunity, shape within-host dynamics but are also subject to numerous feedback loops. Each numbered arrow indicates a causal link between two factors; a brief explanation of each link follows.

(1) The frequency of mixed infections depends on the frequencies of sensitive and resistant strains in the population

(2) The frequency of resistance is determined by relative transmission success of sensitive and resistant parasites, which depends on within-host dynamics

(3) The frequency of mixed (sensitive + resistant) infections increases with transmission intensity

(4) The presence of two strains affects within-host dynamics (e.g. via competition for resources and/or overlapping immune responses)

(5) Transmission intensity affects within-host dynamics by introducing parasites to each host more often; within-host dynamics govern transmission of parasites and thus affect transmission intensity

(6) Acquired immunity develops more rapidly as transmission intensity increases

(7) Within-host dynamics affect immunity by changing how much stimulation the immune system receives; adaptive immunity affects within-host dynamics by reducing proliferation of parasites

(8) Within-host dynamics may determine antimalarial drug use by causing symptoms; antimalarial drugs alter within-host dynamics by eliminating sensitive parasites

The aim of this paper is to explore the complicated relationship between transmission intensity and the evolution of drug resistance in *P. falciparum* using a mathematical model that captures the complex network of factors illustrated in Figure 4.1. Because within-host dynamics appear to be instrumental in determining the success of drug-resistant parasites, and because those dynamics are themselves subject to feedback loops involving several other factors, we felt it was vital to construct a model which allowed for bidirectional feedback between within-host (infection) dynamics and between-host (transmission) dynamics. We therefore constructed a nested individual-based model which describes dynamics on within- and between-host scales and allows these dynamics to interact in virtually all of the ways shown in Figure 4.1.

4.2 Methods

We use a nested model of parasite population dynamics: a model of within-host dynamics embedded into another model that simulates parasite transmission between humans and mosquitoes. Essentially, the model tracks a population of humans, a population of mosquitoes, and the parasites that circulate among them.

Infections in mosquitoes are tracked over time while the dynamics of infection in each human host are modeled using ordinary differential equations. The model simulates within-host dynamics in 24-hour increments interspersed with daily transmission of parasites between humans and mosquitoes; any new parasites that are introduced to a human host are incorporated into the population of parasites tracked by the within-host model. The general structure of the full model is illustrated in Figure 4.2.

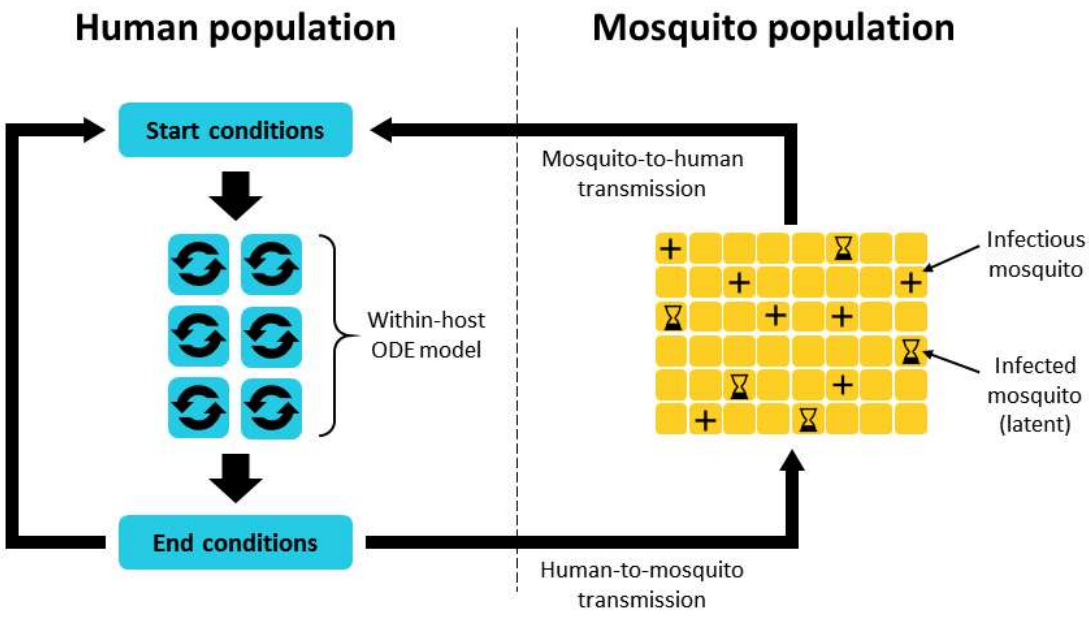

Figure 4.2 Overall structure of the full nested model. Parasites are continually transmitted from humans to mosquitoes and vice versa; dynamics of infections in humans are modeled using a system of ordinary differential equations (ODEs) while infections in mosquitoes are tracked as they progress through a latent period and become infectious. The within-host model tracks infection dynamics over 24-hour intervals punctuated by daily 'contact' between humans and mosquitoes, during which transmission of parasites occurs. Once

parasites are transmitted from a mosquito to a human, their population dynamics are governed by the within-host model.

The model is designed to explore questions related to the evolution of drug resistance; therefore, it actually describes the dynamics of two populations of parasites: drug-sensitive and drug-resistant. For simplicity, we call these populations strains. The actual structure of the parasite population – i.e., the variation within and between strains – is specified by a set of model parameters since it determines the overlap between adaptive immune responses to different strains.

We now give an overview of the within-host model, the between-host (transmission) model, and a few other important aspects. More details, as well as the R code for the model, can be found in the Appendix.

Within-host model

The within-host model consists of a system of ordinary differential equations (ODEs) that describe the dynamics of infection for two parasite strains (sensitive and resistant, denoted strain 1 and strain 2, respectively). The dynamics of the following components are described:

- Uninfected red blood cells (RBCs) (X)
- Infected RBCs of each strain (Y_1, Y_2)
- Merozoites of each strain (S_1, S_2)
- Gametocytes of each strain (G_1, G_2)

- Adaptive immunity to each strain (I_1, I_2)
- Innate immunity (Z)

Below are the ordinary differential equations for the within-host model. Subscripts i and j are used to indicate strain-specific variables and parameters (if $i = 1$ then $j = 2$, and vice versa). The definitions of all parameters in Equations 4.1 - 4.7 are given in Table 4.1 (parameter values can be found in the Appendix) and Figure 4.3 shows a compartment-style schematic of the within-host model.

$$\frac{dX}{dt} = B - \alpha_X X - \beta X(S_i + S_j) \quad \text{(Eq. 4.1)}$$

$$\frac{dY_i}{dt} = \beta X S_i - \left(\frac{1}{1-e_i}\right)\alpha_Y Y_i - \gamma Y_i - \delta_Z Z Y_i - \delta_I\left(I_i + \omega_j I_j\right) Y_i \quad \text{(Eq. 4.2)}$$

$$\frac{dS_i}{dt} = R\alpha_Y(1-\varphi_i)Y_i - \alpha_S S_i - \beta X S_i - \delta_Z Z S_i - \delta_I\left(I_i + \omega_j I_j\right) S_i \quad \text{(Eq. 4.3)}$$

$$\frac{dG_i}{dt} = \gamma Y_i - \alpha_G G_i - \delta_Z Z G_i \quad \text{(Eq. 4.4)}$$

$$\frac{dZ}{dt} = \zeta(1-Z)(S_i + S_j) - \alpha_Z Z \quad \text{(Eq. 4.5)}$$

$$\frac{dI_i}{dt} = \sigma I_i\left(\frac{S_i + \eta S_j}{\theta + S_i + \eta S_j}\right) - \max\left(H_i, H_j\right) * \psi J_i I_i\left(1 - \left(\frac{C_i^k}{C_i^k + A^k}\right)\right) - \alpha_I J_i\left(1 - \max\left(H_i, \eta H_j\right)\right) I_i \quad \text{(Eq. 4.6)}$$

$$\frac{dC_i}{dt} = H_i + \nu H_j \quad \text{(Eq. 4.7)}$$

Table 4.1 Definitions of parameters in the within-host model. Parameter values can be found in the Appendix.

Parameter	Definition
B	Rate of production of new RBCs
α_X	Death rate of uninfected RBCs

β	Rate of infection of RBCs by merozoites
e_i	Increase in death rate due to antimalarial drug treatment, if applicable ($e_i = \varepsilon_i$ if being treated; otherwise $e_i = 0$)
ε_i	Efficacy of antimalarial drug treatment against strain i
α_Y	Death rate of infected RBCs
γ	Gametocyte formation rate
δ_Z	Rate of killing by innate immunity
δ_I	Rate of killing by adaptive immunity
ω_j	Proportion of <u>current</u> strain i antigens recognized by adaptive immunity to strain j
R	Number of merozoites produced per infected RBC
φ_i	Fitness cost ($0 \leq \varphi_i \leq 1$)
α_S	Death rate of merozoites
α_G	Death rate of gametocytes
ζ	Innate immunity activation rate
α_Z	Innate immunity inactivation rate
σ	Maximum growth rate of adaptive immunity
η	Overlap in fixed (non-variant) antigens between strains
θ	Merozoite density at which growth rate of adaptive immunity is $\sigma/2$
H_i	Infection status indicator for strain i ($H_i = 1$ if infected with strain i; otherwise $H_i = 0$)
ψ	Maximum (initial) decay rate of adaptive immunity due to antigenic variation
k	Shape parameter for decay of adaptive immunity due to antigenic variation
A	Shape parameter for decay of adaptive immunity due to antigenic variation

α_I	Decay rate of adaptive immunity in absence of infection
J_i	$J_i = 1$ if $I_i >$ baseline value; otherwise $J_i = 0$
C_i	Amount of exposure to variant antigens of current strain i
ν	Overlap in variant antigens between strains

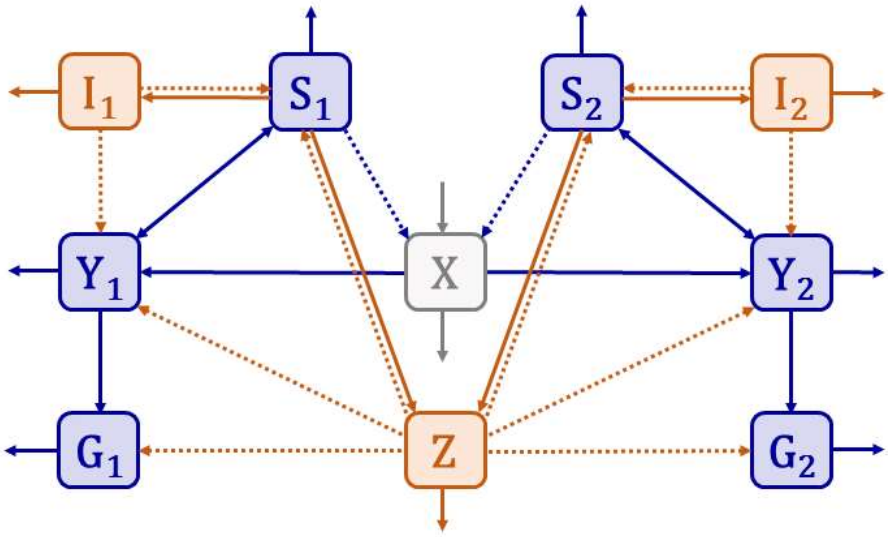

Figure 4.3 Compartment-style schematic of the within-host model. Parasites (infected RBCs, merozoites, gametocytes) and arrows pertaining to parasite replication are shown in blue; immune responses and arrows denoting parasite-immune system interactions are in brown/tan. Solid arrows indicate that one component increases or feeds into another, while dotted arrows indicate that one component reduces another. Strain-specific variables are indicated with subscripts.

The dynamics described by the within-host model boil down to two essential processes: parasite replication and parasite-immune system interactions (shown in Figure 4.3 in blue and brown/tan, respectively). Parasite replication is straightforward: merozoites invade RBCs, turning them into infected RBCs; infected

RBCs either produce more merozoites or differentiate into gametocytes. RBCs are lost during this process, but are continually replaced by new ones. Interactions between parasites and the immune system are more complicated. The model includes two types of immunity: innate and acquired (sometimes called adaptive). Innate immunity acts in a strain-transcending manner and is important for controlling parasite growth during the acute phase of the infection; acquired immunity is at least partly strain-specific (the degree of specificity is determined by the model parameters) and required for eventual clearance of the infection. Both innate and adaptive immune responses are triggered by parasites, and both decay in the absence of continued stimulation; however, the 'on' and 'off' rates for innate immunity are higher, resulting in a fast, self-limiting response. Acquired immunity takes longer to develop, but decays very slowly, and helps to limit parasite growth in subsequent infections. However, the dynamics of acquired immunity are complicated by antigenic variation, which is discussed in more detail below.

Antigenic variation is an evolved strategy for evasion of acquired immunity. The parasite has several dozen "variants" of an immunodominant surface protein, but only expresses one variant at a time; when the immune system learns to recognize the current variant, the parasite switches to a different one [97, 98]. Antigenic variation therefore interferes with recognition and killing by the adaptive immune system and helps to prolong the infection, which may not be cleared for several months (presumably when the variant repertoire has been exhausted). Thus, antigenic variation plays a key role in the dynamics of *P. falciparum* infections; however, explicitly modeling the process is impractical. Instead, our model

implicitly incorporates antigenic variation by describing its effects on the dynamics of infection. Each switch to a novel variant interferes with recognition by the adaptive immune system, which makes the immune response less effective; this loss of effectiveness is mathematically indistinguishable from a loss of immune effectors. We therefore incorporate antigenic variation as a second decay term in the equations for adaptive immunity, which diminishes with the progress of the infection, since the variant repertoire is finite and eventually runs out.

Between-host model

Unlike the within-host model, which is governed by deterministic equations, the between-host model is stochastic; as a result, multiple simulations with the same parameters and starting conditions will tend to yield similar but not identical results – unless the conditions favor highly divergent trajectories, such as scenarios that tip either toward extinction or toward epidemic spread.

The between-host model describes human-to-mosquito and mosquito-to-human transmission of parasites. Each human host is assigned to be bitten by a randomly chosen set of mosquitoes each day (the number of mosquitoes is based on the transmission intensity); these mosquitoes can infect and/or become infected by the human host when they feed. The probability of a mosquito becoming infected is determined by the total gametocyte density in the human host, using a gametocytemia-infectivity function originally described by Churcher et al. [99]. If the mosquito is infected, the number of gametocytes of each strain picked up is determined by the individual gametocyte densities of drug-sensitive and drug-

resistant parasites. If parasites are acquired, there is a latent period (10 days in the model) before the infection reaches the salivary glands and the mosquito becomes infectious.

An infectious mosquito has a constant probability of introducing parasites to the human host it feeds on. If this does occur, a fixed number of sporozoites is introduced; how many of these are drug-sensitive and drug-resistant depends on the ratio of the two strains in the pool of gametocytes the mosquito originally acquired. Once sporozoites are transmitted to the human host, the infection goes through a latent period (i.e. the liver stage), which ends with merozoites being released into the bloodstream, at which point the parasites become subject to the within-host model.

Parasite population structure

An aspect of the model with particularly broad ramifications is the diversity and structure of the parasite population, particularly as it pertains to recognition by the adaptive immune system. There are two important parameters to consider: differences within each strain, and differences between strains. If different isolates of a given strain have very few antigens in common, then exposure to one will offer little protection against another, and it may take many exposures to build up to an effective level of immunity. Thus, within-strain variation determines how well past exposures protect against future ones. Differences between strains, on the other hand, determine how much the acquired immune responses to sensitive and resistant parasites overlap. The greater the overlap, the more each suffers from

acquired immunity to the other – including immunity from past infections – which increases the severity of within-host competition between strains.

Within-strain variation reflects the overall diversity of the parasite population, and in *P. falciparum*, genetic diversity is known to be greater in high-transmission settings [11]. Thus, although it is simpler to compare simulations that differ only in transmission intensity or only in diversity, it may be more relevant to compare high-diversity, high-transmission settings with low-diversity, low-transmission ones. Therefore, we present simulation outputs in sets of four – high and low transmission with high and low within-strain variation – to help disentangle the effects of these two factors.

Between-strain variation describes how similar drug-sensitive and drug-resistant parasites are to each other. When drug-resistant parasites emerge locally, on the same genetic background as the drug-sensitive population, between-strain variation will be similar to within-strain variation. In contrast, if drug-resistant parasites are imported from a distant region, they will likely be on a distinct background, making between-strain variation higher than within-strain variation. We thus use high between-strain variation to simulate the introduction of imported drug-resistant parasites, whereas for local emergence of resistance, we make within- and between-strain variation equal. In the Results section, we focus on simulations of locally emerging resistance, since this is more pertinent to the question of why resistance does not evolve locally in high-transmission settings (the results of simulations with 'imported' resistance can be found in the Appendix, Figures A27-A38). Thus, within the Results section, unless noted otherwise,

'diversity' should be taken to mean both within- *and* between-strain diversity, since these will be equal in the case of locally emerging resistance.

Antimalarial drug treatment

The model allows for considerable flexibility in the 'rules' governing use of antimalarial drugs. Treatment can be made conditional on parasite density exceeding a specified threshold: a high threshold to simulate restriction of treatment to symptomatic infections, a lower threshold to simulate treatment of infections that are detectable by standard diagnostic methods. If an infection 'qualifies' for treatment, there is a fixed probability that antimalarial drug treatment will be initiated (this probability is specified in the model parameters). If started, drug treatment is maintained for a fixed duration (simulating a standard course of treatment), regardless of whether parasite clearance is achieved.

Simulations

We ran a total of 112 simulations with varying transmission intensity, within- and between-strain variation, antimalarial drug use and fitness costs of resistance; the parameters and output for all simulations are available in the Appendix.

All simulations were run with 400 human hosts and 12,000 mosquitoes for a duration of 8,000 days. The drug-sensitive strain was introduced to the human population at an initial prevalence of 10% and the simulation was run for 3,000 days to allow the system to reach equilibrium before introducing the drug-resistant

strain at a prevalence of 2% (this number was chosen to avoid a high incidence of stochastic extinction across all settings). Use of antimalarial drugs, where included, was initiated at the beginning of the simulation, before the introduction of the resistant strain.

4.3 Results

We first give an overview of the general behavior of the model, focusing on the relationships outlined in Figure 4.1.

Within-host dynamics

Figure 4.4 shows the within-host dynamics of infection with a single strain, in the absence of prior immunity and antimalarial drugs. The dynamics of infected red blood cells (top left) are qualitatively similar to those observed in malariotherapy patients (example shown in [100]), which are still one of the best sources of data on malaria infection dynamics in naïve hosts. Gametocyte density (top right), innate immunity (bottom left), and acquired immunity (bottom right) all more or less track the dynamics of infected red blood cells; note that gametocytes persist for several weeks following clearance of asexual parasites, and adaptive immunity fluctuates (a result of the way antigenic variation is built into the model) but eventually stabilizes at a high level that serves to reduce parasite growth in future infections.

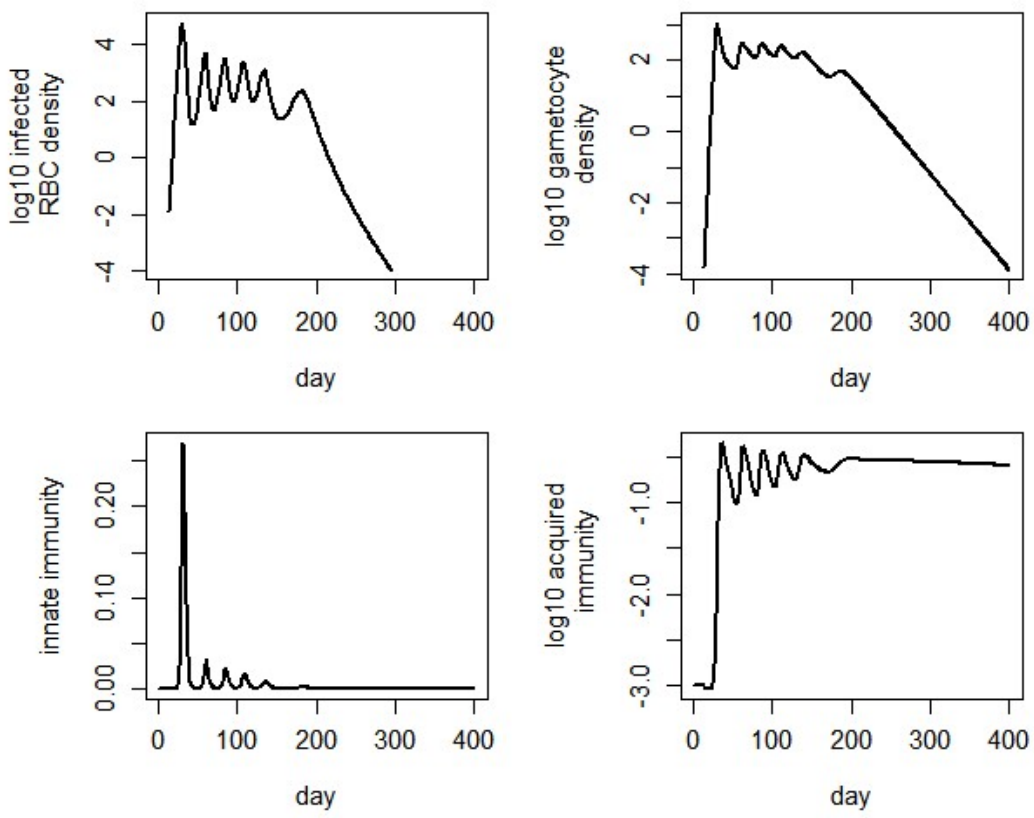

Figure 4.4 Dynamics of infected red blood cells, gametocytes, innate immunity and adaptive immunity. Dynamics are for a single strain in a host with no preexisting immunity.

Figure 4.5 shows the within-host dynamics of two strains, introduced either 20 or 100 days apart – again, no prior immunity or antimalarial treatment – with either high or low overlap among the antigens of the two strains (the greater the overlap, the more each strain is affected by adaptive immunity to the other). With high overlap, when the second strain is introduced 20 days after the first, it immediately goes extinct, whereas when the strains are introduced 100 days apart, the second strain overtakes the first. This illustrates the sensitivity of within-host dynamics to factors – such as the timing of introduction of different strains – that have often been overlooked in the past. In contrast, with low overlap between the

strains, the second strain is able to overtake the first in both cases (a 20-day gap and a 100-day gap), which demonstrates the benefits of being less affected by the immune response to the resident strain.

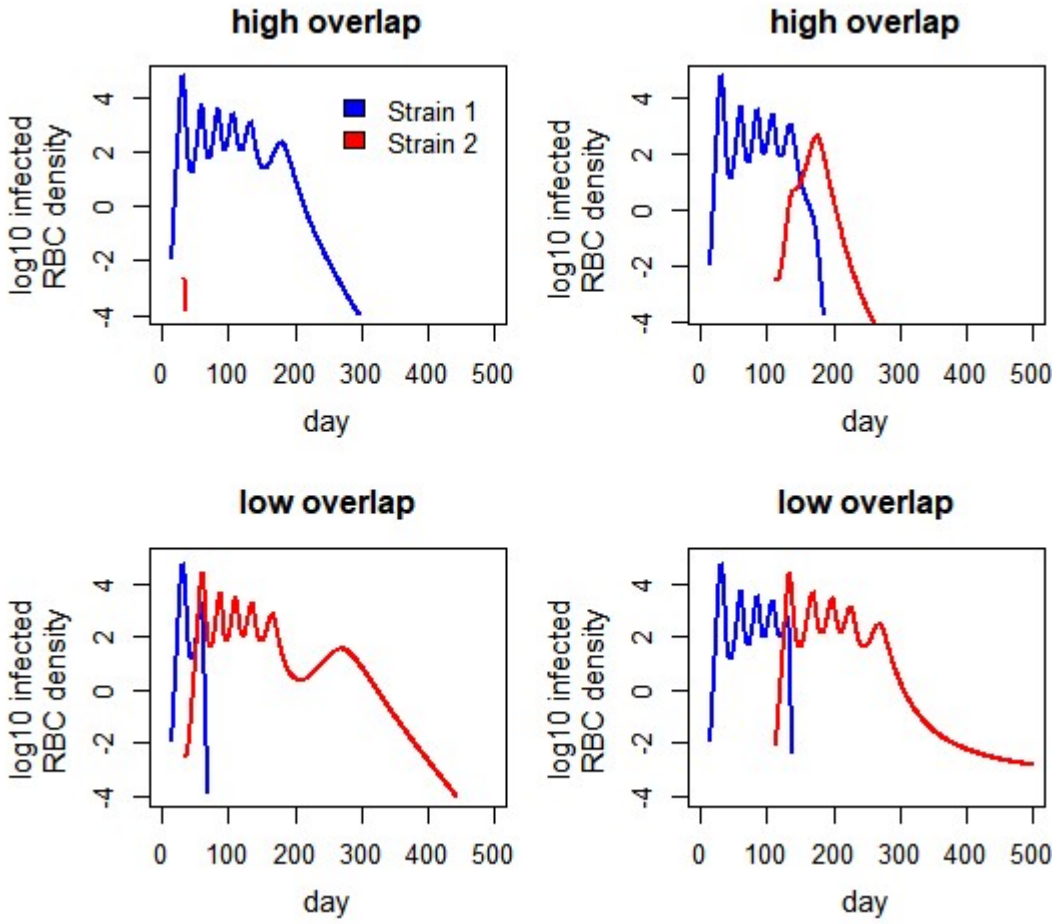

Figure 4.5 Within-host dynamics of two strains. Strains are introduced 20 days apart (left two panels) or 100 days apart (right two panels), with either high or low overlap between antigens of the two strains (top two panels and bottom two panels, respectively).

Epidemiological patterns

Entomological inoculation rate (EIR, the number of potentially infectious mosquito bites per person per year) was estimated for simulations with four different values of b (mean number of mosquito bites per person per day). For simulations with $b = 5, b = 10, b = 15,$ and $b = 20$, respectively, the estimated EIRs were 6.1, 25.3, 47.9, and 72.6 infectious bites per person per year. These values are not constants; EIR depends on the total prevalence of infection in the human population, which can vary both within and between simulations. However, it should be noted that for a two-fold change in biting rate, EIR more than doubles, reflecting the fact that mosquito biting rate affects not only the frequency of contact between humans and mosquitoes, but also the likelihood that any particular mosquito is infectious, since the prevalence of infection among humans increases with transmission intensity as well. This finding is consistent with a well-known feature of the Ross-MacDonald model, in which R_0 is proportional to a^2, where a is the rate of contact between humans and mosquitoes.

Figure 4.6 shows the relationship between transmission intensity and total prevalence of infection. Prevalence increases from slightly over 40% in the lowest-transmission setting (mean of 5 bites per host per day) to over 90% in the highest-transmission setting (mean 20 bites per host per day). These results are consistent with epidemiological observations of the relationship between transmission intensity and infection prevalence [92].

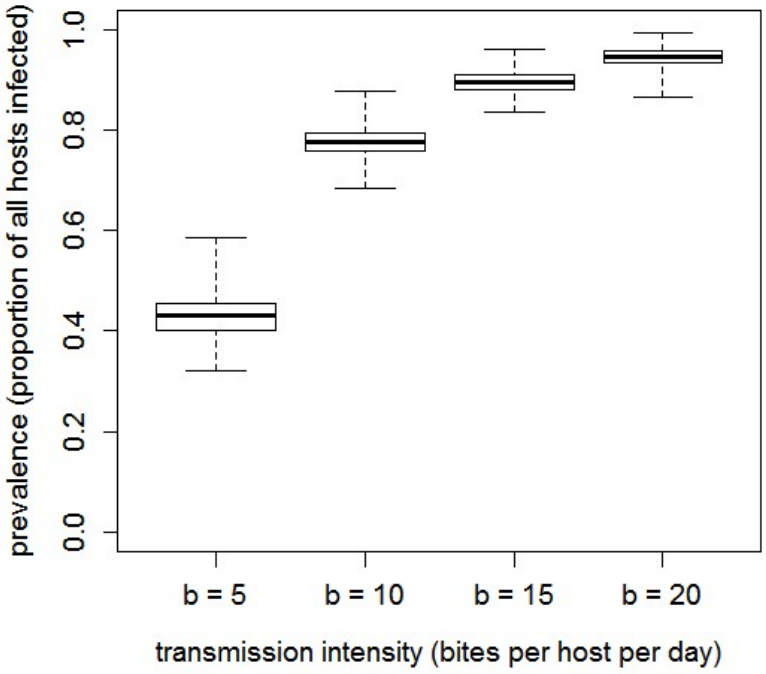

Figure 4.6 Equilibrium prevalence of infection for four different transmission intensities (given as mean number of mosquito bites per host per day). Data shown are daily measurements of prevalence from simulations run at four different transmission intensities.

Figure 4.7 shows the relationship between transmission intensity and the frequency of mixed-strain infections (which, in this context, refers to infections with both drug-sensitive and drug-resistant parasites). The frequency of mixed-strain infections depends on the proportions of the different strains in the population (similar to the frequency of heterozygotes under Hardy-Weinberg assumptions), which, in this case, were roughly equal. The data in Figure 4.7 are consistent with observed correlations between transmission intensity and average multiplicity of infection (number of strains per host) [18].

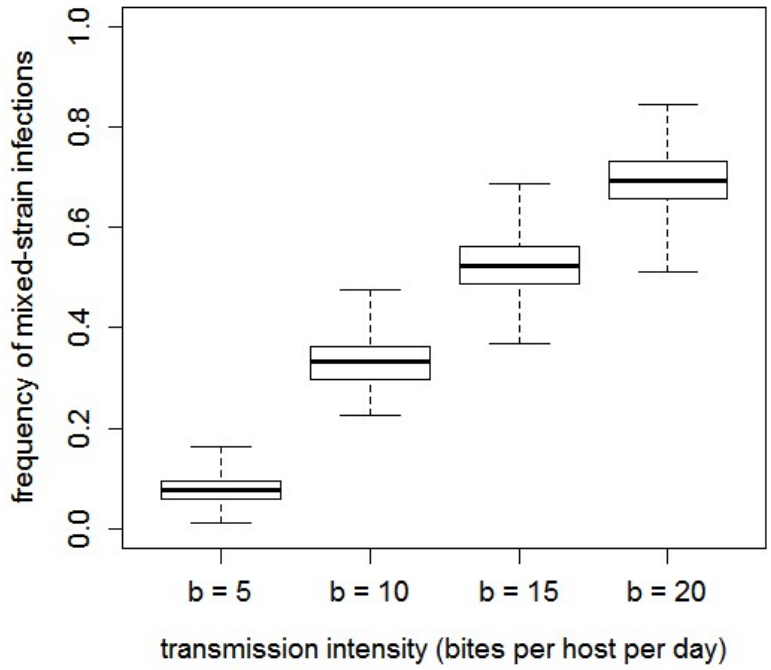

Figure 4.7 Frequency of mixed-strain infections (as a proportion of total infections) increases with transmission intensity. Data shown are daily measurements from simulations run at four different transmission intensities; simulations did not include antimalarial drug use.

Figure 4.8 shows the relationship between age and parasite density for different levels of transmission intensity. In all settings, parasite density decreases with age, but this decrease is more rapid in higher-transmission settings. These results are consistent with observations that immunity develops more rapidly as transmission intensity increases, with clinical immunity to malaria more or less fully developed by five years of age in high-transmission settings [94].

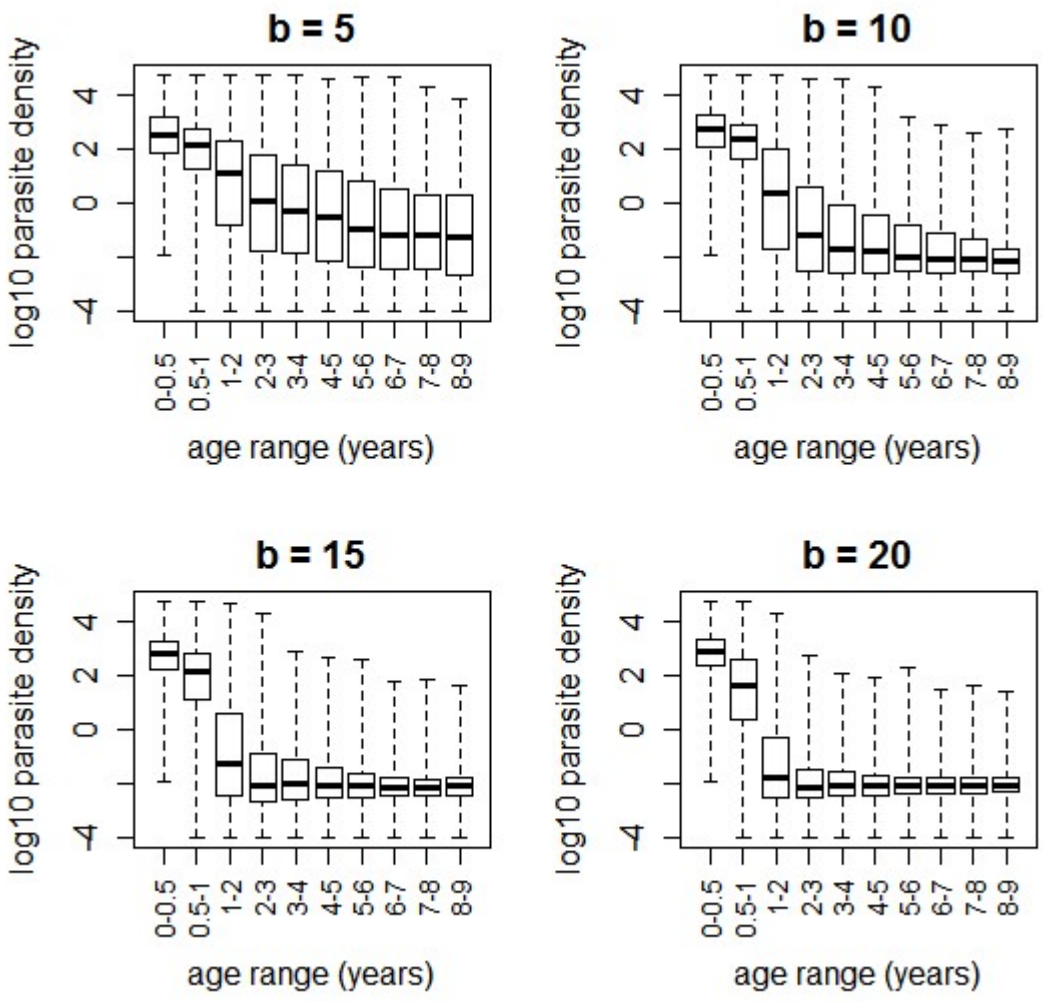

Figure 4.8 Distribution of parasite densities (log_{10}-transformed) for in age groups ranging from 0 to 9 years, for four different levels of transmission intensity (b = number of mosquito bites per person per day).

In some simulations, treatment was made conditional on total parasite density being at or above a certain threshold. Two different thresholds were used: 10 parasites/μL was used to simulate restriction of treatment of infections that could be detected with standard diagnostic methods, while 1000 parasites/μL was used to simulate restriction to symptomatic infections. Due to more rapid

acquisition of immunity in higher-transmission settings (Fig. 4.8), the fraction of infections meeting either of these threshold decreased with transmission intensity, as shown in Figure 4.9.

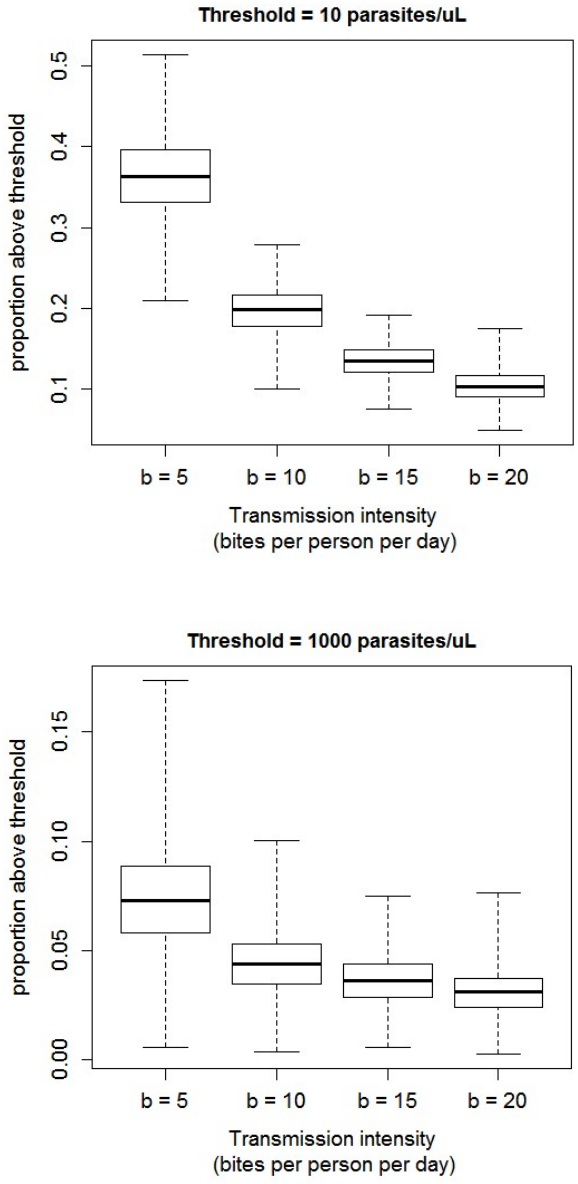

Figure 4.9 The fraction of infections with total parasite density $\geq$ 10 parasites/μL and $\geq$ 1000 parasites/μL for four levels of transmission intensity.

Finally, we show within-host competition appears to exacerbate fitness differences between strains. The top panel of Figure 4.10 shows that, in the absence of a fitness cost, the densities of sensitive and resistant parasites are equal on average, in both single- and mixed-strain infections. In contrast, when the resistant strain suffers a fitness cost, the difference in the average densities of sensitive and resistant parasites is greater in mixed infections than in single infections (Figure 4.10, bottom panel), indicating that the difference in fitness between the two strains is magnified when both infect the same host.

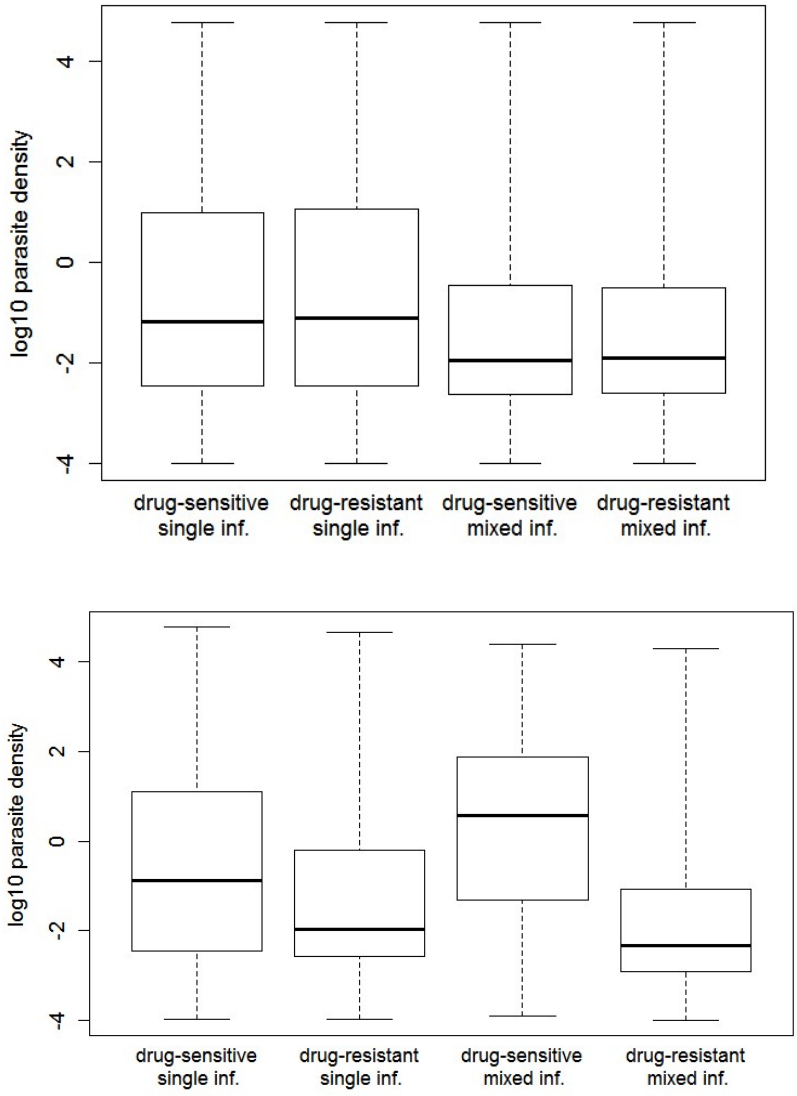

Figure 4.10 Densities of sensitive and resistant parasites in single and mixed infections, with and without a fitness cost of resistance (top and bottom panels, respectively).

Simulation results

In order to understand how selection affects the spread of resistant parasites at the population level, it is helpful to know what happens in the absence of selection (with no antimalarial drug use). As shown in Figure 4.11, drug-resistant strains introduced into high-transmission settings go extinct almost immediately. In

a low-transmission setting with low diversity, the resistant strain persists at low frequency for several years but eventually goes extinct, whereas in a low-transmission setting with high diversity, the resistant strain increases in frequency despite not being under selection from antimalarial drugs. The latter may be due to the fact that, with higher between-strain variation, there is less cross-reactivity between immune responses to sensitive and resistant parasites, and therefore within-host competition (specifically, immune-mediated apparent competition) is somewhat weaker.

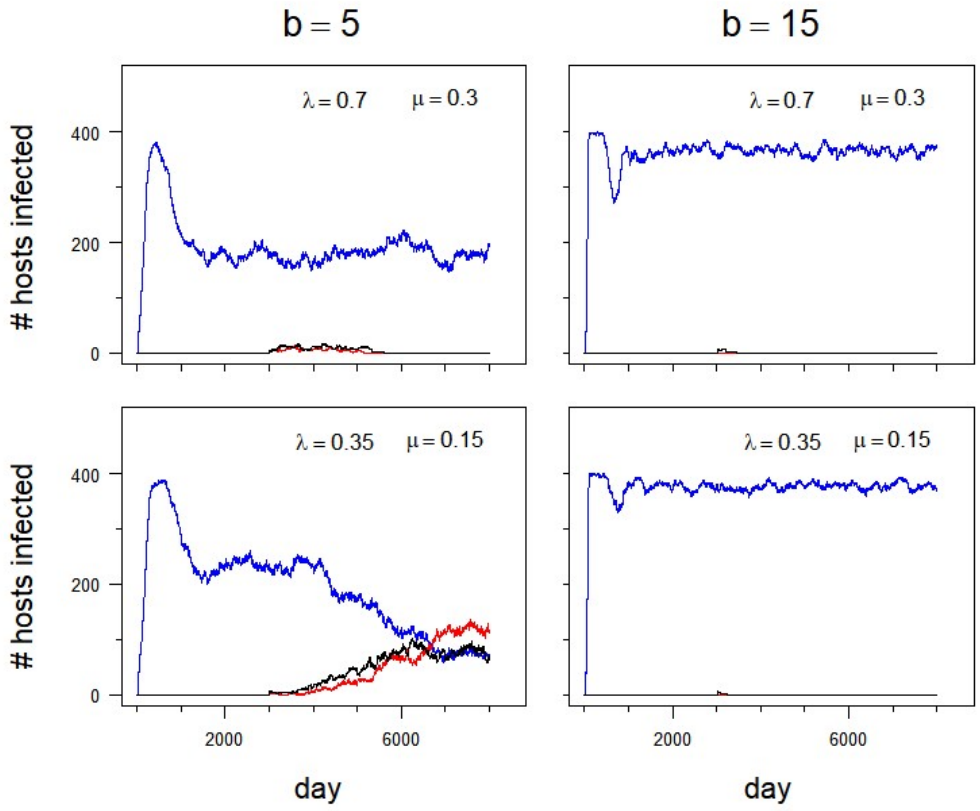

Figure 4.11 Prevalence of sensitive, resistant, and mixed-strain infections (blue, red, and black, respectively) over time in simulations with no antimalarial drug use. Simulation parameters: $\varphi_2 = 0$, $p_{TR} = 0$.

We next examine the spread of resistance when treatment is restricted to infections with parasite density above a set threshold (either 10 or 1,000 parasites/μL). In the absence of a fitness cost of resistance, the resistant strain goes to fixation in all settings, resulting in extinction of the drug-sensitive strain (data in the Appendix). However, when the resistant strain suffers a cost, the results are more variable. For example, Figure 4.12 shows the results of simulations with a

treatment threshold of 1,000 parasites/μL and a fitness cost of resistance (implemented as a 10% reduction in growth rate).

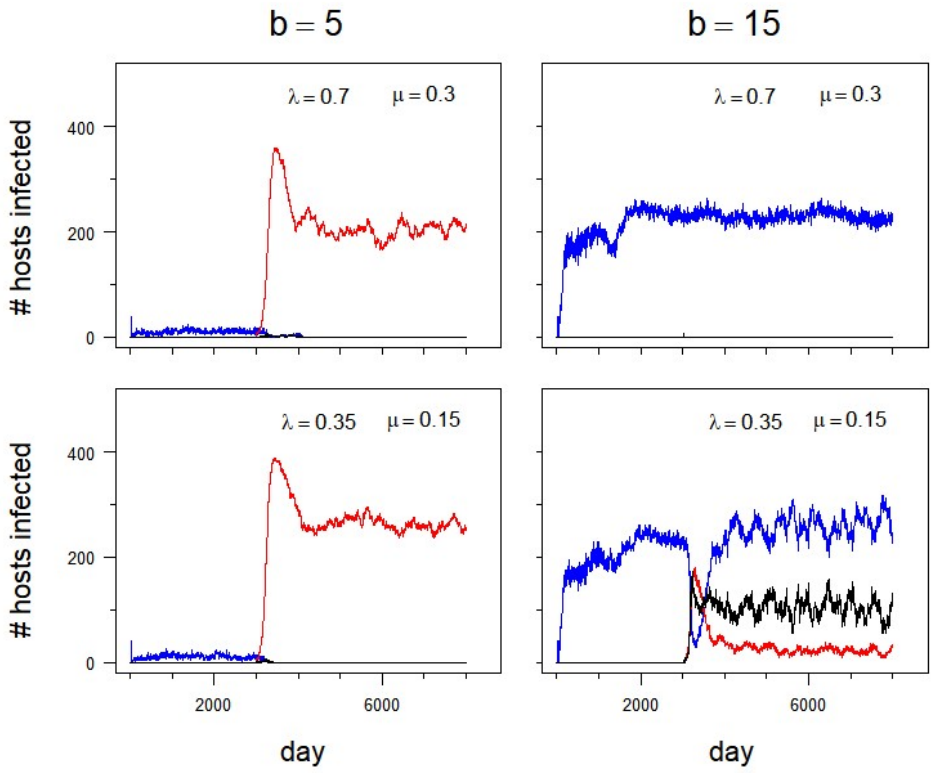

Figure 4.12 Prevalence of sensitive, resistant, and mixed-strain infections (blue, red, and black, respectively) over time in simulations with treatment of symptomatic infections (total parasite density above 1,000 parasites/μL) and a 10% fitness cost of resistance. Simulation parameters: $\varphi_2 = 0.1,\ Y_{TR} = 1000,\ p_{TR} = 0.5$.

These results show that resistance may be favored in low-transmission settings (compared to high-transmission settings) when antimalarial drug use is restricted to infections with parasite density above a threshold. However, this is

probably due to differences in the strength of selection rather than within-host competition between sensitive and resistance parasites.

In order to examine the impact of within-host competition in isolation, we consider equal treatment rates across simulations (making all infected hosts equally likely to be treated). Figure 4.13 shows the outcomes of simulations with four sets of conditions: high and low treatment with no fitness cost of resistance, and high and low treatment with a fitness cost (in the simulations with a cost of resistance, the rates of treatment are increases to compensate for strong selection against the resistance strain).

With lower rates of treatment and no fitness cost (first column of Figure 4.13), resistance spreads at low transmission regardless of parasite diversity, whereas at high transmission, resistance immediately goes extinct in the low-diversity setting but spreads rapidly in the high-diversity setting. In fact, in the high-transmission, high-diversity setting, resistance spreads more rapidly than in the low-transmission settings. With higher rates of treatment, resistance spreads to fixation or near-fixation in all settings (second column), and again, the frequency of resistance increases faster in high-transmission settings.

With a fitness cost of resistance and lower rates of antimalarial drug use, resistance spreads to fixation in the low-transmission settings but rapidly goes extinct in the high-transmission settings (third column). With a higher treatment rate (fourth column), resistance quickly reaches fixation in the low-transmission settings, while in the high-transmission, low-diversity setting, resistance immediately goes extinct; in the high-transmission, high-diversity setting, a quasi-

equilibrium is reached which is dominated by the drug-resistant strain but leaves 5-10% of hosts infected with only the drug-sensitive strain. This could be due to exacerbation of the fitness cost of resistance in mixed-strain infections, which might allow the resistant strain to spread until the additional cost resulting from a higher frequency of mixed-strain infections balances the positive selection from antimalarial drug use, at which point the population may reach a locally stable quasi-equilibrium.

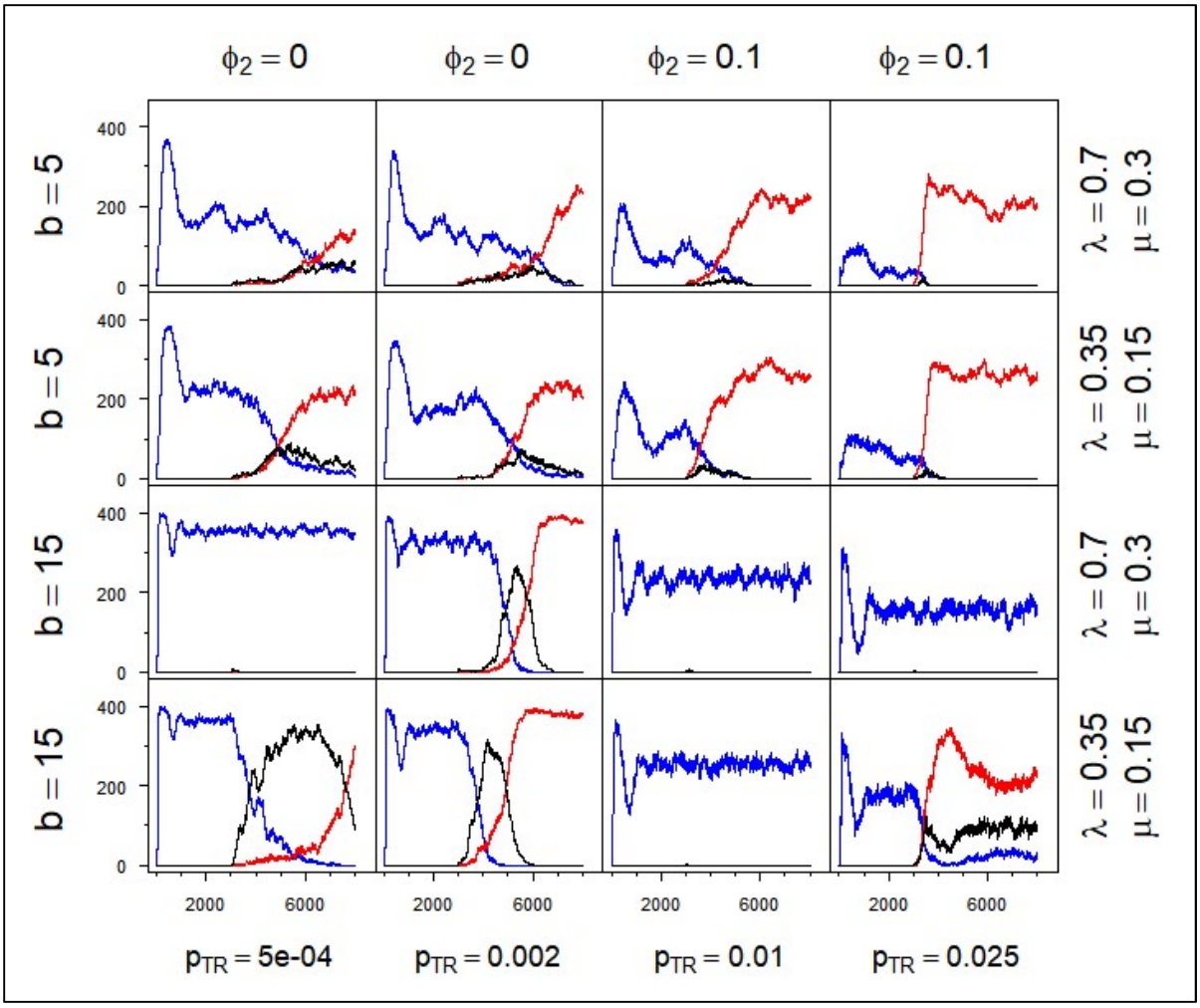

Figure 4.13 Prevalence of sensitive, resistant, and mixed-strain infections (blue, red, and black, respectively) over time in simulations with no threshold for treatment. Simulation parameters $(b, \varphi_2, p_{TR}, \lambda, \mu)$ are shown for each row and column.

4.4 Discussion

One of the most compelling pieces of evidence that within-host competition can suppress the spread of resistance comes from the results of simulations with no selection at all – no cost of resistance, no antimalarial drug use – where the only

forces at work are ecological ones. In a low-transmission, low-diversity setting, a resistant strain introduced at low frequency is maintained in the population for several years before going extinct, whereas at high transmission intensity with comparable diversity, a resistant strain introduced in the same manner goes extinct almost immediately. This suggests that the resistant strain struggles to invade when faced with ubiquitous competition from drug-sensitive parasites. Experiments with the rodent malaria parasite *Plasmodium chabaudi* have shown that within-host competition between strains heavily favors whichever strain infects the host first [27], so if a resistant strain is introduced into a population where virtually every host is infected with sensitive parasites, it may be disproportionately affected by this 'asymmetric competition' even though it is not intrinsically less fit than its competitors.

These results suggest that within-host competition may impede the spread of resistance even in the absence of a fitness cost of resistance. Other theoretical studies have concluded that within-host competition would slow the evolution of resistance in high-transmission settings, but these results are contingent on a fitness cost of resistance being exacerbated in mixed-strain infections [22, 29]. This does occur in the simulations where resistant parasites are assigned a fitness cost (see Appendix), and likely contributes to the suppression of drug resistance in high-transmission settings, but does not appear to be intrinsic to the effects of within-host competition on the spread of resistance.

Simulations where the rate of antimalarial drug use is held constant also show resistance emerging more readily in low-transmission settings – more readily,

but not necessarily more quickly. Where the resistant strain doesn't go extinct, it actually spreads more rapidly in high-transmission settings than in low-transmission settings with comparable levels of diversity. This could be due to so-called 'competitive release' of drug-resistant parasites, in which the removal of drug-sensitive competitors by antimalarial drugs alleviates competitive suppression and allows drug-resistant parasites to expand within the host. It is possible that drug-resistant parasites are at high risk of extinction when first introduced, but if selection is strong enough to avoid extinction, then the gains from competitive release outweigh the losses from competitive suppression, which results in the resistant strain actually spreading faster than in low-transmission settings. This would suggest a 'tipping point' in high-transmission settings, where it takes a high level of antimalarial drug use to overcome within-host competitive suppression of resistant parasites, but if this is achieved, then the rate of evolution of resistance is very high.

Across the board, resistance emerges more readily and spreads more rapidly in high-diversity settings. This effect is even more pronounced in simulations with 'imported' resistance, where between-strain diversity is greater than within-strain diversity (results in the Appendix). This suggests a possible explanation for the rapid spread of Southeast Asian-origin drug-resistant parasites across sub-Saharan Africa, where resistance seldom developed locally. If imported drug-resistant parasites are sufficiently antigenically distinct from local parasites, they will suffer less from cross-reactive immune responses than would a resistant strain derived

from the local parasite population, and as a result, may be able to spread where 'local resistance' cannot.

Taken together, the results presented here suggest that within-host competition, by itself, can inhibit the spread of resistance in high-transmission settings. It appears this inhibition might work mainly by increasing the odds of extinction when resistance is rare, rather than decreasing the rate of spread; indeed, some results suggest that resistance might actually spread more rapidly in high-transmission settings if it can avoid extinction in the early phase. Results also hint that resistance may invade more easily when drug-resistant parasites are dissimilar to the local, drug-sensitive population, which may have some bearing on the global spread of a handful of drug-resistant alleles.

Overall, the results here suggest that simple ecological competition might be an important force in the evolution of drug resistance in *P. falciparum* (possibly acting in conjunction with other forces, such as differences in selection pressure). We also note the important distinction between emergence of resistance, which is a function of opportunity and may be hindered by competition, and spread of resistance, which is a function of selection and may, in some cases, be aided by competitive release. Thus, understanding and managing the evolution of drug resistance in *P. falciparum* can best be achieved by considering the impacts of selection pressure and ecological competition together; future work may explore the combined effects of these factors to identify the optimal strategies for resistance prevention and containment across a range of transmission settings.

Chapter 5: Discussion

It was and is my hope that the work presented in this dissertation might fill some key gaps in the current understanding of within-host competition and its effects on the evolution of drug resistance in *Plasmodium falciparum*. Specifically, the aims were to address deficiencies in three areas, as follows:

(1) Empirical evidence for within-host competition in *P. falciparum*

(2) Empirical evidence (in *P. falciparum*) for competitive release of resistant parasites following treatment of mixed infections

(3) Understanding of the relationship between transmission intensity and evolution of resistance in *P. falciparum* and the role of within-host dynamics, including competition

I believe that the research summarized in Chapters 2-4 represents forward progress in all of these areas, but there are, as always, caveats and further questions to be considered. A brief summary and discussion of the findings from Chapters 2, 3, and 4 follows.

5.1 Discussion of Chapter 2: Within-host competition in *Plasmodium falciparum*

The study described in Chapter 2 was motivated by the fact that, although there was a large body of evidence for within-host competition in the rodent malaria model *Plasmodium chabaudi*, the evidence for competition in *P. falciparum* was extremely limited. Bruce et al. analyzed longitudinal data on the dynamics of mixed-species infections and found evidence for density-dependent regulation of

multiple species, which suggested within-host interspecific competition [48]; Harrington et al. found increased parasitemia and higher frequencies of drug-resistant genotypes in the placentas of women who had received antimalarial drugs during pregnancy, compared with women who had not, which was suggestive of competitive release and facilitation of drug-resistant parasites [49]. However, in both studies, the support for competition and/or competitive release was indirect and of uncertain relevance to *P. falciparum* in the general population. Surprisingly, the most straightforward studies of competition (comparing parasite densities of single- and mixed-strain infections) and competitive release (comparing pre- and post-treatment densities of drug-sensitive and drug-resistant parasites) had never been done; and yet, there was a growing body of literature predicated on the assumption that within-host competition and competitive release would occur in *P. falciparum.*

As described in Chapter 2, we tackled the question of whether within-host competition occurs in *P. falciparum* by measuring the densities of drug-sensitive and drug-resistant parasites in (naturally acquired) single- and mixed-strain infections. We found that the total parasite density of mixed-strain infections was no greater than single-strain infections, suggesting that different strains were indeed competing for a shared niche within the host, and also found that the densities of drug-sensitive and drug-resistant parasites were reduced in mixed infections, suggesting competitive suppression of individual strains. The findings, for the most part, were highly consistent with observations of within-host competition in the *Plasmodium chabaudi* model.

An important caveat regarding these results is that the study was – necessarily – an observational one without the experimental manipulation needed to rigorously demonstrate competition. (To do the experiment properly requires intentionally infecting hosts with malaria parasites, which is allowed in mice, but not in people.) The *P. falciparum* infections examined were naturally acquired infections, and therefore the influence of confounding factors, such as acquired immunity, cannot be completely ruled out. The fact that the findings were based on a large number of infections (1,341 in total) and were replicated in three populations from different countries gives us a high degree of confidence that the results themselves are not spurious; however, without the ability to control for external factors, the underlying mechanisms cannot be pinned down with a high degree of certainty.

Another limitation of the work in Chapter 2 is that all of the samples came from children (up to 5 years old in Ghana and Tanzania and up to 9 years old in Angola). Many studies relating to the treatment of malaria are focused on young children because they comprise the population that is at highest risk for severe disease and death, especially in Africa. However, in this case, it means that our observations reflect within-host dynamics in hosts that have less immunity than the rest of the population. Acquired immunity to *P. falciparum* is thought to be at least partly strain-specific, and increases with age [94]; so it is possible that regulation of parasite growth may be more strain-specific in older children and adults, resulting in weaker competition between strains. Thus, it is currently not known whether

competition is the rule (occurring in all hosts) or the exception (occurring only in children and others with limited immunity).

In the rodent parasite *Plasmodium chabaudi*, within-host competition has been shown to exacerbate differences in performance between strains, including between drug-sensitive and drug-resistant parasites [27]. We found strong evidence for a fitness cost of chloroquine resistance in *P. falciparum,* both in reduced densities of resistant parasites compared to drug-sensitive ones, and in the rapid decline of chloroquine resistance in Ghana following the retirement of chloroquine as a first-line treatment for malaria (similar declines had previously been observed in numerous countries [53, 64, 101, 102]). However, in a potentially important divergence from the rodent model, we found little evidence that this fitness cost was exacerbated by competition in mixed-strain infections – at least that we could detect, since we were unable to account for cases where either strain was present but below the detection threshold of the assay used. Thus, the assumptions that others have sometimes made, that fitness costs of resistance would be magnified in mixed infections, or even limited to mixed infections, may not be justified [22, 88]. This may be important, because if the cost of resistance is amplified by within-host competition, then the conclusion that competition slows the spread of resistance is trivial, since it increases the strength of selection against resistant parasites. The notion that within-host competition alone, absent any competition-dependent effects on fitness or even any fitness differences whatsoever, has not received much consideration.

5.2 Discussion of Chapter 3: Competitive release of drug-resistant parasites following treatment

Similar to within-host competition, there was ample evidence for competitive release in *Plasmodium chabaudi* [19, 41, 42], but extremely limited evidence for similar dynamics in *P. falciparum* [49]. Even so, there was a growing body of literature predicated on the idea that competitive release would also occur in *P. falciparum*, which highlighted the need for empirical studies. We therefore took the basic approach of examining dynamics of drug-sensitive and drug-resistant parasites in a population of hosts, some of whom were treated with antimalarial drugs while others were not. Despite considerable variation in the dynamics of both treated and untreated infections, we observed a negative correlation between the changes in drug-sensitive and drug-resistant alleles following treatment – meaning that when the sensitive alleles went down, the resistant alleles tended to go up, and vice versa – which was not observed in the infections that were not treated. This is consistent with competitive release, although the decrease in sensitive parasites accompanied by increase in resistant that defines the phenomenon was actually observed in only a minority of treated infections, even when analysis was restricted to cases where both sensitive and resistant alleles were present before treatment. One reason for this may be that, as was seen when analysis was stratified by the interval separating pre- and post-treatment samples, the total parasite density was markedly decreased following treatment – a hundred-fold, on average. Thus, when sensitive and resistant populations are both reduced, the actual definition of

competitive release is not met. It seems likely that this decrease in both populations may be the result of incomplete resistant to the drug, which was sufficient to avoid complete clearance in some cases but did not offer complete protection against the effects of the drug. Resistance to SP, which was the drug used in treating these infections, is encoded by several different loci in two different genes (*dhps* and *dhfr*) and the degree of resistance is known to be positively correlated with the number of mutations present (although mutations do not all contribute equally to resistance). Thus, some of the parasites that had resistant *alleles* were probably only partially resistant in phenotypic terms, which complicates the picture. We were also limited by the lack of reconstructed haplotypes for the two genes. Although we considered each allele independently, in reality these loci are intrinsically linked due to asexual reproduction of the parasite within the host; thus, the change in alleles at one locus is tied to the changes at all the other loci.

Future studies looking at competitive release in *P. falciparum* may take a few lessons from the results laid out in Chapter 3. First, it may be useful to have time series for individual infections, with multiple post-treatment samples that can be used to track changes in drug-sensitive and drug-resistant alleles. While longitudinal sample sets were in fact obtained for the study described in Chapter 3, the individual samples were too far apart to give a clear picture of within-host dynamics. The standard follow-up schedule used in antimalarial drug efficacy studies, with samples taken on days 0, 1, 2, 3, 7, 14, 21, and 28 (sometimes 35 and 42) would be ideal for such longitudinal analysis, although these studies have the drawback of lacking untreated control infections. Another challenge is that, at

present, efficacy studies generally focus on response to ACTs, and the prevalence of resistance to ACTs is still low in most places, meaning that the potential to observe competitive release may be quite limited.

Second, reconstruction of haplotypes would greatly simplify the analysis of competitive release in cases where resistance is encoded at multiple loci. The reconstruction of haplotypes, especially in mixed infections, can be a challenge; however, such methods have been developed and used previously, including for *P. falciparum* [103]. Such methods could be utilized to advance the analysis in Chapter 3 from individual alleles to discrete parasite populations, which would help to develop a clearer picture of how drug-sensitive and drug-resistant parasite populations actually changed in response to treatment.

Studies of competitive release in *P. chabaudi* have gone beyond changes in asexual parasite populations and looked at the impact on gametocyte densities and transmission of sensitive and resistant parasites to mosquitoes; these studies give a better indication of the size of the benefit experienced by resistant parasites that undergo competitive release. Not all of these studies can be replicated in humans; however, it is possible that follow-up in a drug efficacy study might be expanded to include collection of whole blood samples that could be used for membrane feeding of mosquitoes, which would allow within-host changes in sensitive and resistant parasite densities to be linked to changes in transmission potential.

Finally, based on studies of competitive release in rodent malaria models, some have suggested alternative approaches to antimalarial drug use that would seek to reduce the advantage competitive release affords resistant parasites. The

idea is that eliminating every last drug-sensitive parasite from the host, which is ostensibly the goal of aggressive therapy that seeks to achieve total clearance of the infection, maximizes the benefit to resistant parasites by completely eliminating competitive suppression. It has been suggested, and also demonstrated in mice, that the dosing of antimalarial drugs could be reduced in order to alleviate symptoms without entirely clearing the drug-sensitive population, which would reduce competitive release of any resistant parasites. However, even if the theory is sound, this proposal is likely to encounter pushback due to the aggressive push in many countries to achieve malaria elimination or pre-elimination status in the near future; changes to treatment policy that explicitly aim *not* to clear infections obviously run counter to these goals.

5.3 Discussion of Chapter 4: Transmission intensity, within-host dynamics, and the evolution of drug resistance

One of the primary motivations for the model presented in Chapter 4 is that the predictions of previously published mathematical models regarding the impact of within-host competition on the spread of drug resistance were highly inconsistent. Some predicted that competitive release of resistance would drive faster spread of resistance at high transmission intensity [20, 21], while others suggested the opposite, often due more to costs of resistance being exacerbated by competition than the intrinsic effects of competition alone [22, 29]. None of these models accounted for the fact that between-host factors, like transmission intensity

and the population-level frequency of drug resistance, could influence within-host dynamics in ways that would affect the fate of drug-resistant parasites. For example, it is shown in Chapter 4 that in the absence of any selection at all (no antimalarial drug use, no fitness cost of resistance), drug-resistant parasites introduced at low frequency go extinct faster in high-transmission settings than low-transmission settings. This is most likely a result of the fact that, as shown in *P. chabaudi*, it is hard for a parasite to invade an established infection. Thus, since resistant parasites will have to invade drug-sensitive infections in nearly every host they encounter, the resistant strain is at a disadvantage simply by virtue of being rare; and this disadvantage is greater in high-transmission settings because there are so few uninfected hosts where the resistant strain can obtain a foothold.

The results of the model in Chapter 4 thus address a key question that was left open in the literature, which was whether within-host competition *alone* could suppress the spread of resistance in high-transmission settings; the results obtained suggest it can. This underscores the fact that the strength of selection is not the only determinant of the rate of resistance evolution; parasite population dynamics also play a major role. In particular, feedbacks between within-host infection dynamics and population-level transmission dynamics appear to be, potentially, quite important. While models allowing within-host dynamics to influence population-level dynamics are not uncommon, it is extremely rare for models to allow feedbacks in the other direction. In cases where superinfection is rare and immunity is acquired after a single exposure, such feedbacks are probably not very important; however, for infections like malaria, where mixed infections are common and

immunity is acquired gradually, the heterogeneity of infection dynamics, and the responsiveness of these dynamics to changes in the composition of the parasite population, is likely to be an important factor in epidemiological phenomena.

Overall, our results are largely consistent with the general findings of the existing literature – even those parts that initially appear irreconcilable. We find within-host competition can inhibit the spread of resistance (with or without fitness costs), as others have suggested [22, 29], and yet also find that resistance can spread more rapidly in high-transmission settings, as others have described [20, 21]. It appears that, in most cases, resistance is favored in low-transmission settings not because of a faster rate of spread, but because of a lower probability of extinction when rare. In cases where the strength of selection was sufficient for the resistant strain to avoid extinction, resistance actually spread more quickly in high-transmission settings. Going forward, the within-host dynamics underlying these outcomes can be examined (using saved model output) to determine the extent to which competitive suppression and competitive release may be driving the extinction and spread, respectively, of the resistant strain in high-transmission settings.

A significant limitation of the model is its complexity, as well as the lack of empirical data on the dynamics of *P. falciparum* infections in humans (especially chronic infections) against which to compare the model. It seems likely that the general findings can be reproduced with a simpler model that incorporates key features, including competition, acquisition of immunity, and different degrees of antigenic overlap between strains; such a model would be more amenable to more

comprehensive study of the impact of competition on the evolution of resistance under a wide range of conditions, as well as exploration of the optimal methods for malaria control and resistance management in a variety of settings.

Chapter 6: Appendix

6.1 Appendix to Chapter 2: Within-host competition in *Plasmodium falciparum*

Methods: Quantitative real-time PCR

DNA was used in a quantitative real-time PCR assay which amplifies codons 72-76 of the *PfCRT* gene on chromosome 7 (Tables A2-A3). TaqMan® probes (Life Technologies) were designed to bind to two different genotypes, one encoding the amino acid sequence CVMNK, which is chloroquine-sensitive (abbreviated CQS), and the other encoding CVIET, which is chloroquine-resistant (abbreviated CQR). Each probe was tagged with a different fluorophore (FAM™ for CVMNK and HEX™ for CVIET) such that samples could be analyzed with both probes simultaneously (multiplexing). Parasite strains 3D7 and Dd2, which have *PfCRT* genotypes CVMNK and CVIET, respectively, were used as positive controls. Samples from Angola were analyzed with a third probe designed to bind to SVMNT (tagged with CAL Fluor® Red 610), using strain HB3 as a positive control. Samples positive for SVMNT ($n = 13$) were excluded from analysis.

Samples were run in triplicate on a Stratagene Mx3000P real-time PCR machine. Control strains (3D7, Dd2, and HB3) were cultured, synchronized to ring stages, and standardized to a density of $2x10^5$ parasites/µl [104]. DNA was extracted using QIAamp DNA Mini Kit and serially diluted to densities of $2x10^4$, $2x10^3$, $2x10^2$, and $2x10^1$ genomes/µl for a total of five standards (including $2x10^5$ genomes/µl). The 3D7 and Dd2 standards (as well as HB3 when analyzing samples

from Angola) were included in triplicate on each qPCR plate and used to generate standard curves for CVMNK and CVIET, respectively, by plotting C_t values against $\log_{10}$ parasite density. Runs with efficiency below 85% for any genotype were repeated and replaced by runs with higher efficiency. Fluorescence baselines and thresholds were set manually for each sample in MxPro qPCR software (Agilent Technologies). Standard curves were used to convert C_t values to $\log_{10}$ parasite densities. Samples with parasite density below 2 p/μl for any genotype were ruled negative for that genotype; samples negative for both genotypes were excluded from analysis.

Control mixtures of 3D7 and Dd2 at various densities and in different proportions were analyzed to determine the relationships between actual parasite densities and proportions and those determined by qPCR (Fig. A3, A4). The results (polynomial regression relating the observed proportions and parasite densities to actual values) were used to ensure accurate quantification of CQS and CQR parasites in mixed-genotype infections.

Figures

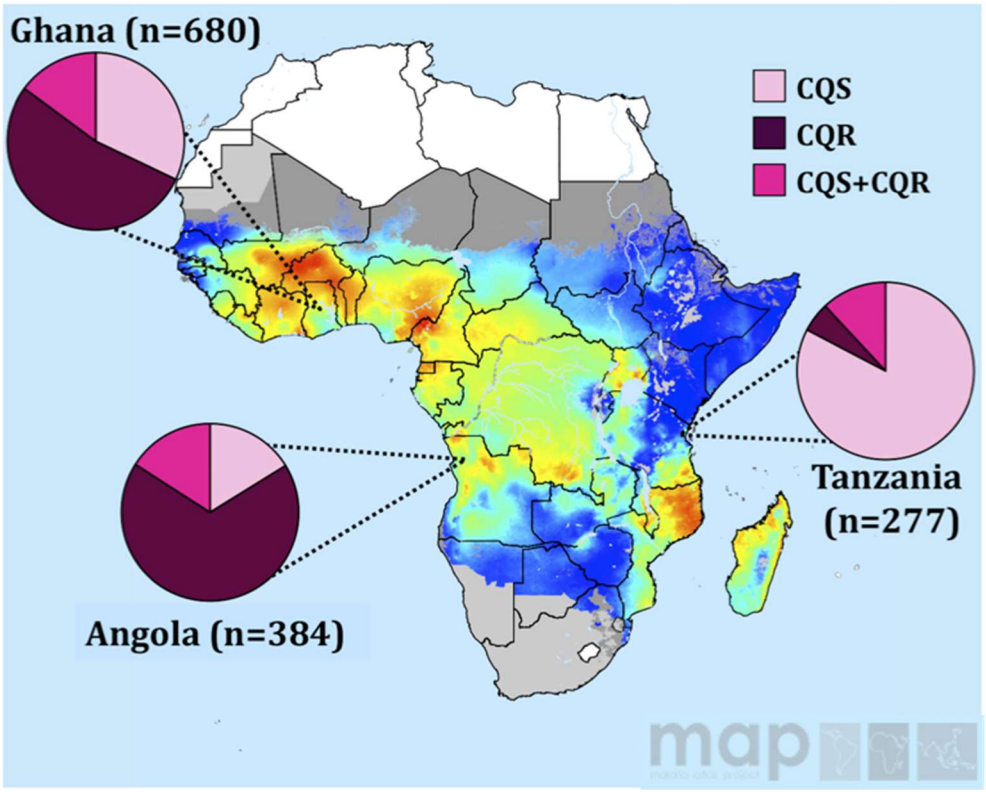

Figure A1. *PfCRT* genotypes of samples from different countries, superimposed on map showing *P. falciparum* endemicity. Pie charts show proportions of infections harboring chloroquine-sensitive (CQS, light pink), chloroquine-resistant (CQR, dark pink), or both alleles (CQS+CQR, medium pink) in samples from Angola, Ghana, and Tanzania. Numbers of samples analyzed from each country are given in parentheses. Shading on the African continent shows endemicity (*Plasmodium falciparum* point prevalence in children ages 2-10 years), ranging from 0% (dark blue) to 70% (red). Map modified from [65].

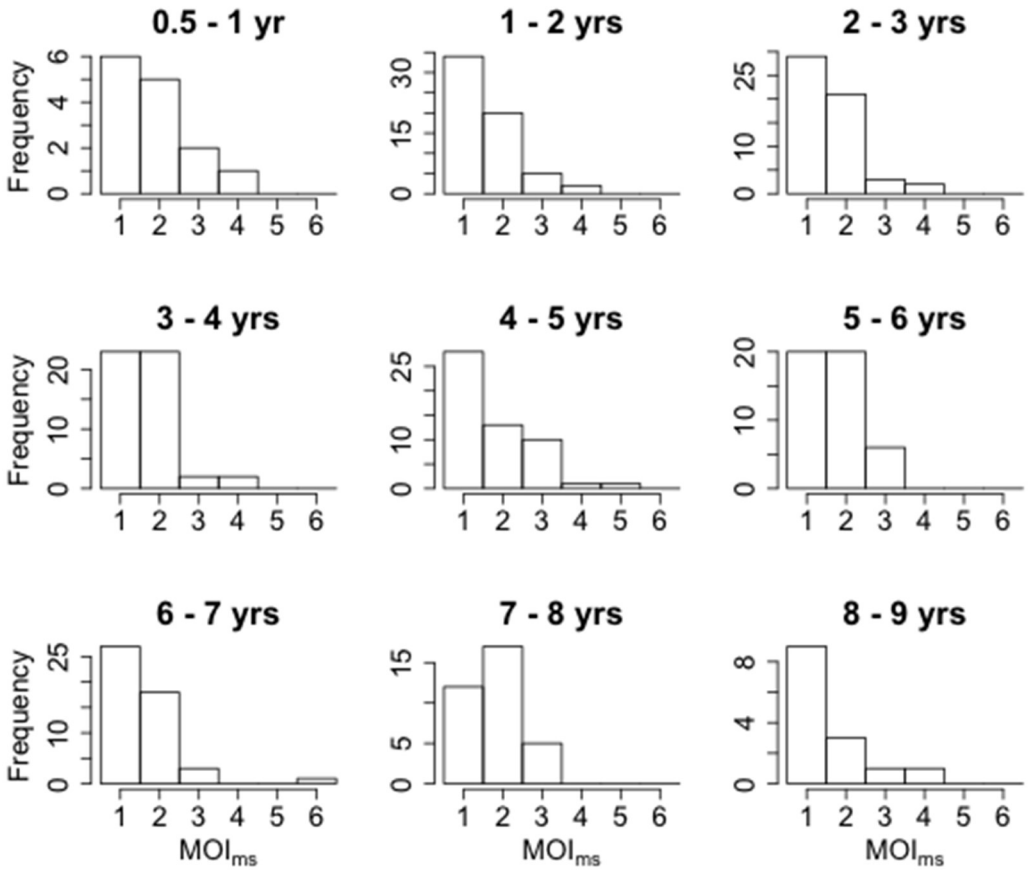

Figure A2. Distribution of MOI_{ms} (number of strains per host) stratified by host age. Each histogram shows the number of hosts in each age group with a given MOI_{ms}.

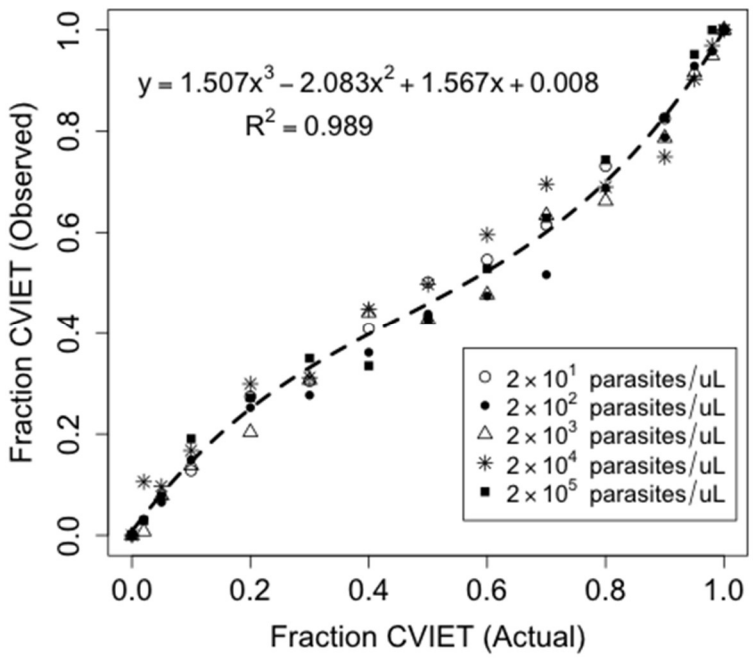

Figure A3. Fraction CVIET (observed) vs. fraction CVIET (actual). The y-axis shows fraction CVIET as determined using qPCR data from control mixtures of 3D7 (CVMNK) and Dd2 (CVIET) at different concentrations (see legend). Dashed line shows polynomial regression (equation on figure).

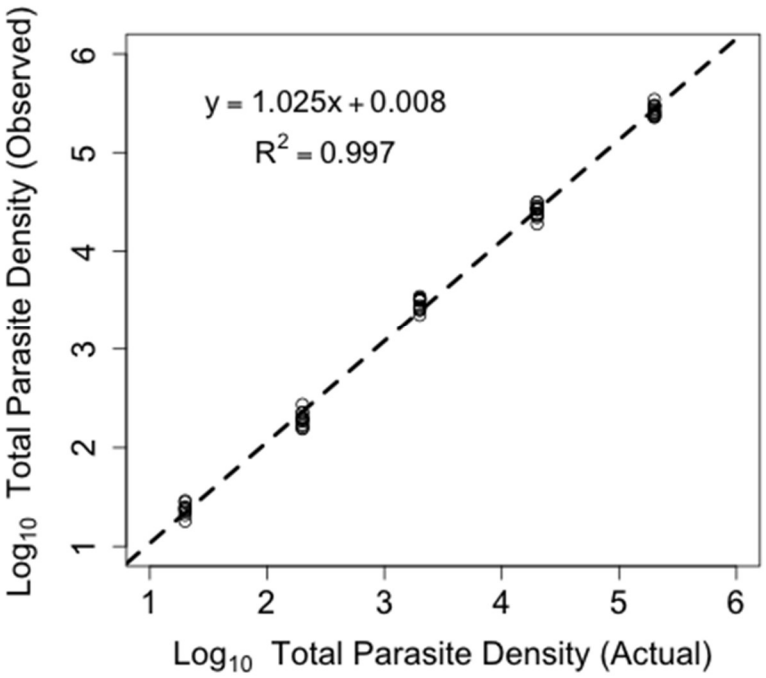

Figure A4. Log_{10} total parasite density: observed values vs. true values. The y-axis shows log_{10} total parasite density as determined using qPCR data from control mixtures of 3D7 and Dd2 (in various proportions; see Fig. A3) at different densities. Dashed line shows linear regression (equation on figure).

Tables

Table A1. Study locations and sample sizes. Numbers in parentheses are samples positive for CVMNK and/or CVIET and – for samples from Angola - negative for SVMNT.

Country	**Study Site**	**# Samples Collected (# Positive by qPCR)**
Angola	Uíge, Uíge Province	196 (190)
	M'banza Congo, Zaire Province	201 (194)

Ghana	Hohoe	199 (177)
	Navrongo	229 (216)
	Sunyani	117 (107)
	Yendi	200 (180)
Tanzania	Bagamoyo District	280 (277)

Table A2. Primer and probe sequences used in *PfCRT* quantitative real-time PCR. Mutant bases in CVIET probe are underlined. FAM™ and HEX™ dyes are owned by Glen Research; CAL Fluor® Red 610 dye and Black Hole Quenchers® (BHQ1 and BHQ2) are owned by Biosearch.

Oligo	Sequence
PFCRT-Fwd	5'-TGG TAA ATG TGC TCA TGT GTT T-3'
PFCRT-Rev	5'-AGT TTC GGA TGT TAC AAA ACT ATA GT-3'
CVMNK	5'-FAM-TGT GTA ATG AAT AAA ATT TTT GCT AA-BHQ1-3'
CVIET	5'-HEX-TGT GTA ATT GAA ACA ATT TTT GCT AA-BHQ1-3'
SVMNT	5'-CalRd610-AGT GTA ATG AAT ACA ATT TTT GCT AA-BHQ2-3'

Table A3. *PfCRT* quantitative real-time PCR master mix and thermal cycling protocol.

Master Mix
Invitrogen™ Platinum® Quantitative PCR Supermix-UDG 12.5 µl
$MgCl_2$ (50 mM) 1.25 µl
Fwd primer (10 µM) 0.75 µl

Rev primer (10 µM) 0.75 µl CVMNK probe (10 µM) 0.25 µl CVIET probe (10 µM) 0.25 µl SVMNT probe (10 µM) 0.25 µl ROX reference dye 0.25 µl H_2O 3.75 µl DNA 5 µl Total volume 25 µl *This reaction can also be run with a total volume of 12.5 µl; in this case all volumes are reduced by half.*
Thermal Cycling Protocol 95˚ (6 min.) [95˚ (15 sec.), 57˚ (1 min.)] x 50 4˚ (hold)

Table A4. Primer sequences for microsatellite loci [105, 106].

Microsatellite	**Primer**	**Sequence**
TA1 Chromosome 6 Nested PCR	Fwd. (primary)	5'-CTA CAT GCC TAA TGA GCA-3'
	Rev.	5'-TTT TAT CTT CAT CCC CAC-3'
	Fwd. (secondary)	5'-HEX-CCG TCA TAA GTG CAG AGC-3'
Polyα Chromosome 4 Nested PCR	Fwd.	5'-AAA ATA TAG ACG AAC AGA-3'
	Rev. (primary)	5'-ATC AGA TAA TTG TTG GTA-3'
	Rev. (secondary)	5'-FAM-GAA ATT ATA ACT CTA CCA-3'

PfPK2	Fwd.	5’-CTT TCA TCG ATA CTA CGA-3’
Chromosome 12	Rev. (primary)	5’-CCT CAG ACT GAA ATG CAT-3’
Nested PCR	Rev. (secondary)	5’-HEX-AAA GAA AGG AAC AAG CAG A-3’
TA109	Fwd. (primary)	5’-TAG GGA ACA TCA TAA GGA T-3’
Chromosome 6	Rev.	5’-CCT ATA CCA AAC ATG CTA AA-3’
Nested PCR	Fwd. (secondary)	5’-FAM-GGT TAA ATC AGG ACA ACA T-3’
C2M34	Fwd.	5’-FAM-TCCCTTTTAAAATAGAAGAAA-3’
Chromosome 2	Rev.	5’-GAT TAT ATG AAA GGA TAC ATG-3’
Non-nested PCR		
C3M69	Fwd.	5’-HEX-AAT AGG AAC AAA TCA TAT TG-3’
Chromosome 3	Rev.	5’-AGA TAT CCA GGT AAT AAA AAG-3’
Non-nested PCR		

Table A5. PCR master mixes and thermal cycling protocols for amplifying neutral microsatellites. Protocols for non-nested PCRs are from [107] and for nested PCRs are from [90].

Non-nested PCR: Master Mix

Promega PCR Master Mix 7.5 µl

H_2O 4.3 µl

Fwd primer (stock conc. 10 µM) 0.6 µl

Rev primer (stock conc. 10 µM) 0.6 µl

DNA 2 µl

Total volume 15 µl

Non-nested PCR: Thermal Cycling Protocol
94˚ (2 min.)
[94˚ (30 sec.), 50˚ (30 sec.), 60˚ (30 sec.)] x 5
[94˚ (30 sec.), 45˚ (30 sec.), 60˚ (30 sec.)] x 40
4˚ (hold)
Nested PCR Master Mix (Primary and Secondary Reactions)
Promega PCR Master Mix 7.5 µl
H_2O 5.3 µl
Fwd primer (stock conc. 10 µM) 0.6 µl
Rev primer (stock conc. 10 µM) 0.6 µl
DNA 1 µl
Total volume 15 µl
Nested PCR Thermal Cycling Protocol: Primary Reaction
94˚ (2 min.)
[94˚ (30 sec.), 42˚ (30 sec.), 40˚ (30 sec.), 65˚ (40 sec.)] x 25
65˚ (2 min.)
4˚ (hold)
Nested PCR Thermal Cycling Protocol: Secondary Reaction
94˚ (2 min.)
[94˚ (20 sec.), 45˚* (20 sec.), 65˚ (30 sec.)] x 25
65˚ (2 min.)
4˚ (hold)
*For TA109 change 45˚ to 59˚

Table A6. Distributions of multiplicity of infection (MOI) for Angola (based on microsatellite genotyping) and Tanzania (based on Carlsson et al. [108]).

	MOI=1	MOI=2	MOI=3	MOI=4	MOI=5	MOI=6
Frequency (Angola)	0.50	0.36	0.10	0.03	0.003	0.003
Frequency (Tanzania)	0.22	0.40	0.24	0.08	0.04	0.02

Table A7. Number and frequency of infections positive for CQS and/or CQR alleles in Angola, Ghana, and Tanzania. Prevalence of mixed-genotype infections (CQS+CQR) did not vary significantly between countries ($X^2 = 2.898$, d.f. = 2, $p = 0.235$) but the frequencies of CQS and CQR varied markedly ($X^2 = 326.974$, d.f. = 2, $p = 9.967\text{x}10^{-72}$).

	Angola (*n*)	**Ghana (*n*)**	**Tanzania (*n*)**	**All (*n*)**
CQS only	65 (16.9%)	218 (32.1%)	229 (82.7%)	512 (38.2%)
CQR only	255 (66.4%)	361 (53.1%)	15 (5.4%)	631 (47.1%)
CQS + CQR	64 (16.7%)	101 (14.9%)	33 (11.9%)	198 (14.8%)
Total	384	680	277	1,341

Structure and implementation of null model of CQS+CQR mixed-genotype infections

The data required for the null model are CQS and CQR allele frequencies and the distribution of multiplicity of infection (MOI) in the population. Using these data, it is possible to estimate the probability of an infection with any given composition (for example, the probability that a host will have three strains, of which one is CQR and two are CQS). With these probabilities, and working under the null assumption that the numbers of CQS and CQR parasites in a host will be strictly proportional to the numbers of strains of each genotype, the model is used to calculate the expected mean proportion of CQR parasites in all CQS+CQR mixed infections in a population.

CQS and CQR allele frequencies were estimated from single-genotype samples used in our study. Data on multiplicity of infection (MOI) for Angola were also collected in our study, and data on MOI for Tanzania were obtained from contemporaneous work on the within-host diversity of malaria infections in Bagamoyo District, Tanzania [108]. From the published data, the estimation of MOI was similar to the method we used for Angola: MOI = maximum number of alleles observed at *msp1* or *msp2*. Given the distributions of MOI and CQS/CQR allele frequencies, we can calculate the expected proportion CQR in CQS+CQR mixed infections for each population, as follows. Let m be the maximum MOI observed in the population, f_i the frequency of infections with MOI=i, p the frequency of the CQR allele and q the frequency of the CQS allele. The expected proportion CQR is obtained by summing over all possible values multiplied by their probabilities. For an infection with i total strains, of which j are resistant, the expected proportion CQR (under the null model) is j / i; the rest of the summand gives the probability of

such an infection. The denominator is the total probability of all mixed-genotype infections; dividing by this ensures that the estimated probabilities sum to 1.

$$\frac{\sum_{i=2}^{m}\sum_{j=1}^{i-1} f_i\left(\frac{j}{i}\right)\binom{i}{j}p^j q^{i-j}}{\sum_{i=2}^{m}\sum_{j=1}^{i-1} f_i\binom{i}{j}p^j q^{i-j}}$$

Both Angola and Tanzania were found to have MOI ranging from 1 to 6 (frequencies shown in Table A6), and our estimate of the CQR allele frequencies in Tanzania and Angola were 0.06 and 0.80, respectively. Calculating the denominator of the formula above gives the expected proportion of all infections expected to have both CQS and CQR genotypes; this value comes out to be 0.122 for Tanzania and 0.185 for Angola, which are not statistically different from the observed frequencies of mixed-genotype infections in our sample (0.119 for Tanzania, p=0.96; 0.169 for Angola, p=0.25). Therefore, the MOI distributions derived from Carlsson et al. and from our microsatellite data are consistent with the observed frequencies of CQS+CQR mixed-genotype infections. The formula above gives the expected proportion CQR in mixed-genotype infections, which is found to be 0.544 for Angola and 0.377 for Tanzania. For each of these countries, the observed average proportion CQR is significantly lower than expected (one-sample, two-sided *t*-tests of logit-transformed proportion data ($p = 0.01$ for Angola, $p = 9\text{x}10^{-5}$ for Tanzania).

Information on MOI was not available for Ghana, but it is possible to test against a simplified null model, which makes no assumptions about the distribution of MOI in the population. Since the frequency of the CQR allele in Ghana was 0.62, a neutral model would predict the proportion CQR to be greater than or equal to 0.5. A one-sample, two-sided *t*-test of logit-transformed proportion data (two-sided to be conservative, although a one-sided test would also be appropriate) shows that the average proportion CQS is significantly less than 0.5 ($p=4x10^{-8}$). The rejection of the simplified null model, in this case, also allows us to reject the full null model. Adding information about the distribution of MOI will always yield an expected mean between 0.5 and the CQR allele frequency (0.62). If the average proportion CQR in Ghana is significantly less than 0.5, it will also be significantly less than any value greater than 0.5; therefore, we know that the prediction of the more sophisticated null model will also be rejected.

The null model can be modified to incorporate the differences observed between CQS and CQR parasites in single-genotype infections. If the average density of CQR in single infections is some fraction x of the average density of CQS in single infections, then the expected proportion CQR in a host with j resistant and i-j sensitive strains becomes $(xj)\div(i+j(x-1))$ and the rest of the model is unchanged.

The primary limitation of this null model stems from the fact that methods such as microsatellite genotyping will tend to underestimate MOI. As a result, the proportions predicted by this null model will tend to err toward 0.5, regardless of whether this is above or below the predicted value. With this in mind, this model provides estimates that fall in between two extremes, the first being 0.5 (the

proportion CQR expected if all CQS+CQR mixed infections comprise one strain of each genotype) and the second being the frequency of the CQR allele in the population (which is the limit approached by the model as multiplicity of infection goes to infinity).

6.2 Appendix to Chapter 3: Competitive release of drug-resistant parasites following treatment

Table A8. PCR master mix for amplification of *dhps* and *dhfr*:

Reagent	Volume (µL)	Final Concentration (µM)
Sample DNA	4	-
5x GC Buffer[1]	10	1X
dNTPs (10 µM)	1	0.2
Forward primer (µM)	2.5	0.5
Reverse primer (µM)	2.5	0.5
H_2O	29.5	-
HF Phusion DNA polymerase[1]	0.5	1 unit
Total	50	-

[1]New England Biolabs (catalog no. M0530L)

Table A9. Primers used for whole-gene amplification of *dhps* and *dhfr* (adapted from [109]).

Gene	Primer direction	Primer sequence
dhfr	Forward	5'-TTT TTA CTA GCC ATT TTT GTA TTC C-3'
	Reverse	5'-TTA ACC GTT CAG GTA ATT TTG TCA-3'
dhps	Forward	5'-AAT ATT TGC GCC AAA CTT TTT A-3'
	Reverse	5'-TTT ATT TCG TAA TAG TCC ACT TTT GAT-3'

Table A10. PCR thermal cycling protocol for amplification of *dhps* and *dhfr*:

Step	Temperature & duration	Number of cycles
1	98°C for 3:00 minutes	1
2	98°C for 0:30 minutes 58°C for 0:30 minutes 65°C for 5:00 minutes	30
3	65°C for 10:00 minutes	1
4	Hold at 4°C	1

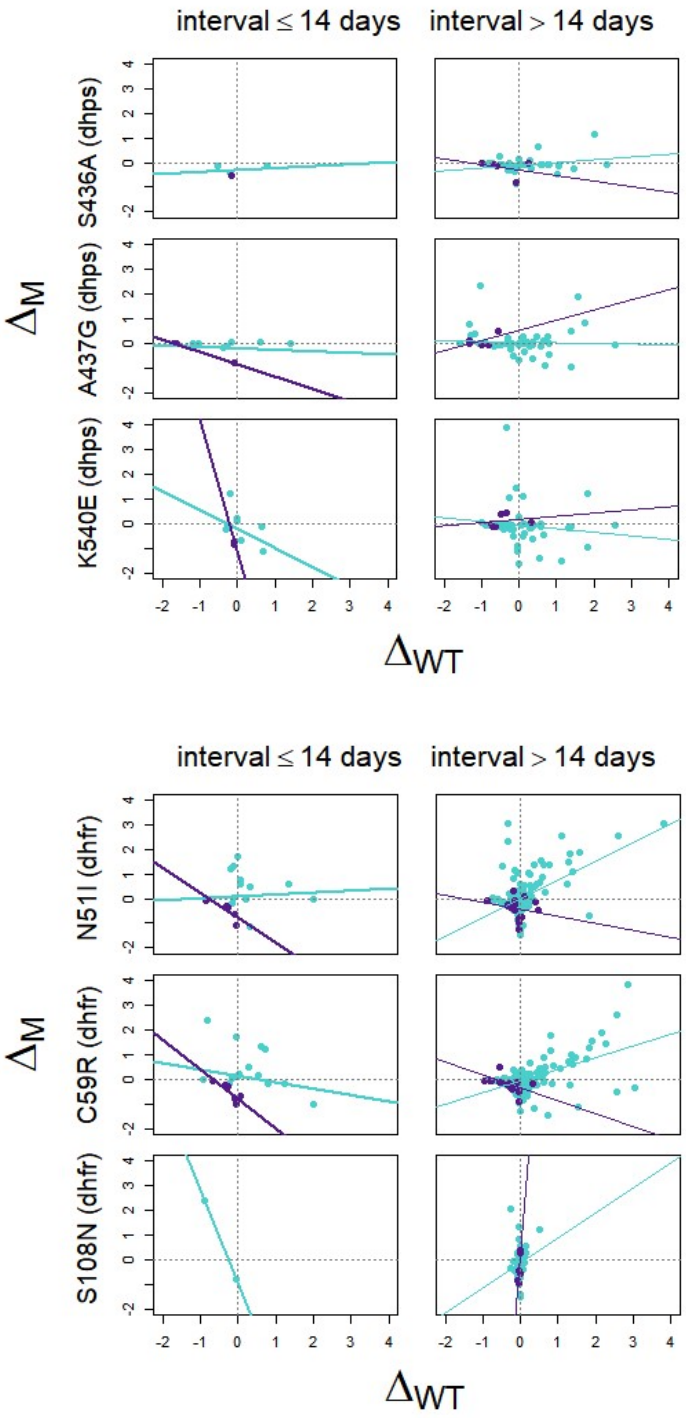

Figure A5. Relative changes in densities of mutant (drug-resistant) and WT (drug-sensitive) alleles for each resistance locus, shown separately for sample pairs with intervals of ≤14 days and pairs with intervals of >40 days. Data points and regression lines are shown in turquoise and purple for control and treated sample pairs.

Appendix to Chapter 4: Transmission intensity, within-host dynamics, and the evolution of drug resistance

Methods

Within-host model

The within-host model describes the infection dynamics of two strains of *Plasmodium falciparum*, one drug-sensitive and the other drug-resistant (these are denoted strain 1 and strain 2). The model is comprised of a system of ordinary differential equations that describe the dynamics of the following components:

- Red blood cells (X)
- Infected red blood cells of each strain (Y_1, Y_2)
- Merozoites of each strain (S_1, S_2)
- Gametocytes of each strain (G_1, G_2)
- Adaptive immunity to each strain (I_1, I_2)
- Innate immunity (Z)

In the following equations and explanations, we use subscripts i and j to denote strain-specific variables and parameters; thus $(i, j) = (1,2)$ or $(2,1)$.

The differential equation for uninfected red blood cells is as follows:

$$\frac{dX}{dt} = \underbrace{B}_{\text{RBC production}} - \overbrace{\alpha_X X}^{\text{RBC death}} - \underbrace{\beta X(S_1 + S_2)}_{\text{Infection by merozoites}}$$

where B is the rate of production of new RBCs, α_X is the death rate of uninfected RBCs, and β is the rate of infection of RBCs by free merozoites (parameter values can be found in Table A11).

Infected RBCs of strain i are described by the following equation:

$$\frac{dY_i}{dt} = \underbrace{\beta X S_i}_{\text{Infection of RBCs by merozoites}} - \underbrace{\left(\frac{1}{1-e_i}\right)}_{\text{Death rate increase from antimalarial drug treatment}} \underbrace{\alpha_Y Y_i}_{\text{Infected RBC death}} \overbrace{-\gamma Y_i}^{\text{Gametocyte formation}} - \underbrace{\delta_Z Z Y_i}_{\text{Killing by innate immunity}} - \overbrace{\delta_I\left(I_i + \omega_j I_j\right) Y_i}^{\text{Killing by adaptive immunity}}$$

where α_Y is the background death rate of infected RBCs; in the absence of antimalarial drug treatment, $e_i = 0$ (making the death rate α_Y). If the host is being treated with antimalarial drugs, then $e_i = \varepsilon_i$ where ε_i represents the efficacy of drug treatment against strain i. γ is the per capita rate of gametocyte formation. δ_I and δ_Z are the rates of killing by adaptive and innate immune responses, respectively. ω_j is the proportion of I_j (the adaptive immune response to strain j) that is effective against strain i. The relationship of ω_j to the antigenic overlap between the two strains is discussed later on.

The equation for free merozoites of strain i is:

$$\frac{dS_i}{dt} = \underbrace{R\alpha_Y\overbrace{(1-\varphi_i)}^{\text{Fitness cost}}Y_i}_{\text{Merozoite production by infected RBCs}} - \overbrace{\alpha_S S_i}^{\text{Merozoite death}} - \underbrace{\beta X S_i}_{\text{Merozoite invasion of RBCs}} - \overbrace{\delta_Z Z S_i}^{\text{Killing by innate immunity}} - \underbrace{\delta_I\left(I_i + \omega_j I_j\right) S_i}_{\text{Killing by adaptive immunity}}$$

where R is the burst size (number of merozoites released by a single infected red blood cell), φ_i is the fitness cost of strain i, and α_S is the death rate of free merozoites. δ_I, δ_Z, and ω_j are as described above.

The equation for gametocytes of strain i is below:

$$\frac{dG_i}{dt} = \underbrace{\gamma Y_i}_{\text{Gametocyte formation}} - \overbrace{\alpha_G G_i}^{\text{Gametocyte death}} - \underbrace{\delta_Z Z G_i}_{\text{Killing by innate immunity}}$$

where α_G is the death rate of mature gametocytes and γ and δ_Z are as described above. Due to the scarcity of gametocytes in the human host, we assume that adaptive immune responses to gametocytes are negligible. Therefore, "natural" death and killing by innate immunity are the only mechanisms by which gametocytes are eliminated in the model.

Innate immunity is described by the following equation:

$$\frac{dZ}{dt} = \underbrace{\zeta(1-Z)(S_1+S_2)}_{\text{Innate immunity activation}} - \underbrace{\alpha_Z Z}_{\text{Innate immunity inactivation}}$$

where Z is considered the fraction of a fixed pool of innate immune effectors that are currently "activated." ζ is the activation rate of these effectors, and α_Z is the inactivation rate.

The dynamics of adaptive immunity to strain i are described by the following equations:

$$\frac{dI_i}{dt} = \overbrace{\sigma I_i \left(\frac{S_i + \eta S_j}{\theta + S_i + \eta S_j}\right)}^{\text{Growth of adaptive immunity}} \overbrace{- \max(H_1, H_2) * \psi J_i I_i \left(1 - \left(\frac{C_i^k}{C_i^k + A^k}\right)\right)}^{\text{“Loss” of adaptive immunity due to antigenic variation}}$$

$$\underbrace{- \alpha_I J_i \left(1 - \max\left(H_i, \eta H_j\right)\right) I_i}_{\text{Decay of adaptive immunity}}$$

$$\frac{dC_i}{dt} = \underbrace{H_i + \nu H_j}_{\text{Exposure to antigenic variants}}$$

The parameter σ is the maximum growth rate of the adaptive immune response and θ is the density of merozoites $\left(S_i + \eta S_j\right)$ at which the growth rate is $\sigma/2$ (Fig. A6). η is the proportion of fixed (non-variant) antigens or epitopes that are shared between strains i and j. Thus, the contribution of strain j merozoites to stimulation of I_i is proportional to this overlap.

Although both merozoites and infected RBCs will stimulate adaptive immune responses, the above equation is written such that only merozoites drive growth of adaptive immunity. This simplification is justified because infected RBCs and free merozoites maintain a relatively fixed ratio in the host, such that $S + Y \approx \rho S$; thus, this ratio ρ can simply be incorporated into the parameters σ and θ instead.

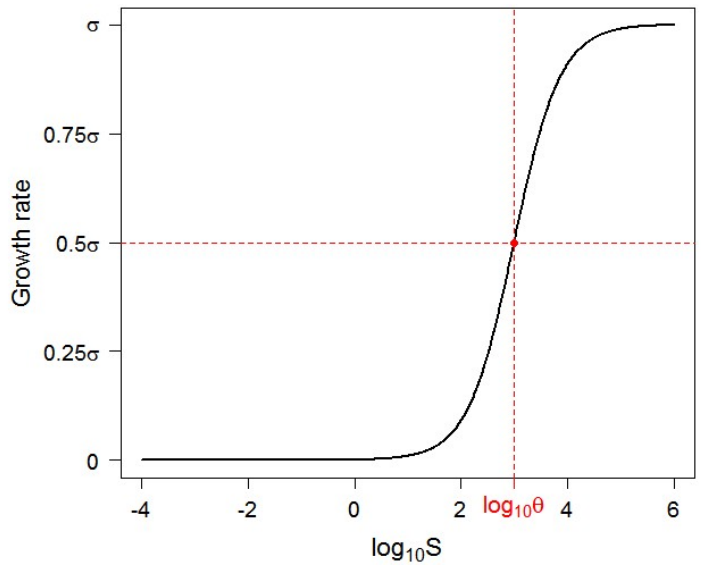

Figure A6. Growth rate of adaptive immunity $\left(\text{the positive term of } \frac{dI}{dt}\right)$ as a function of merozoite density (S). For simplicity, S here stands for $S_i + \eta S_j$. Intersection of dashed lines identifies the point at which $S = \theta$ and the growth rate equals $\sigma/2$.

The equations for the adaptive immune responses each includes two decay terms, but the application of these terms depends on which strain(s) are present in the host. The variable H_i is definied such that $H_i = 1$ if strain i is present, and $H_i = 0$ otherwise. In addition, the variable J_i ensures that I_i does not decline below the baseline value I_N: $J_i = 0$ if $I_i \leq I_N$, and $J_i = 1$ otherwise.

Thus, the first decay term, with coefficient $\max(H_1, H_2)$, is applied whenever the host is infected with either strain. The second term, with the coefficient $\left(1 - \max\left(H_i, \eta H_j\right)\right)$, is applied "in full" when neither strain is present, to a lesser degree when only strain i is present, and not at all if the host if strain i is present (regardless of whether strain j is also present).

The latter decay term is simply the slow, exponential decline of adaptive immunity in the absence of continued stimulation (the half-life being measured in years). If strain i is absent, and as long as $I_{ij} > I_N$, the applicable decay term is $-\alpha_I(1-\eta j)I_i$. If strain j is also absent, the decay term simplifies to $-\alpha_I I_i$.

When the host is infected – with either or both strains - and as long as $I_i > I_N$, the applicable decay term is $-\psi I_{ij}\left(1-\left(\frac{C_{ij}^k}{C_{ij}^k+A^k}\right)\right)$. As described in more detail below, C_i increases with time, the fraction $\left(\frac{C_{ij}^k}{C_{ij}^k+A^k}\right)$ approaches 1, and the decay rate approaches zero. The relationship between C_i and the decay rate is depicted in Figure A7.

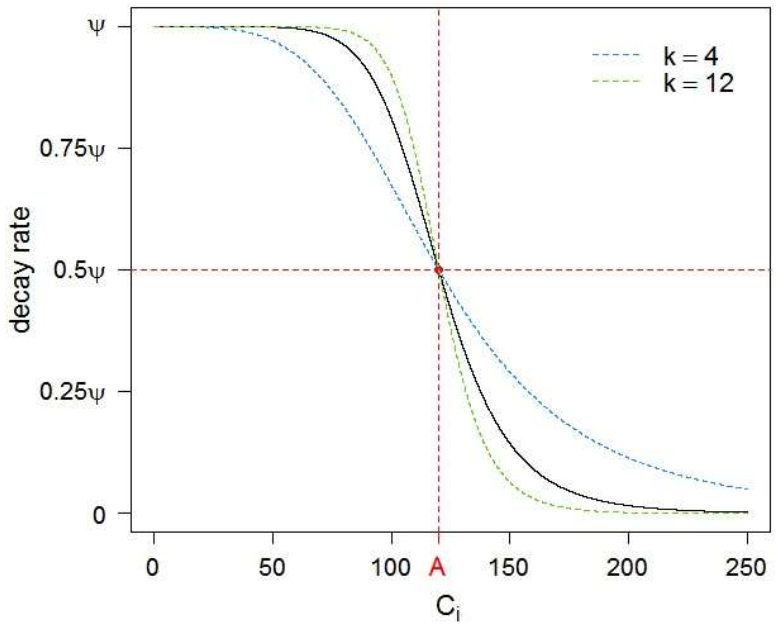

Figure A7. Decay rate of I_i as a function of C_i (black line). Intersection of dashed red lines indicates the point where $C = A$ and the decay rate equals $\psi/2$. Dashed blue and green lines

show what the function looks like for alternative values of k ($k = 4$, blue; $k = 12$, green; black line with $k = 8$).

The function of this second decay term is to approximate the process of immune evasion through antigenic variant switching. Variant switching is thought to be stochastic in nature, although the degree of randomness is not known. For what follows, we assume that switching is at least approximately random (not heavily biased toward particular switching patterns).

P. falciparum has a large, but finite, pool of variant antigens to switch through; for example, the size of the *var* gene repertoire is generally around 60 variants. If variant switching is approximately random, the time it takes to "find" a variant that is not recognized by the adaptive immune response is primarily a function of how many variants are already recognized. Early in the infection, almost any variant will not be recognized, so "escape" through switching should happen rapidly. However, when most variants have been seen by the immune system, it will take many more random switches to find one that has not been seen before. A simple model assuming completely random switching (and no cross-reactivity between variants) shows that the mean number of tries required to find a novel variant increases non-linearly with the number of variants already seen (Figure A8).

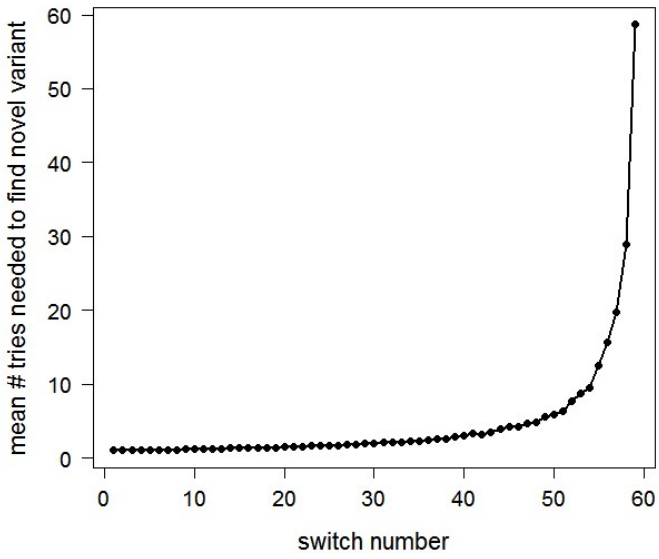

Figure A8. A simulation was written which, given a starting variant, iterates a process of randomly choosing variants until it finds one that has not been "expressed" before. Shown here is the mean number of random picks needed to find a "novel" variant at each step of the process ($n = 1000$ simulations).

Rather than explicitly model the dynamics of variants and variant-specific immune responses, we use this hypothesized relationship between the number of variants already seen and the time required to "find" a novel variant to implicitly model the process of antigenic variation. The switch to a novel variant impairs the ability of the adaptive immune system to recognize and kill parasites; this loss of effectiveness is mathematically indistinguishable from a loss of immune effectors, and can thus be represented by a decay term in the equation for adaptive immunity.

As described above, novel variants should be found rapidly at the start of an infection, but much more slowly as the pool of variants is exhausted. Therefore, the rate of decay of adaptive immunity should be high initially and decrease as the

infection progresses. The variable C_i exists to track the "progress" of an infection – i.e. how much of the variant repertoire has been "seen" by the adaptive immune system. We assume that only one variant is expressed at any given time, and therefore C_i increases linearly with time. However, different strains can have variants in common, and any shared variant expressed by one has been "used up" for all. Therefore, strain j contributes to the increase of C_i over time at a rate that is proportional to the overlap in the variant repertoires of strains i and j (the parameter v).

Parasite population structure and acquired immunity

For the purposes of this model, we define *strain* simply on the basis of drug susceptibility or resistance. Drug-sensitive parasites are considered to comprise one strain, and drug-resistant parasites another. We refer to subpopulations of a given strain (such as the drug-sensitive populations within different hosts) as *isolates*. The amount of variation between isolates of a given strain affects the acquisition of immunity; the greater the variation, the less any previous exposure will protect against a future one, and the more exposures it will take to reach a given "degree" of protection. Variation between strains, on the other hand, determines how much cross-reactivity there is between acquired immune responses to each strain; with less variation there will be more overlap, and hence a greater degree of cross-reactivity. Immune responses that target both strains can result in 'immune-mediated apparent competition' – a form of indirect competition mediated by

strain-transcending immune responses. Greater overlap will tend to increase the severity of immune-mediated apparent competition.

We define parameters that govern the overlap between isolates of the same strain as well as between isolates of different strains. In addition, we make a distinction between overlap in fixed (non-variant) antigens and overlap in variant antigen repertoires, for reasons that are discussed below. The overlap parameters are as follows:

- η – fixed antigen overlap between isolates of different strains
- ν – variant antigen repertoire overlap between isolates of different strains
- λ – fixed antigen overlap between isolates of the same strain
- μ – variant antigen repertoire overlap between isolates of the same strain

There are two reasons that overlap of fixed antigens and overlap of variant antigens are considered separately. The first is simply that overlap in variant repertoires is typically small (sometimes approaching zero). The second is that fixed and variant antigens have different effects on the dynamics of immunity. When fixed antigens are shared, it has the effect of boosting the immune response, whereas when variant antigens are shared, it hastens the exhaustion of each strain's variant repertoire. The logic is as follows: suppose two strains in the same host share a particular antigenic variant. When one of the strains expresses this variant, the adaptive immune system mounts a response against it. However, when the other strain switches to expressing this variant, the specific immunity acquired from previous exposure will not contribute much to control of parasite growth; instead, it will simply exert selection for other variants that are not yet recognized. Thus, any

variant expressed by either strain has been 'used up' for both, which decreases the time until both strains run out of novel variants.

Although the possibilities for combinations of these four parameters are vast, we boil the possibilities down to four configurations that are relevant to the spread of drug resistance. We set two combinations of λ and μ that correspond to high and low within-strain variation, and then either set $\eta = \lambda$ and $\nu = \mu$, which makes between-strain variation equal to within-strain variation, or set η and ν to very low values, which makes within-strain variation less than between-strain variation. (Keep in mind that the overlap parameters describe *similarity*, so lower values indicate greater variation). These four configurations are illustrated in Figure A9.

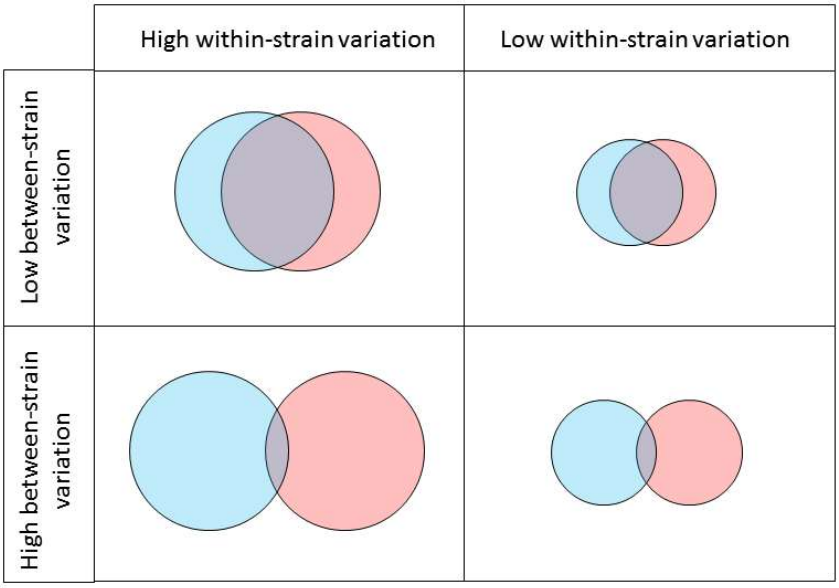

Figure A9. The four parasite population structure configurations used. The size of the circles (blue for drug-sensitive, red for drug-resistant) indicates the amount of genetic diversity within each strain (bigger = more diverse), while the amount of overlap indicates how

similar the two strains are to each other (less overlap = less similar). Note that the drug-sensitive and drug-resistant parasite populations are always equally diverse.

Where η and ν appear in the equations of the within-host model, they are mediating interactions between the strains that are currently in the host. However, as mentioned above, antigenic overlap between isolates of the same strain affects the ability of acquired immunity from previous infections to control future infections. Thus, in the model, each time a new isolate of strain i is introduced into a host, I_i is multiplied by the proportion of the new isolate's antigens that are recognizable based on past exposures: $I_i \times (1 - (1 - \lambda)^{n_i})$ where n_i is the number of past encounters with strain i.

Something similar is done for the variable C_i, which tracks how much of the current isolate's antigenic variant repertoire the immune system has seen. When a new isolate of strain i is introduced, C_i is multiplied by the proportion of the new isolate's variants that have been seen before: $C_i \times (1 - (1 - \mu)^{n_i}(1 - \nu)^{n_j})$ where n_i and n_j are the number of past exposures to strain i and strain j, respectively.

Finally, the number of previous exposures affects the degree of cross-reactivity between the strains. The rate of killing of strain i by acquired immunity to strain j is proportional to ω_j where $\omega_j = 1 - (1 - \eta)^{n_j}$ (n_j is as defined above).

Human-mosquito contact and parasite transmission

Every day, each human host is assigned to be bitten by a number of mosquitoes that is drawn from a Poisson distribution with mean b. Each mosquito

bites only one host per day, and which mosquitoes bite on any given day is random (mosquitoes can bite on sequential days but do not necessarily do so).

The probability that a mosquito is infected upon feeding on a host is determined by a function described by Churcher et al. [99]:

$$P = \left(1 - \left(1 + \frac{(G_1 + G_2)}{2d}\right)^{d-1}\right)\left(g_0 + g_1 \exp\left(-g_2 \exp\left(-g_3(G_1 + G_2)\right)\right)\right)(1 + p + q)$$

$$\text{where } p = \begin{cases} 0 & \text{if } (Y_1 + Y_2) < 100 \\ f_1 & \text{if } 100 \leq (Y_1 + Y_2) < 1000 \\ f_2 & \text{if } (Y_1 + Y_2) \geq 1000 \end{cases} \quad \text{and } q = \begin{cases} 0 & \text{if age} < 5 \text{ years} \\ 1 & \text{otherwise} \end{cases}$$

If a mosquito is determined to be infected, the number of gametocytes of strain i picked up is drawn from a Poisson distribution with mean $G_i * V$ where $G_i =$ strain i gametocytes/μL and V is the volume of a mosquito blood meal in μL. (Draws of zero gametocytes are disallowed because the number of mosquitoes infected is determined by the gametocyte density-infectivity function shown above.)

Infection in the mosquito has a latent period of y days. After the latent period ends (simulating the appearance of sporozoites in the salivary glands), the mosquito becomes infectious. When an infectious mosquito bites a host, there is a fixed probability f that sporozoites are transmitted to the host; if this occurs, the mosquito introduces n sporozoites to the host. If m_i gametocytes of strain i were originally, then drawing from a binomial distribution with size n and probability $m_1/(m_1 + m_2)$ determines the number of sporozoites of each strain transmitted. If

parasites from K blood meals have reached the infectious stage, assuming m_{ix} is the number of strain i gametocytes acquired from blood meal x $(1 \leq x \leq K)$, then a draw of size n is made from a multinomial distribution with probability $\left(\frac{1}{K}\right)\left(\frac{m_{ix}}{(m_{ix}+m_{jx})}\right)$ for strain i from blood meal x. The sporozoites from different blood meals are considered separately for the purposes of tracking the human host's exposure to each strain. If the host receives sporozoites of strain i that were derived from 3 different blood meals, then the 'count' of strain i isolates the host has encountered increases by 3, even though the parasites were introduced by the same mosquito. However, when a mosquito acquires gametocytes from a host, the gametocytes of each strain are considered to constitute one isolate, even if they were derived from multiple introductions.

Infection in the human host also has a latent period of w days, which simulates the liver stage of the infection. At the end of the latent period, M merozoites are released for each sporozoite introduced w days before and are added to the circulating merozoites tracked by the within-host model. At this point, the host's 'exposure count' for each strain is updated to reflect the number of isolates represented among the newly-emerged parasites.

Populations and turnover

The human population consists of N_H hosts with ages uniformly distributed between zero and the human lifespan, a. A host that reaches age a is replaced by a host of age zero with a 'clean slate' – no current infection or latent infection, no history of infection, no immunity. The mosquito population is similar (except for

having a much higher rate of turnover); the population consists of N_M mosquitoes that are evenly divided between ages zero to z (the mosquito lifespan), and each day the oldest mosquitoes are removed and replaced with new mosquitoes of age zero.

Treatment

The simulated use of antimalarial drugs is flexible in a few ways. Treatment can be made conditional on the total parasite density $(Y_1 + Y_2)$ exceeding a threshold, which can simulate treating only symptomatic infections or only infections detectable by standard diagnostic methods. Antimalarial drug use can be started in the middle of a simulation, to simulate introduction of a drug into a population at equilibrium. Treatment can also be restricted to start only on certain days, which can simulate mass drug administration (MDA) or mass screening and treatment (MSAT) where antimalarial drugs are administered en masse at regular intervals. Not all of these options are used in the simulations presented, but they provide opportunities to further explore the fate of drug resistance in scenarios not considered here.

Model parameters

Table A11. Default model parameters; those varied for the simulations presented in this work are noted as such.

Variable or Parameter	Value	Definition
B	$(5/12) \times 10^5$	Production rate of new RBCs (per μL per day)
α_X	$1/120$	Death rate of uninfected RBCs
β	2.4×10^{-6}	Infection rate (merozoite invasion of RBCs)
ε_i	$\varepsilon_1 = 0.95,\ \varepsilon_2 = 0$	Antimalarial drug efficacy against strain i
α_Y	0.5	Death rate of infected RBCs
γ	0.02	Gametocyte formation rate
δ_I	4	Rate of killing by adaptive immunity
ω_i	depends on infection history	Effect of adaptive immunity to strain i on other strain
δ_Z	4	Rate of killing by innate immunity
R	16	Burst size (merozoites per infected erythrocyte)
φ_i	varies	Fitness cost (growth reduction) of strain i
α_S	48	Death rate of free merozoites
α_G	0.0625	Death rate of gametocytes
ζ	3×10^{-5}	Growth rate of innate immunity
α_Z	0.5	Decay rate of innate immunity
σ	1	Maximum growth rate of adaptive immunity

θ	10^3	Shape parameter (adaptive immunity growth curve)
ψ	0.1	Decay rate of adaptive immunity due to antigenic escape
A	120	Shape parameter (adaptive immunity decay due to antigenic escape)
k	8	Shape parameter (adaptive immunity decay due to antigenic escape)
α_I	10^{-3}	Background decay rate of adaptive immunity
I_N	10^{-3}	Starting value of adaptive immunity to each strain
Ω	10^{-4}	Extinction threshold (infected RBC density)
L	14	Duration of treatment (days)
z	14	Mosquito lifespan (days)
y	10	Latent period in mosquito (days)
w	12	Latent period (liver stage) in humans
V	2	Blood meal volume (μL)
n	12	Number of sporozoites introduced by each mosquito bite
M	10^4	Number of merozoites produced per sporozoite (liver stage)
a	3000	Human lifespan (days)
N_H	400	Human population size
N_M	1.2×10^4	Mosquito population size
b	Varies	Mean number of mosquito bites per person per day

λ	varies	Proportion of fixed antigen epitopes shared between substrains of the same strain
μ	varies	Proportion of variant antigen epitopes shared between substrains of the same strain
η	varies	Proportion of fixed antigen epitopes shared between strains
ν	varies	Proportion of variant antigen epitopes shared between strains
Y_{TR}	varies	Minimum infected RBC density required for detection and treatment
p_{TR}	varies	Probability host treated if other conditions met
τ	1	Interval (days) at which hosts are screened and treatment initiated
ι_i	$\iota_1 = 0.1, \iota_2 = 0.02$	Initial fraction of hosts infected with strain i
d	0.0446	Mosquito infection function parameter [99]
f_1	0.181	Mosquito infection function parameter [99]
f_2	0.881	Mosquito infection function parameter [99]
f_3	0.0904	Mosquito infection function parameter [99]
g_0	0.0382	Mosquito infection function parameter [99]
g_1	0.165	Mosquito infection function parameter [99]
g_2	51.4	Mosquito infection function parameter [99]
g_3	0.0129	Mosquito infection function parameter [99]

Simulation parameters

Simulations were run with a semi-factorial design (Figure A10).

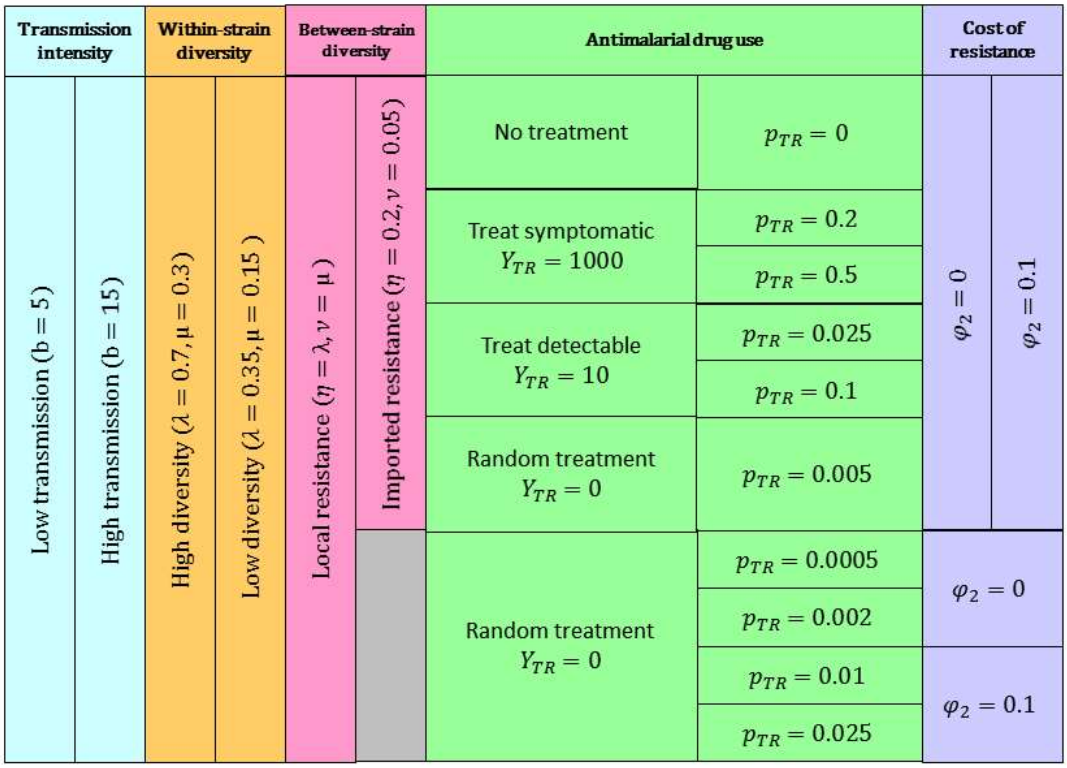

Figure A10. Combinations of parameters used for simulations; the actual parameter combinations are shown in Table A12.

Table A12. Parameter combinations used for simulations. Organization is hierarchical and follows that in Figure A10. The 'Figure' column gives the number of the figure showing the simulation output for each parameter set.

Sim #	Figure	b	lambda	mu	eta	nu	Y_TR	p_TR	phi_2
1	A11	5	0.7	0.3	0.7	0.3	1E+06	0	0

2	A12	5	0.7	0.3	0.7	0.3	1E+06	0	0.1
3	A13	5	0.7	0.3	0.7	0.3	1000	0.2	0
4	A14	5	0.7	0.3	0.7	0.3	1000	0.2	0.1
5	A15	5	0.7	0.3	0.7	0.3	1000	0.5	0
6	A16	5	0.7	0.3	0.7	0.3	1000	0.5	0.1
7	A17	5	0.7	0.3	0.7	0.3	10	0.025	0
8	A18	5	0.7	0.3	0.7	0.3	10	0.025	0.1
9	A19	5	0.7	0.3	0.7	0.3	10	0.1	0
10	A20	5	0.7	0.3	0.7	0.3	10	0.1	0.1
11	A21	5	0.7	0.3	0.7	0.3	0	5E-04	0
12	A22	5	0.7	0.3	0.7	0.3	0	0.002	0
13	A23	5	0.7	0.3	0.7	0.3	0	0.005	0
14	A24	5	0.7	0.3	0.7	0.3	0	0.005	0.1
15	A25	5	0.7	0.3	0.7	0.3	0	0.01	0.1
16	A26	5	0.7	0.3	0.7	0.3	0	0.025	0.1
17	A27	5	0.7	0.3	0.2	0.05	1E+06	0	0
18	A28	5	0.7	0.3	0.2	0.05	1E+06	0	0.1
19	A29	5	0.7	0.3	0.2	0.05	1000	0.2	0
20	A30	5	0.7	0.3	0.2	0.05	1000	0.2	0.1
21	A31	5	0.7	0.3	0.2	0.05	1000	0.5	0
22	A32	5	0.7	0.3	0.2	0.05	1000	0.5	0.1
23	A33	5	0.7	0.3	0.2	0.05	10	0.025	0
24	A34	5	0.7	0.3	0.2	0.05	10	0.025	0.1
25	A35	5	0.7	0.3	0.2	0.05	10	0.1	0

26	A36	5	0.7	0.3	0.2	0.05	10	0.1	0.1
27	A37	5	0.7	0.3	0.2	0.05	0	0.005	0
28	A38	5	0.7	0.3	0.2	0.05	0	0.005	0.1
29	A11	5	0.35	0.15	0.35	0.15	1E+06	0	0
30	A12	5	0.35	0.15	0.35	0.15	1E+06	0	0.1
31	A13	5	0.35	0.15	0.35	0.15	1000	0.2	0
32	A14	5	0.35	0.15	0.35	0.15	1000	0.2	0.1
33	A15	5	0.35	0.15	0.35	0.15	1000	0.5	0
34	A16	5	0.35	0.15	0.35	0.15	1000	0.5	0.1
35	A17	5	0.35	0.15	0.35	0.15	10	0.025	0
36	A18	5	0.35	0.15	0.35	0.15	10	0.025	0.1
37	A19	5	0.35	0.15	0.35	0.15	10	0.1	0
38	A20	5	0.35	0.15	0.35	0.15	10	0.1	0.1
39	A21	5	0.35	0.15	0.35	0.15	0	5E-04	0
40	A22	5	0.35	0.15	0.35	0.15	0	0.002	0
41	A23	5	0.35	0.15	0.35	0.15	0	0.005	0
42	A24	5	0.35	0.15	0.35	0.15	0	0.005	0.1
43	A25	5	0.35	0.15	0.35	0.15	0	0.01	0.1
44	A26	5	0.35	0.15	0.35	0.15	0	0.025	0.1
45	A27	5	0.35	0.15	0.2	0.05	1E+06	0	0
46	A28	5	0.35	0.15	0.2	0.05	1E+06	0	0.1
47	A29	5	0.35	0.15	0.2	0.05	1000	0.2	0
48	A30	5	0.35	0.15	0.2	0.05	1000	0.2	0.1
49	A31	5	0.35	0.15	0.2	0.05	1000	0.5	0

50	A32	5	0.35	0.15	0.2	0.05	1000	0.5	0.1
51	A33	5	0.35	0.15	0.2	0.05	10	0.025	0
52	A34	5	0.35	0.15	0.2	0.05	10	0.025	0.1
53	A35	5	0.35	0.15	0.2	0.05	10	0.1	0
54	A36	5	0.35	0.15	0.2	0.05	10	0.1	0.1
55	A37	5	0.35	0.15	0.2	0.05	0	0.005	0
56	A38	5	0.35	0.15	0.2	0.05	0	0.005	0.1
57	A11	15	0.7	0.3	0.7	0.3	1E+06	0	0
58	A12	15	0.7	0.3	0.7	0.3	1E+06	0	0.1
59	A13	15	0.7	0.3	0.7	0.3	1000	0.2	0
60	A14	15	0.7	0.3	0.7	0.3	1000	0.2	0.1
61	A15	15	0.7	0.3	0.7	0.3	1000	0.5	0
62	A16	15	0.7	0.3	0.7	0.3	1000	0.5	0.1
63	A17	15	0.7	0.3	0.7	0.3	10	0.025	0
64	A18	15	0.7	0.3	0.7	0.3	10	0.025	0.1
65	A19	15	0.7	0.3	0.7	0.3	10	0.1	0
66	A20	15	0.7	0.3	0.7	0.3	10	0.1	0.1
67	A21	15	0.7	0.3	0.7	0.3	0	5E-04	0
68	A22	15	0.7	0.3	0.7	0.3	0	0.002	0
69	A23	15	0.7	0.3	0.7	0.3	0	0.005	0
70	A24	15	0.7	0.3	0.7	0.3	0	0.005	0.1
71	A25	15	0.7	0.3	0.7	0.3	0	0.01	0.1
72	A26	15	0.7	0.3	0.7	0.3	0	0.025	0.1
73	A27	15	0.7	0.3	0.2	0.05	1E+06	0	0

74	A28	15	0.7	0.3	0.2	0.05	1E+06	0	0.1
75	A29	15	0.7	0.3	0.2	0.05	1000	0.2	0
76	A30	15	0.7	0.3	0.2	0.05	1000	0.2	0.1
77	A31	15	0.7	0.3	0.2	0.05	1000	0.5	0
78	A32	15	0.7	0.3	0.2	0.05	1000	0.5	0.1
79	A33	15	0.7	0.3	0.2	0.05	10	0.025	0
80	A34	15	0.7	0.3	0.2	0.05	10	0.025	0.1
81	A35	15	0.7	0.3	0.2	0.05	10	0.1	0
82	A36	15	0.7	0.3	0.2	0.05	10	0.1	0.1
83	A37	15	0.7	0.3	0.2	0.05	0	0.005	0
84	A38	15	0.7	0.3	0.2	0.05	0	0.005	0.1
85	A11	15	0.35	0.15	0.35	0.15	1E+06	0	0
86	A12	15	0.35	0.15	0.35	0.15	1E+06	0	0.1
87	A13	15	0.35	0.15	0.35	0.15	1000	0.2	0
88	A14	15	0.35	0.15	0.35	0.15	1000	0.2	0.1
89	A15	15	0.35	0.15	0.35	0.15	1000	0.5	0
90	A16	15	0.35	0.15	0.35	0.15	1000	0.5	0.1
91	A17	15	0.35	0.15	0.35	0.15	10	0.025	0
92	A18	15	0.35	0.15	0.35	0.15	10	0.025	0.1
93	A19	15	0.35	0.15	0.35	0.15	10	0.1	0
94	A20	15	0.35	0.15	0.35	0.15	10	0.1	0.1
95	A21	15	0.35	0.15	0.35	0.15	0	5E-04	0
96	A22	15	0.35	0.15	0.35	0.15	0	0.002	0
97	A23	15	0.35	0.15	0.35	0.15	0	0.005	0

98	A24	15	0.35	0.15	0.35	0.15	0	0.005	0.1
99	A25	15	0.35	0.15	0.35	0.15	0	0.01	0.1
100	A26	15	0.35	0.15	0.35	0.15	0	0.025	0.1
101	A27	15	0.35	0.15	0.2	0.05	1E+06	0	0
102	A28	15	0.35	0.15	0.2	0.05	1E+06	0	0.1
103	A29	15	0.35	0.15	0.2	0.05	1000	0.2	0
104	A30	15	0.35	0.15	0.2	0.05	1000	0.2	0.1
105	A31	15	0.35	0.15	0.2	0.05	1000	0.5	0
106	A32	15	0.35	0.15	0.2	0.05	1000	0.5	0.1
107	A33	15	0.35	0.15	0.2	0.05	10	0.025	0
108	A34	15	0.35	0.15	0.2	0.05	10	0.025	0.1
109	A35	15	0.35	0.15	0.2	0.05	10	0.1	0
110	A36	15	0.35	0.15	0.2	0.05	10	0.1	0.1
111	A37	15	0.35	0.15	0.2	0.05	0	0.005	0
112	A38	15	0.35	0.15	0.2	0.05	0	0.005	0.1

Model output (all simulations)

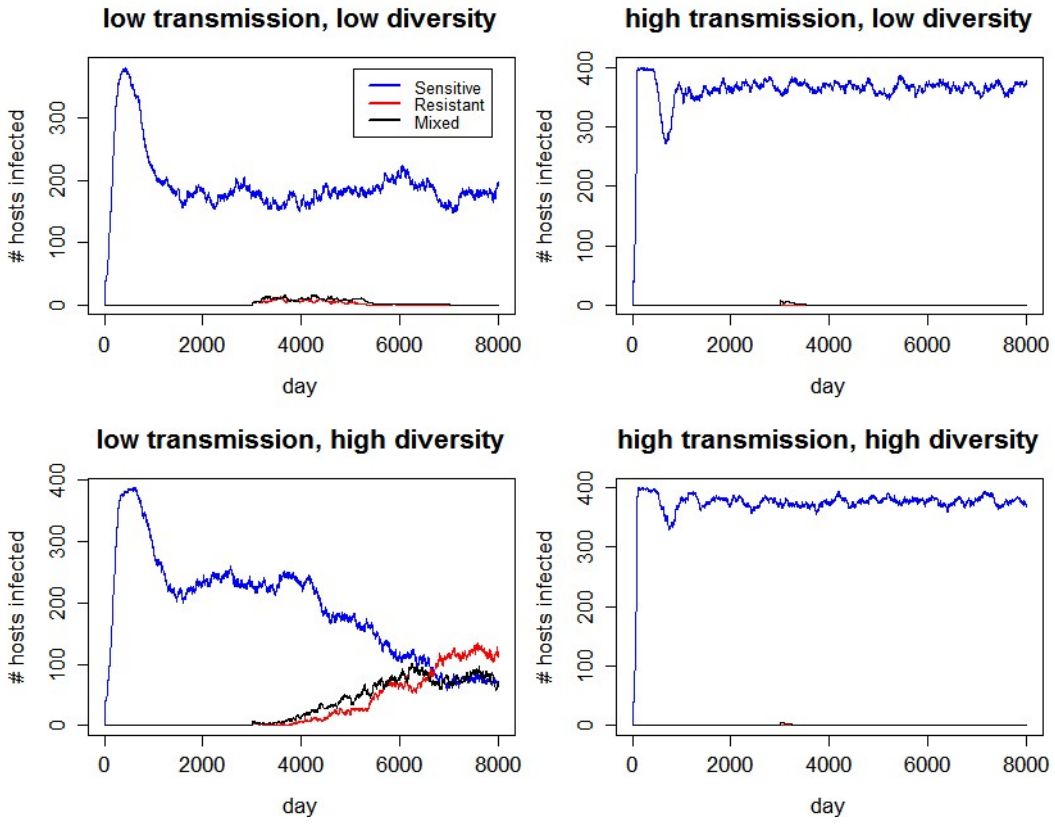

Figure A11. Simulation parameters: $\eta = \lambda, \nu = \mu, p_{TR}$=0, $\varphi_2 = 0$. Simulation numbers: 1 (top left), 29 (bottom left), 57 (top right), 85 (bottom right).

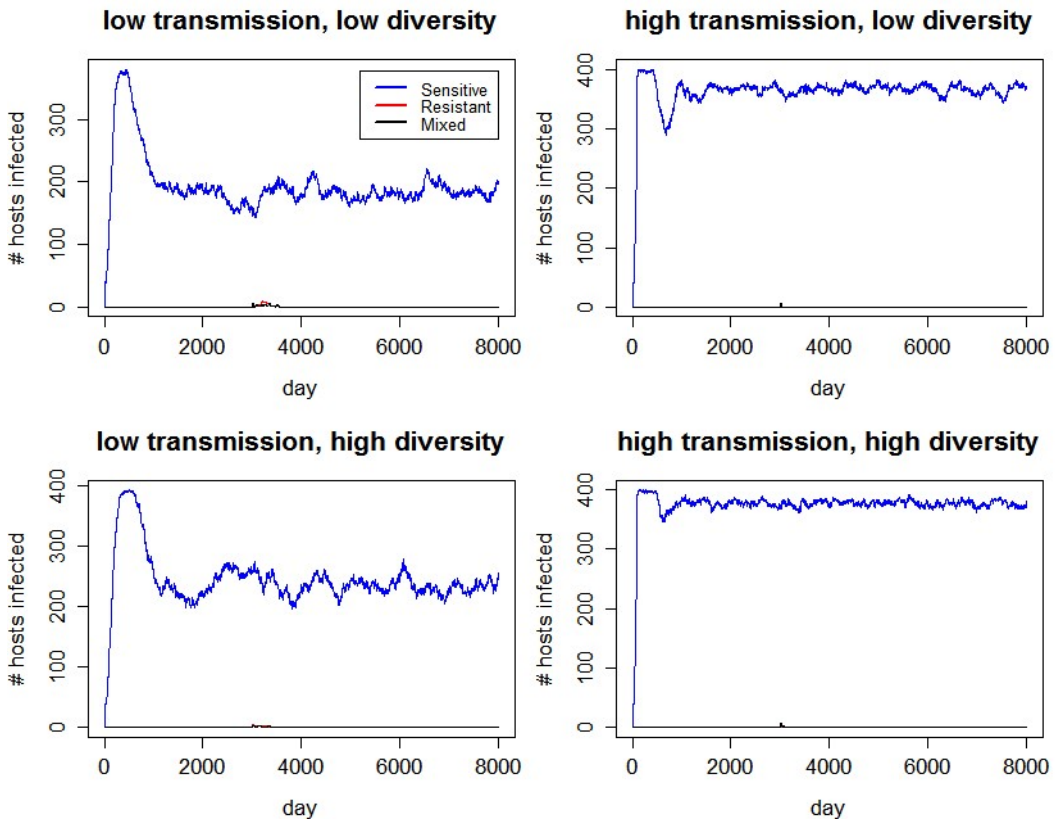

Figure A12. Simulation parameters: $\eta = \lambda, \nu = \mu, p_{TR}$=0, $\varphi_2 = 0.1$. Simulation numbers: 2 (top left), 30 (bottom left), 58 (top right), 86 (bottom right).

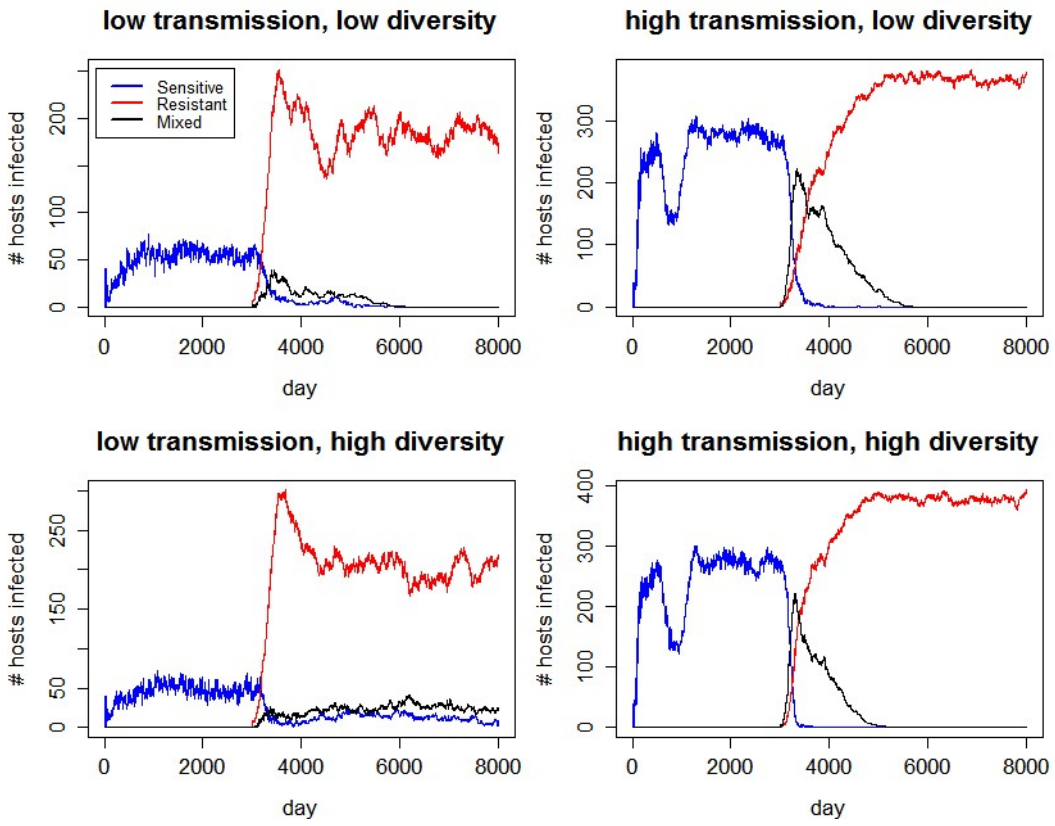

Figure A13. Simulation parameters: $\eta = \lambda, \nu = \mu$, Y_{TR}=1000, p_{TR}=0. 2, $\varphi_2 = 0$. Simulation numbers: 3 (top left), 31 (bottom left), 59 (top right), 87 (bottom right).

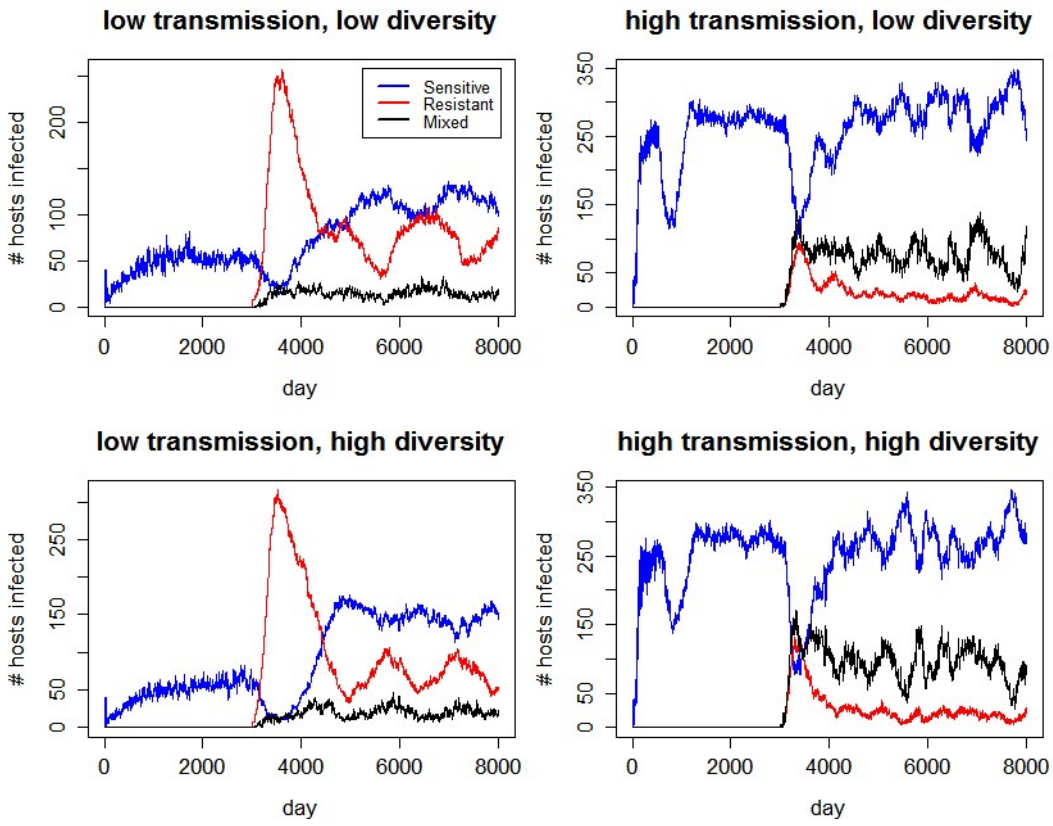

Figure A14. Simulation parameters: $\eta = \lambda, \nu = \mu$, Y_{TR}=1000, p_{TR}=0. 2, $\varphi_2 = 0.1$. Simulation numbers: 4 (top left), 32 (bottom left), 60 (top right), 88 (bottom right).

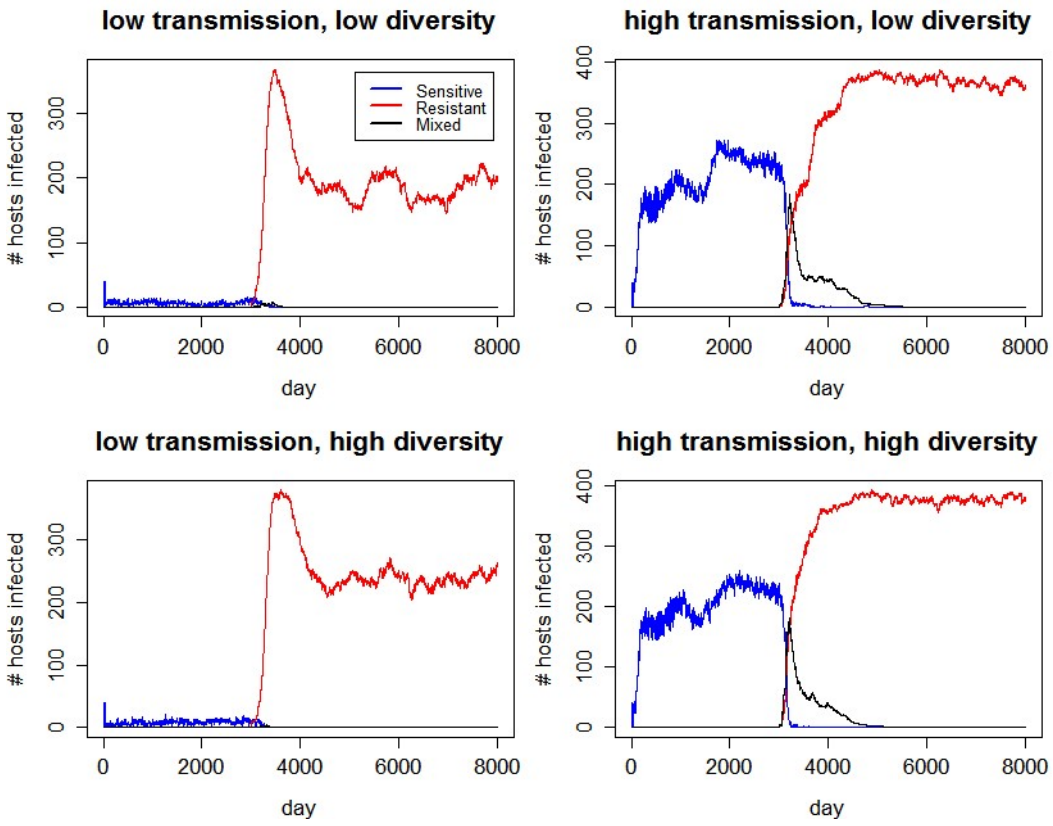

Figure A15. Simulation parameters: $\eta = \lambda, \nu = \mu, Y_{TR}$=1000, p_{TR}=0. 5, $\varphi_2 = 0$. Simulation numbers: 5 (top left), 33 (bottom left), 61 (top right), 89 (bottom right).

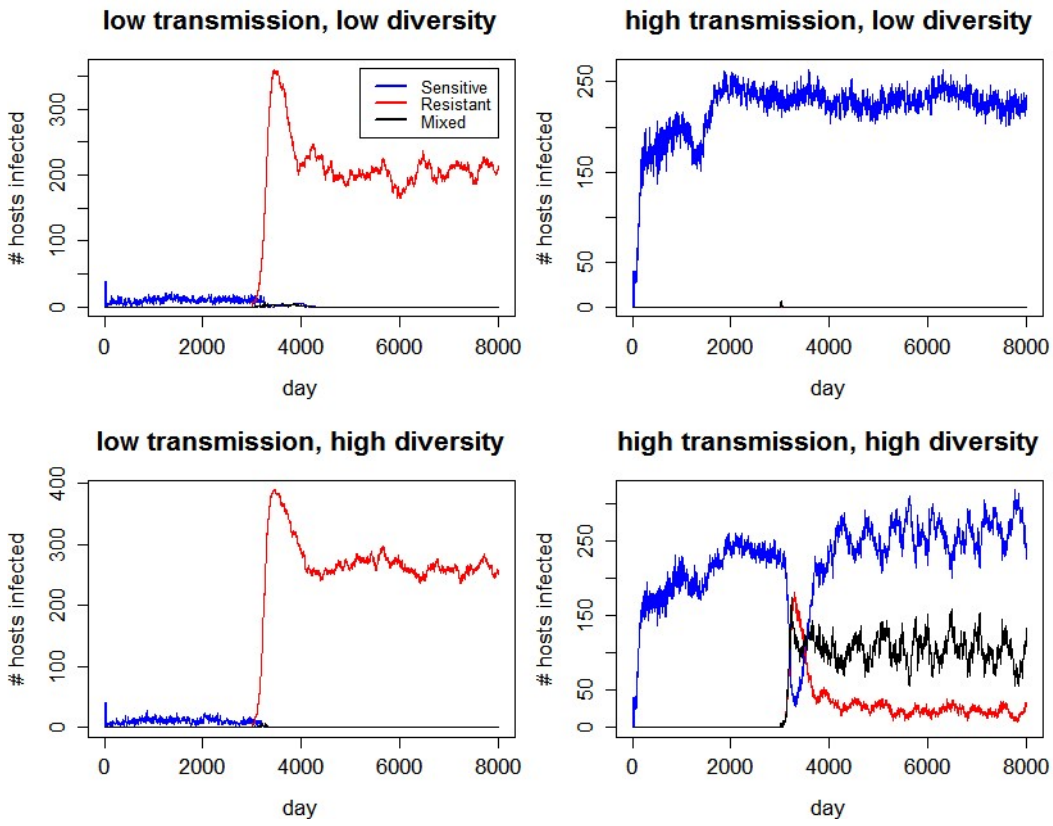

Figure A16. Simulation parameters: $\eta = \lambda, \nu = \mu$, Y_{TR}=1000, p_{TR}=0. 5, $\varphi_2 = 0.1$. Simulation numbers: 6 (top left), 34 (bottom left), 62 (top right), 90 (bottom right).

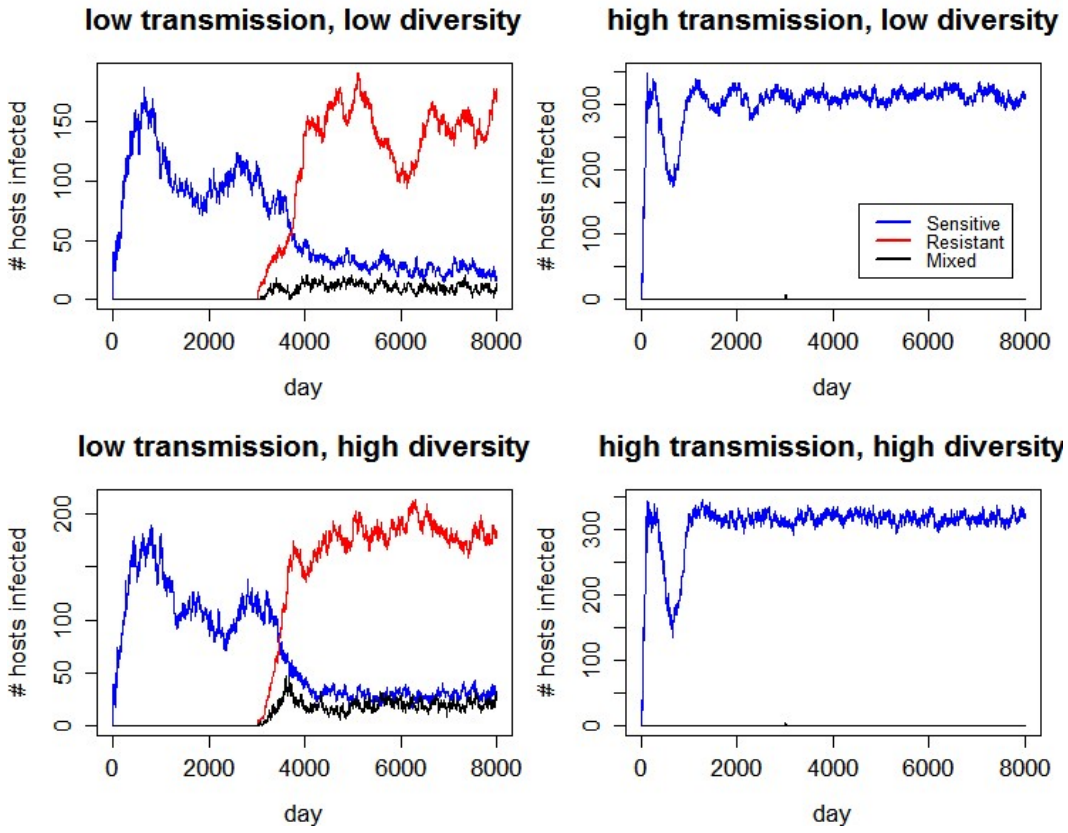

Figure A17. Simulation parameters: $\eta = \lambda, \nu = \mu$, Y_{TR}=10, p_{TR}=0.025, $\varphi_2 = 0$. Simulation numbers: 7 (top left), 35 (bottom left), 63 (top right), 91 (bottom right).

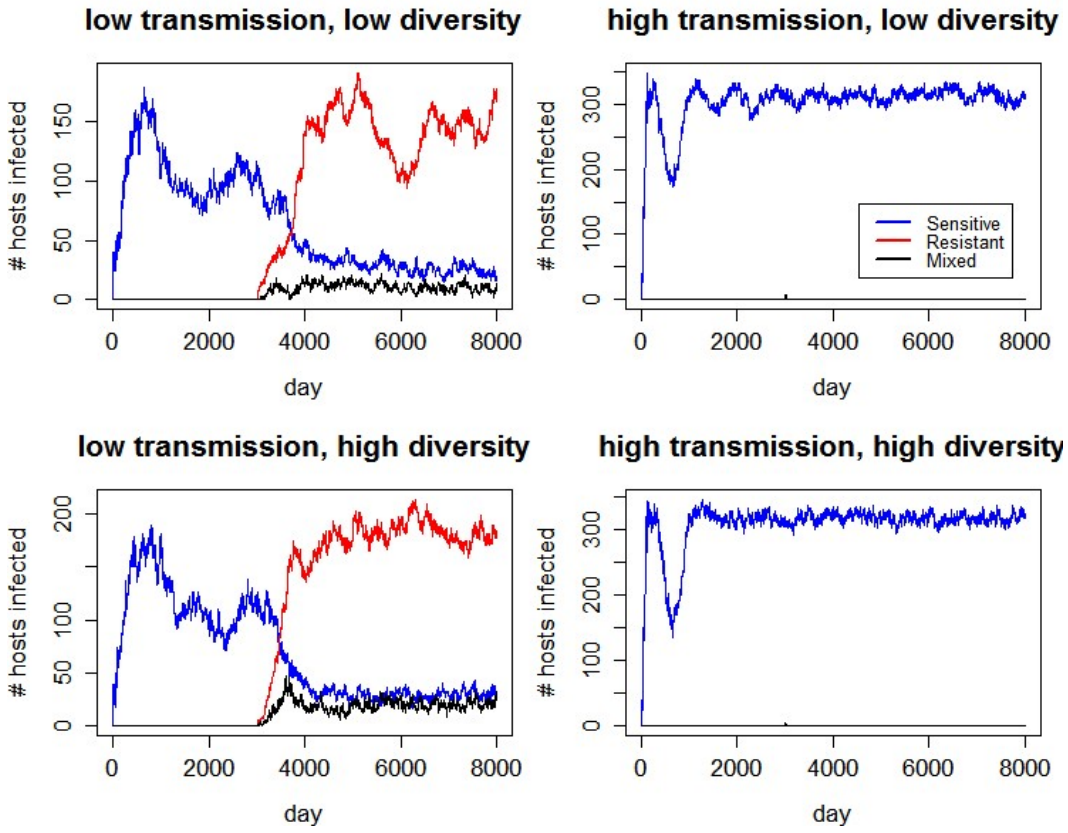

Figure A18. Simulation parameters: $\eta = \lambda, \nu = \mu$, Y_{TR}=10, p_{TR}=0.025, $\varphi_2 = 0.1$. Simulation numbers: 8 (top left), 36 (bottom left), 64 (top right), 92 (bottom right).

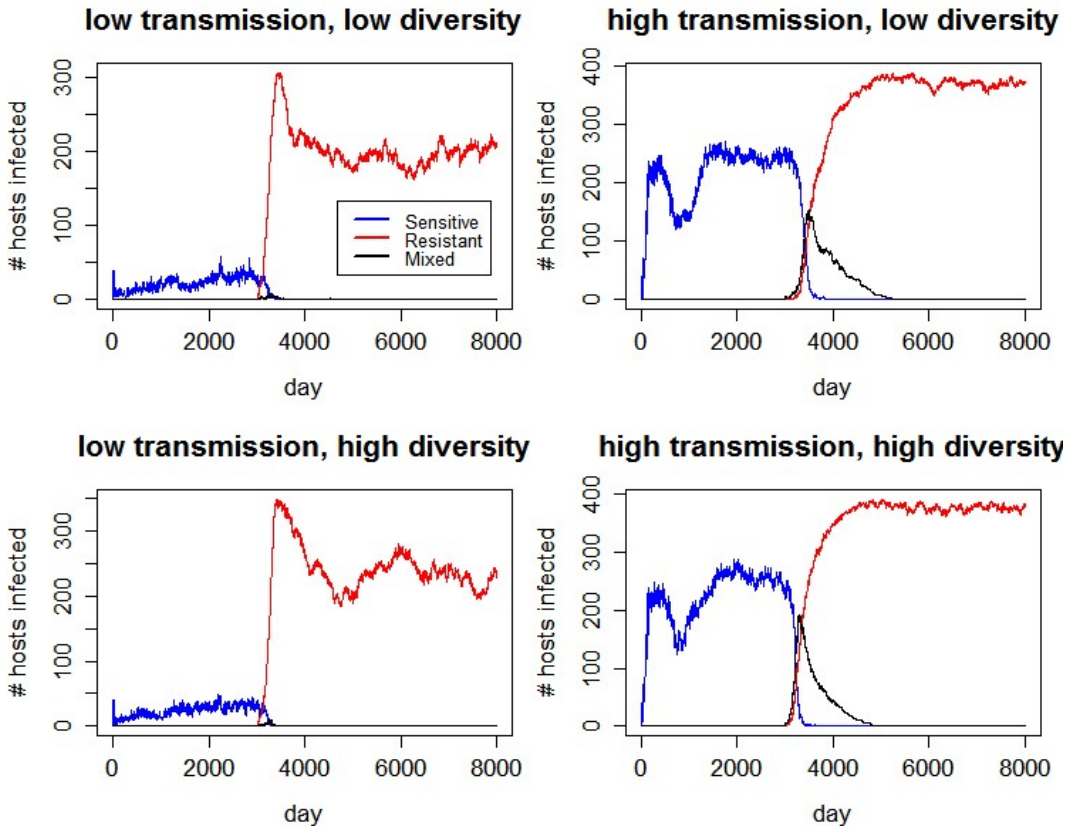

Figure A19. Simulation parameters: $\eta = \lambda, \nu = \mu$, Y_{TR}=10, p_{TR}=0.1, $\varphi_2 = 0$. Simulation numbers: 9 (top left), 37 (bottom left), 65 (top right), 93 (bottom right).

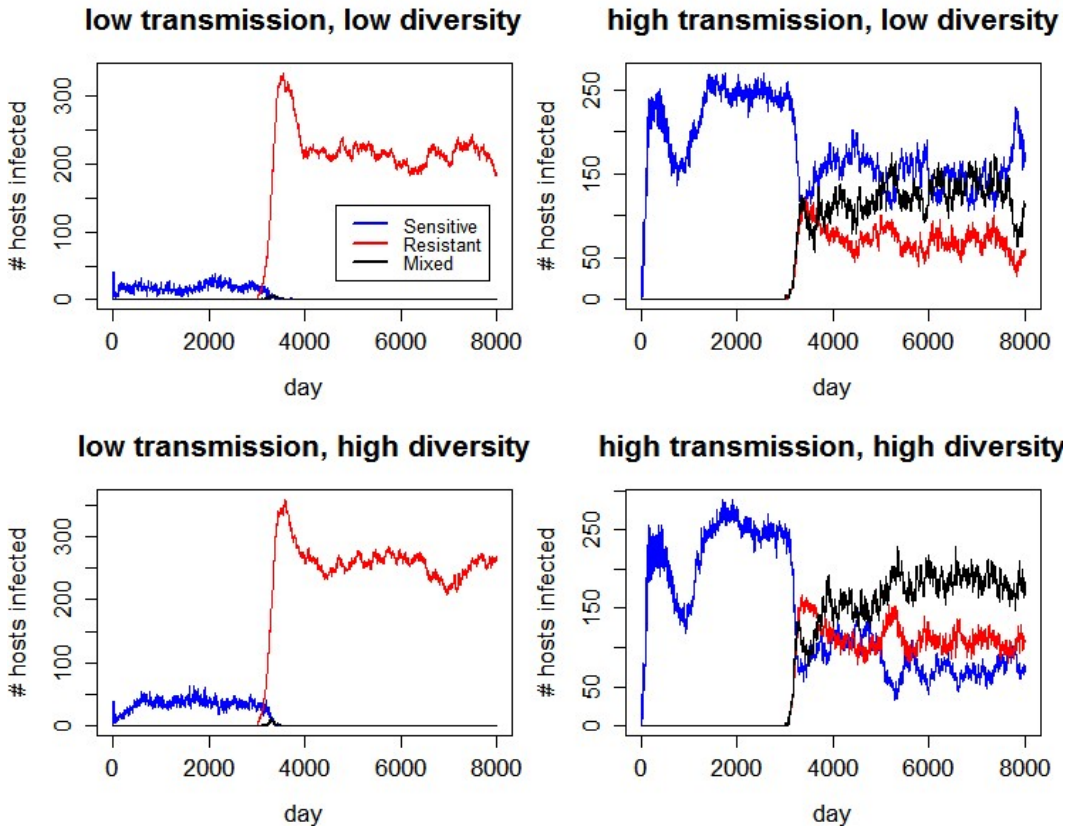

Figure A20. Simulation parameters: $\eta = \lambda, \nu = \mu$, Y_{TR}=10, p_{TR}=0.1, $\varphi_2 = 0.1$. Simulation numbers: 10 (top left), 38 (bottom left), 66 (top right), 94 (bottom right).

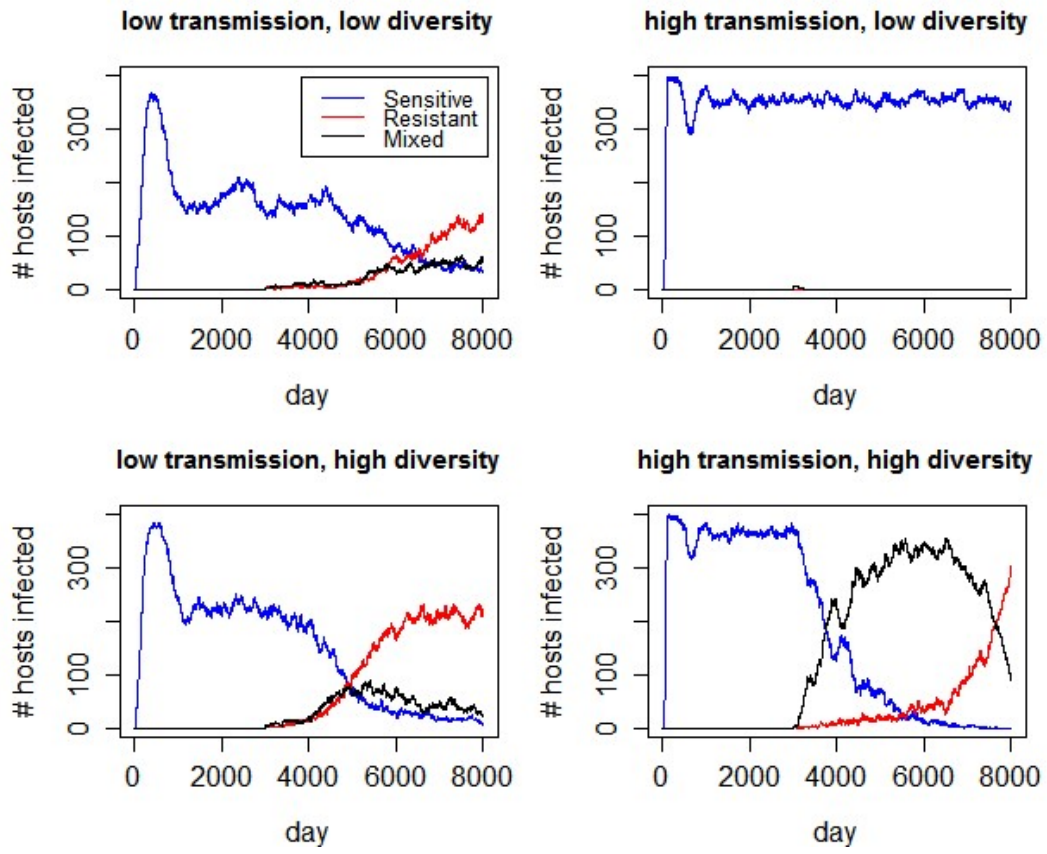

Figure A21. Simulation parameters: $\eta = \lambda, \nu = \mu$, Y_{TR}=0, p_{TR}=0.0005, $\varphi_2 = 0$. Simulation numbers: 11 (top left), 39 (bottom left), 67 (top right), 95 (bottom right).

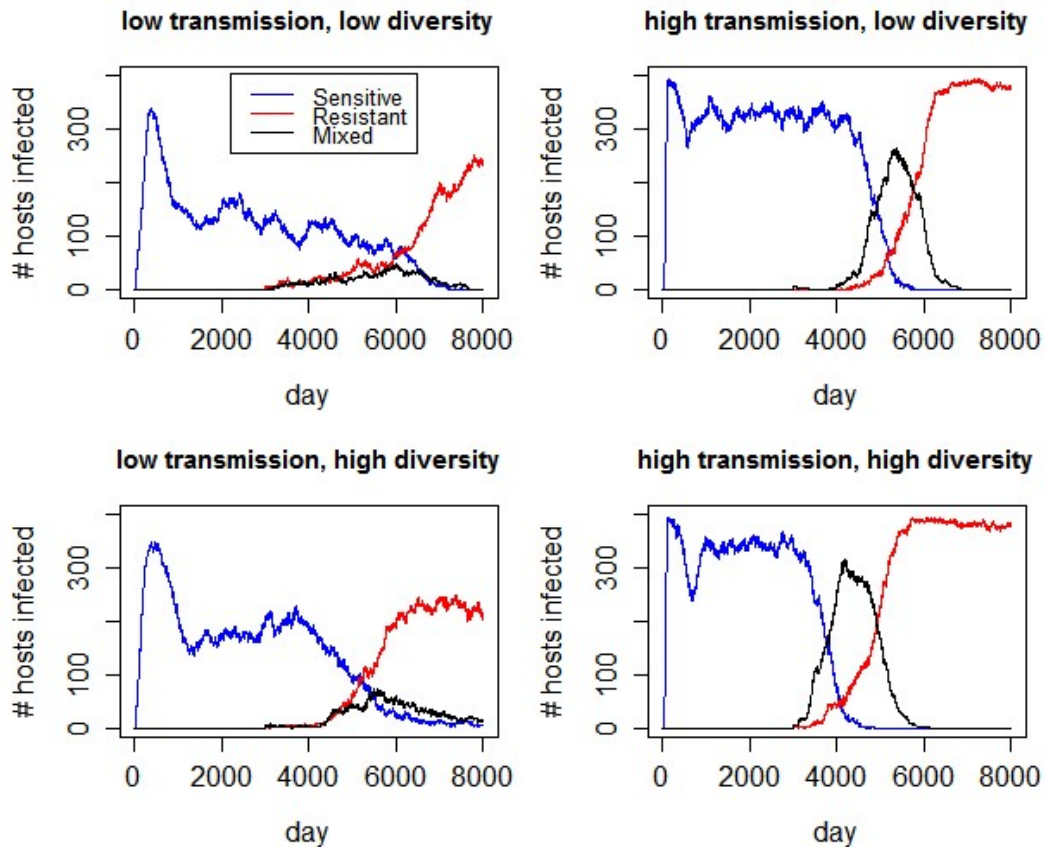

Figure A22. Simulation parameters: $\eta = \lambda, \nu = \mu$, Y_{TR}=0, p_{TR}=0.002, $\varphi_2 = 0$. Simulation numbers: 12 (top left), 40 (bottom left), 68 (top right), 96 (bottom right).

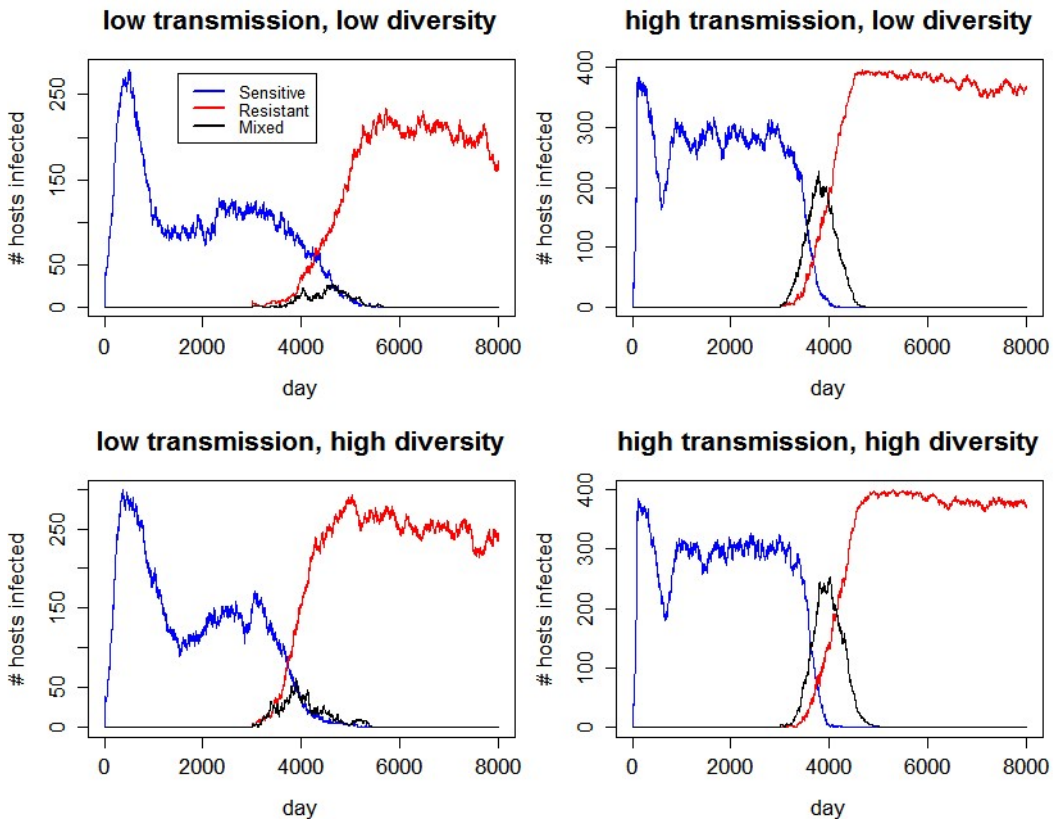

Figure A23. Simulation parameters: $\eta = \lambda, \nu = \mu$, Y_{TR}=0, p_{TR}=0.005, $\varphi_2 = 0$. Simulation numbers: 13 (top left), 41 (bottom left), 69 (top right), 97 (bottom right).

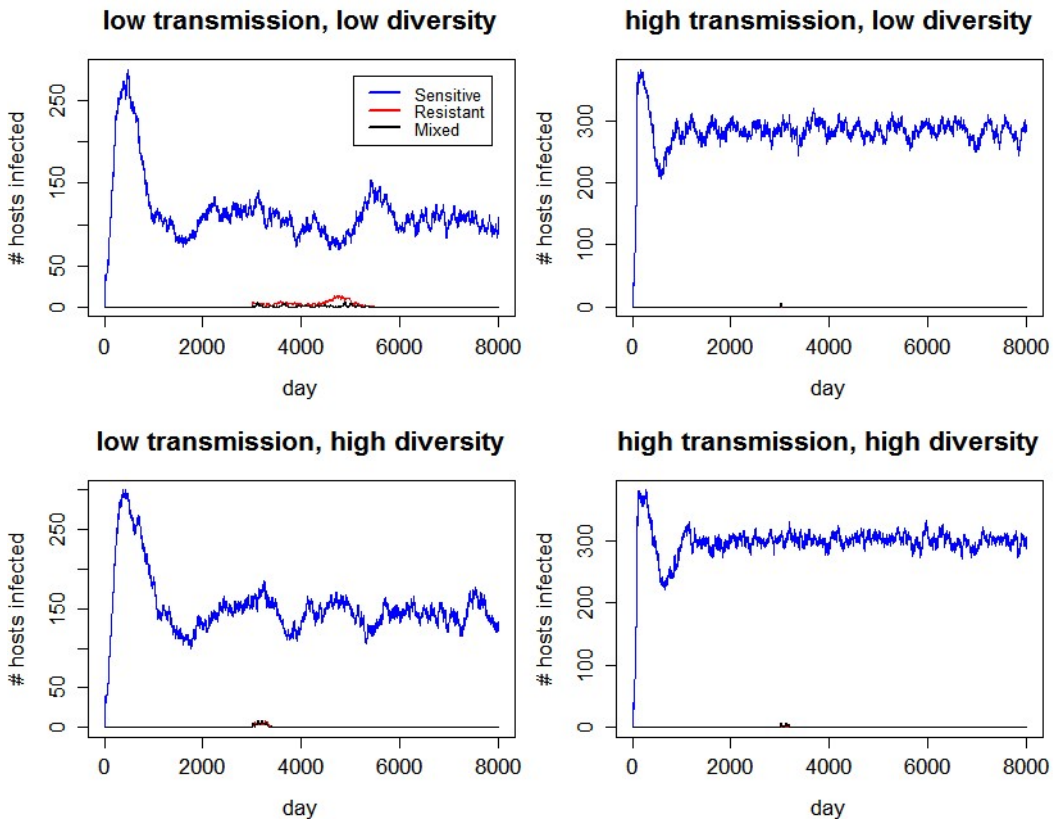

Figure A24. Simulation parameters: $\eta = \lambda, \nu = \mu$, Y_{TR}=0, p_{TR}=0.005, $\varphi_2 = 0.1$. Simulation numbers: 14 (top left), 42 (bottom left), 70 (top right), 98 (bottom right).

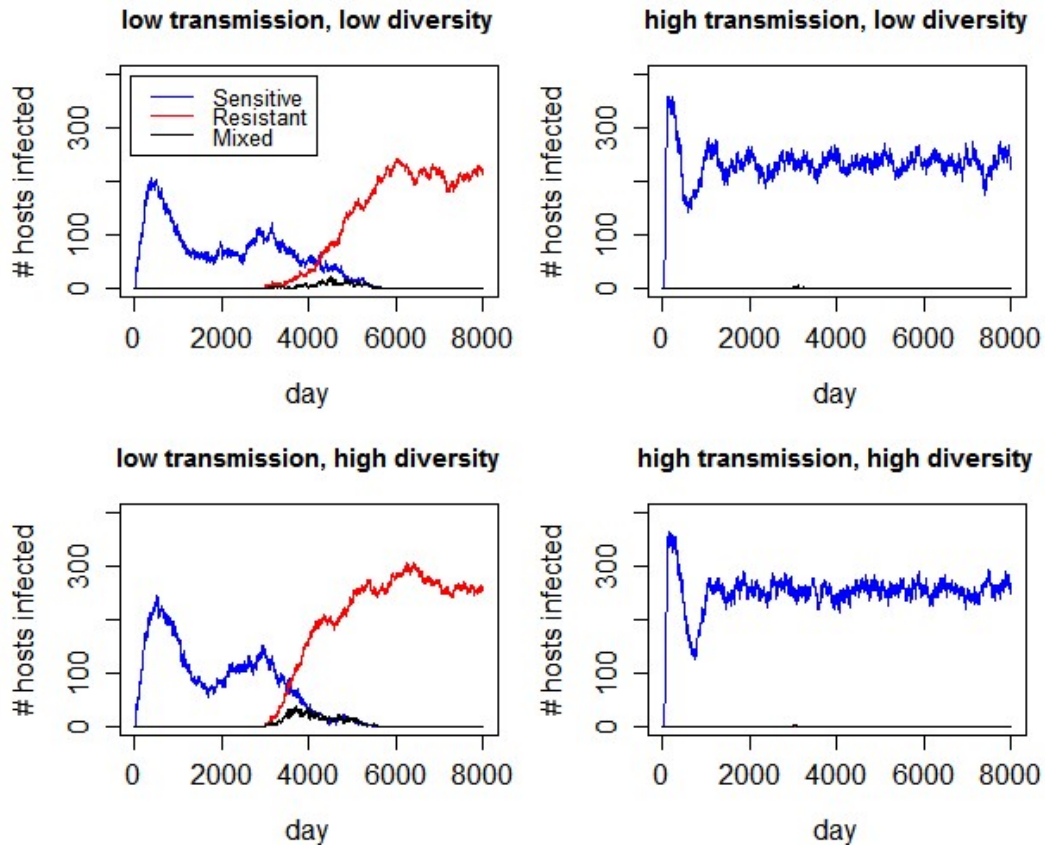

Figure A25. Simulation parameters: $\eta = \lambda, \nu = \mu$, Y_{TR}=0, p_{TR}=0.01, $\varphi_2 = 0.1$. Simulation numbers: 15 (top left), 43 (bottom left), 71 (top right), 99 (bottom right).

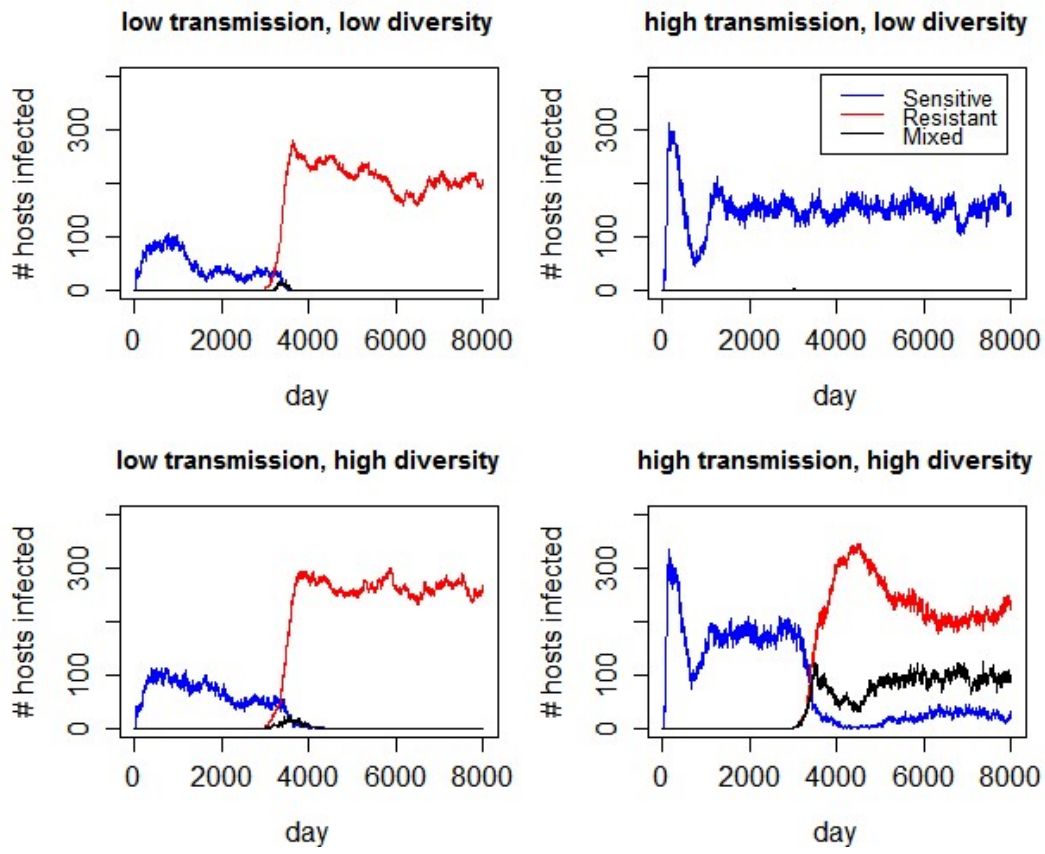

Figure A26. Simulation parameters: $\eta = \lambda, \nu = \mu$, Y_{TR}=0, p_{TR}=0.025, $\varphi_2 = 0.1$. Simulation numbers: 16 (top left), 44 (bottom left), 72 (top right), 100 (bottom right).

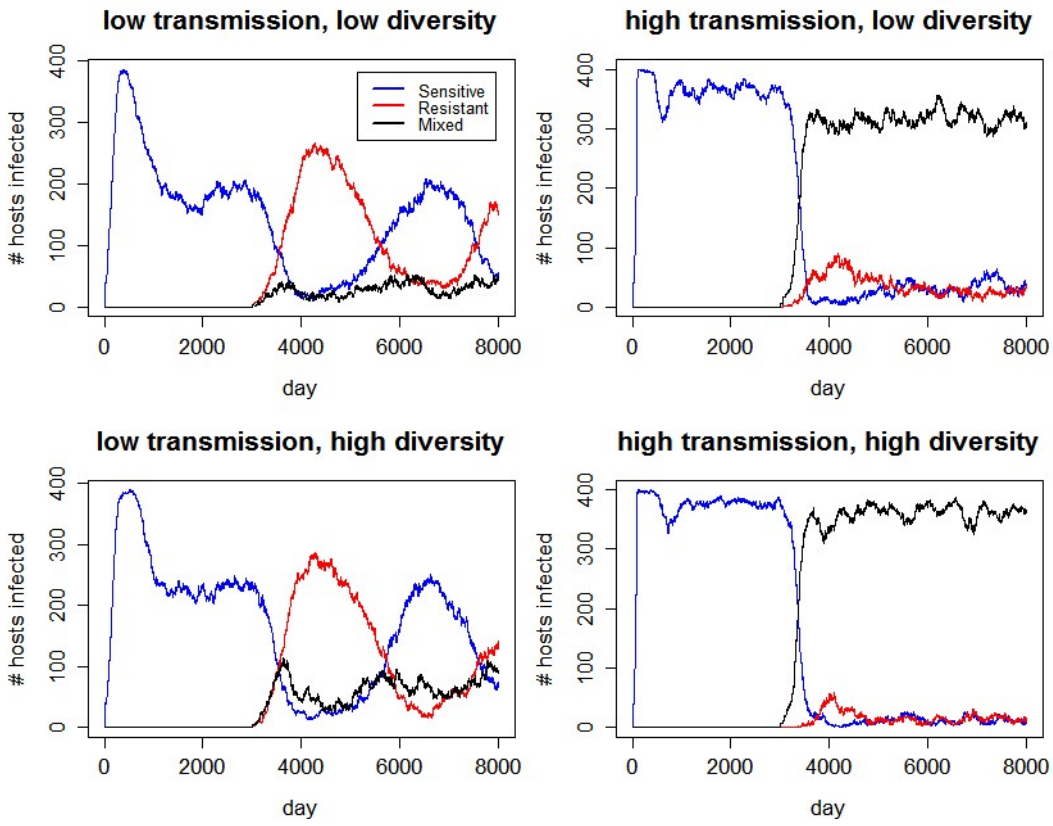

Figure A27. Simulation parameters: $\eta = 0.2, \nu = 0.05, p_{TR}$=0, $\varphi_2 = 0$. Simulation numbers: 17 (top left), 45 (bottom left), 73 (top right), 101 (bottom right).

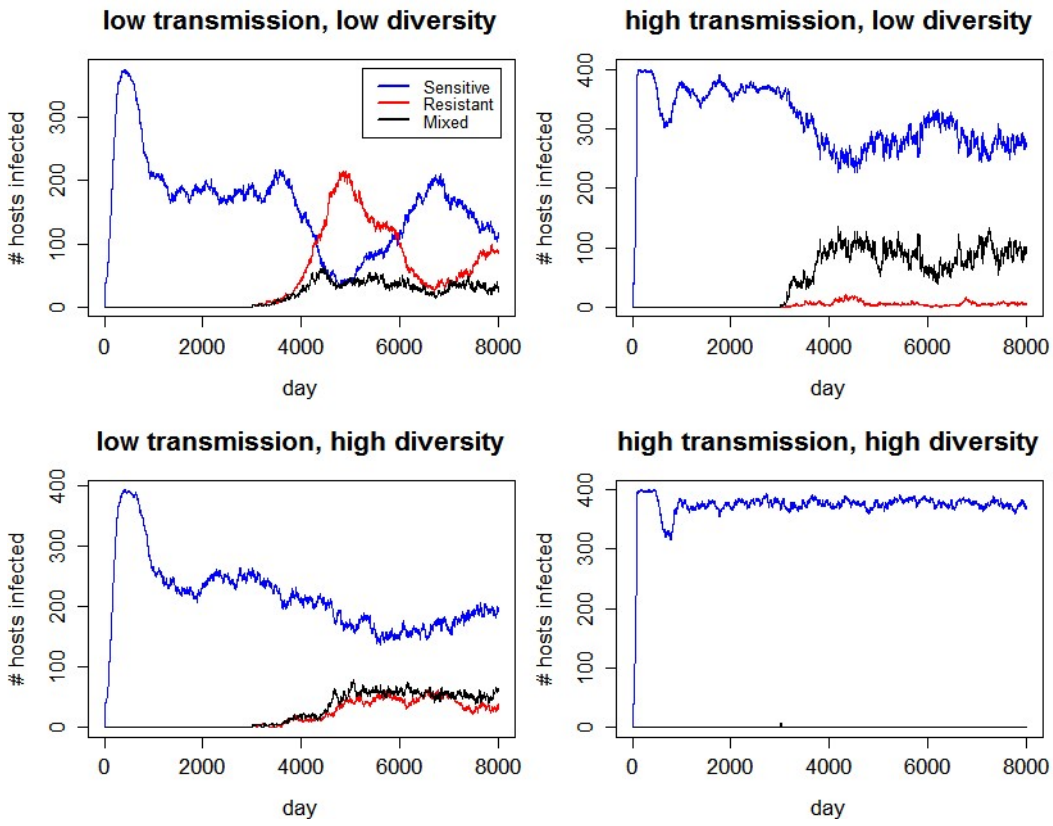

Figure A28. Simulation parameters: $\eta = 0.2, \nu = 0.05, p_{TR}$=0, $\varphi_2 = 0.1$. Simulation numbers: 18 (top left), 46 (bottom left), 74 (top right), 102 (bottom right).

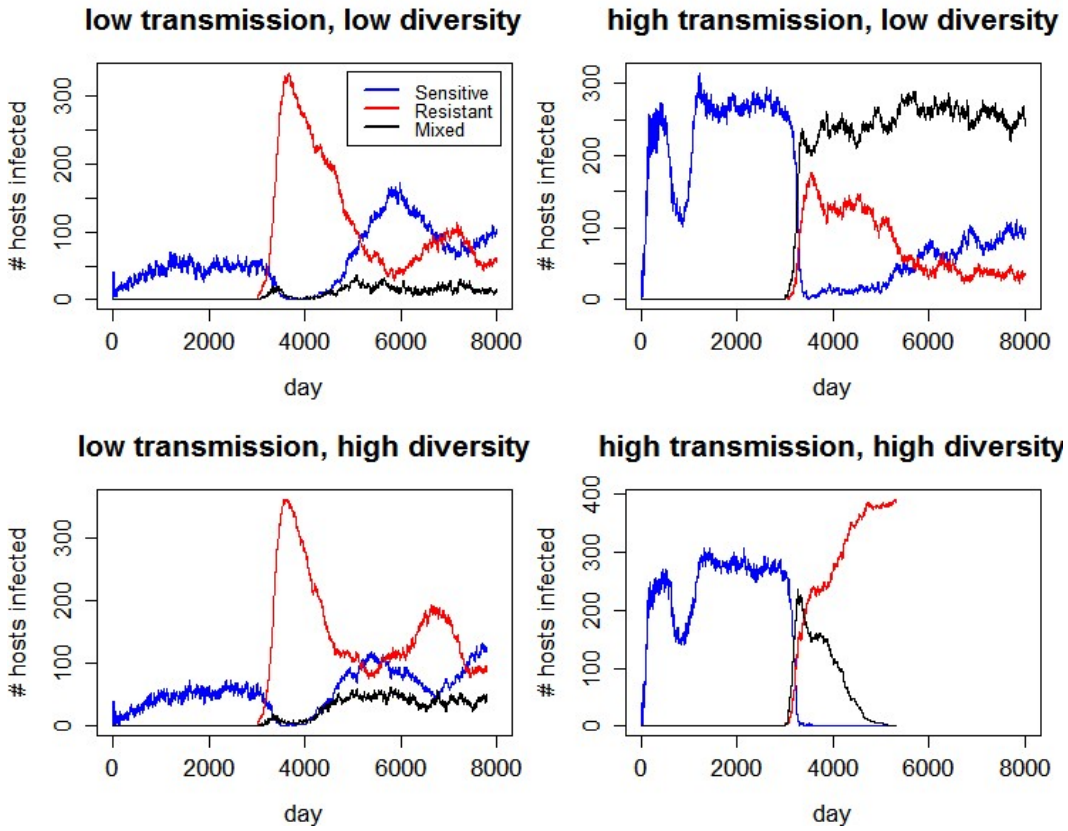

Figure A29. Simulation parameters: $\eta = 0.2, \nu = 0.05, Y_{TR} = 1000, p_{TR}$=0.2, $\varphi_2 = 0$.

Simulation numbers: 19 (top left), 47 (bottom left), 75 (top right), 103 (bottom right).

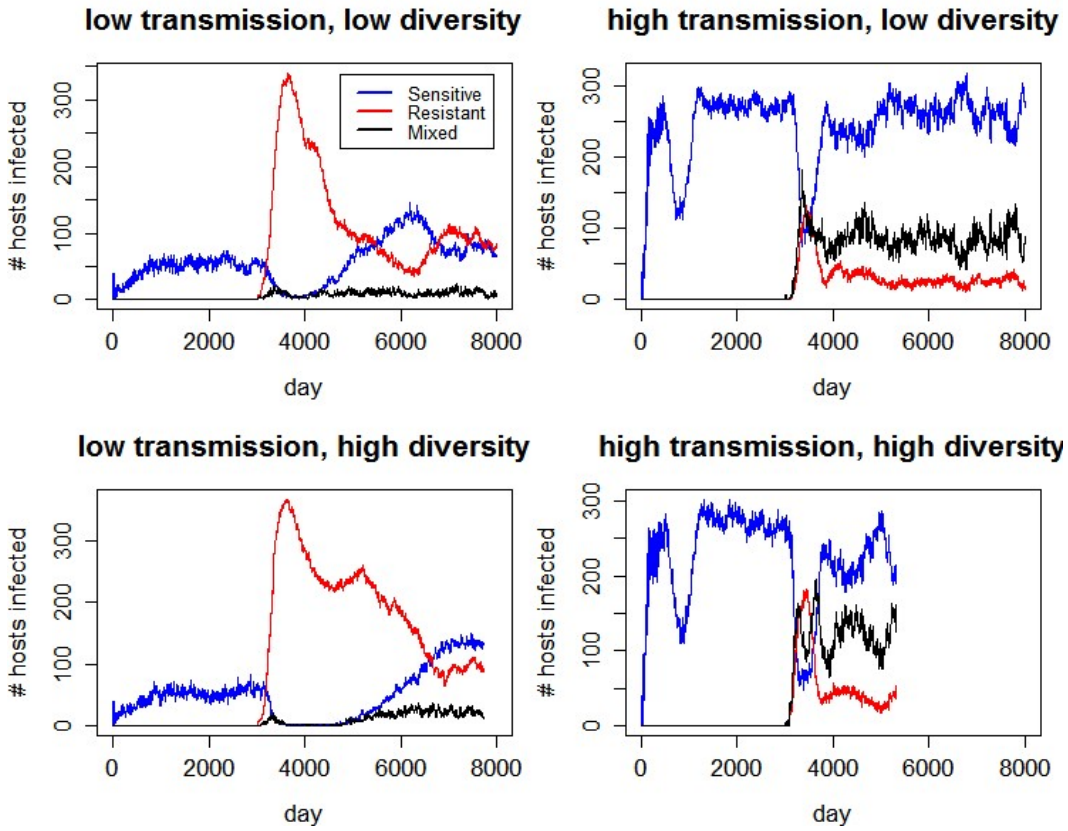

Figure A30. Simulation parameters: $\eta = 0.2, \nu = 0.05, Y_{TR} = 1000, p_{TR}$=0.2, $\varphi_2 = 0.1$.

Simulation numbers: 20 (top left), 48 (bottom left), 76 (top right), 104 (bottom right).

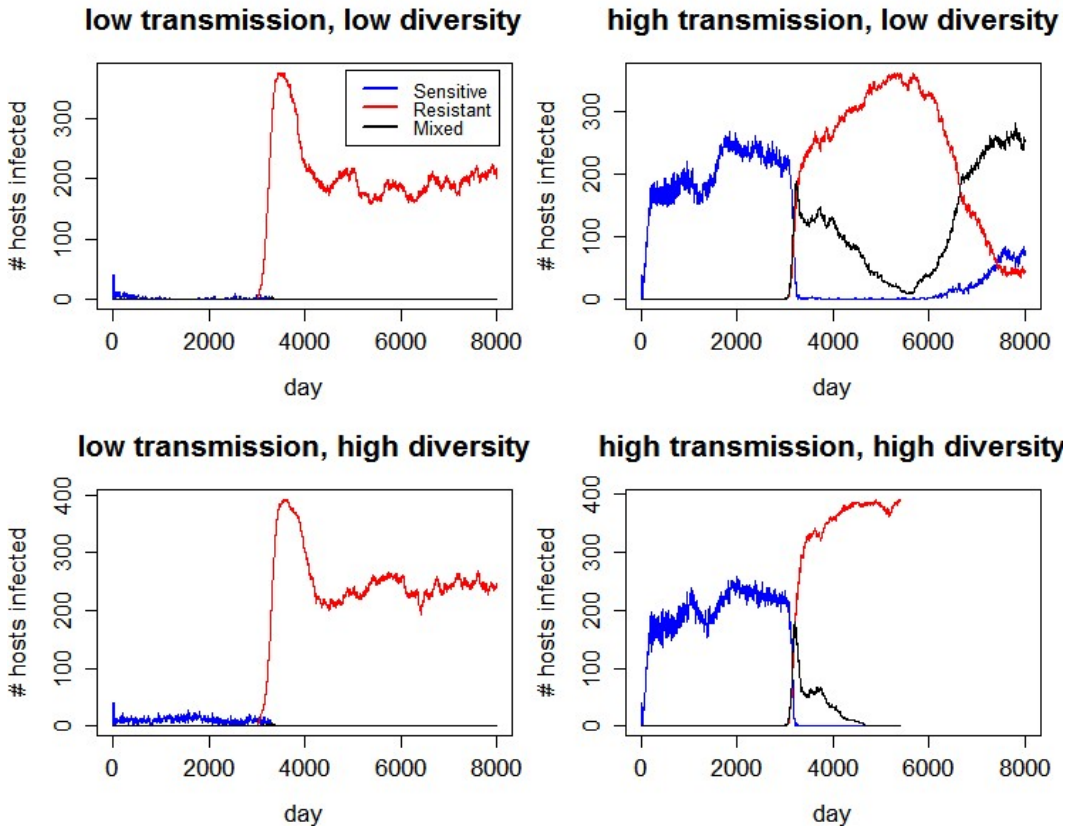

Figure A31. Simulation parameters: $\eta = 0.2, \nu = 0.05, Y_{TR} = 1000, p_{TR}$=0.5, $\varphi_2 = 0$.

Simulation numbers: 21 (top left), 49 (bottom left), 77 (top right), 105 (bottom right).

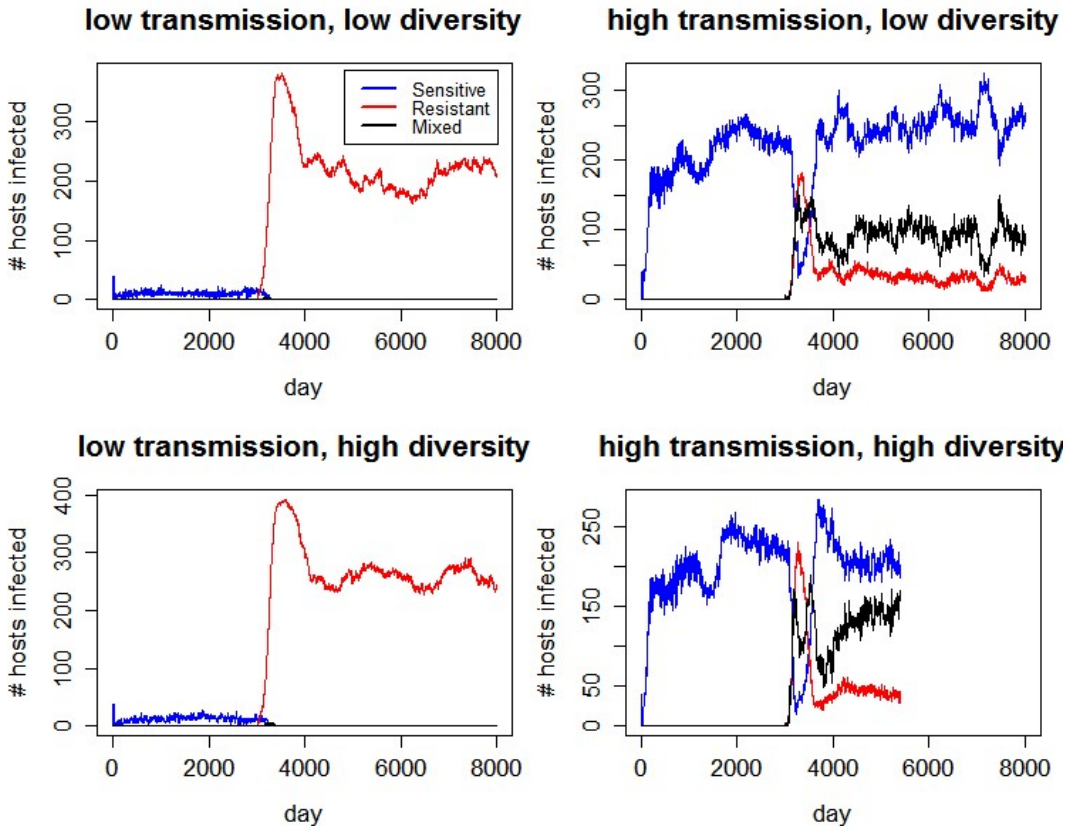

Figure A32. Simulation parameters: $\eta = 0.2, \nu = 0.05, Y_{TR} = 1000, p_{TR}$=0.5, $\varphi_2 = 0.1$.

Simulation numbers: 22 (top left), 50 (bottom left), 78 (top right), 106 (bottom right).

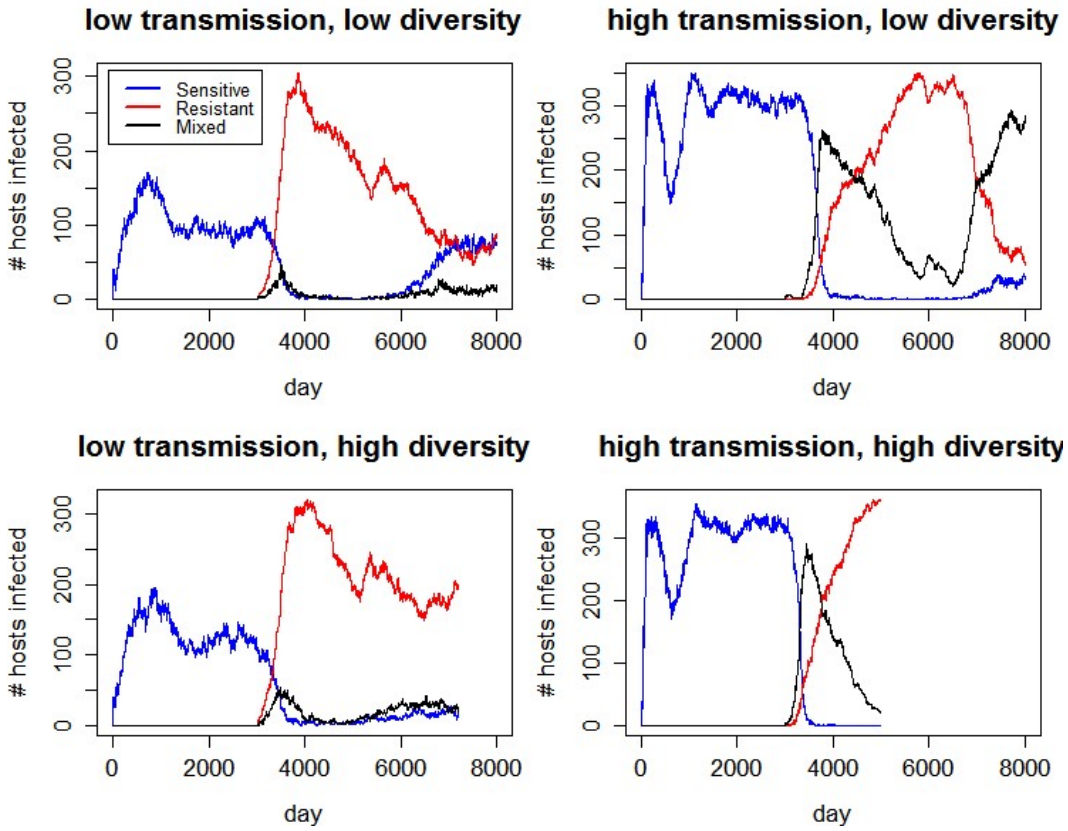

Figure A33. Simulation parameters: $\eta = 0.2, \nu = 0.05, Y_{TR} = 10, p_{TR}$=0.025, $\varphi_2 = 0$.

Simulation numbers: 23 (top left), 51 (bottom left), 79 (top right), 107 (bottom right).

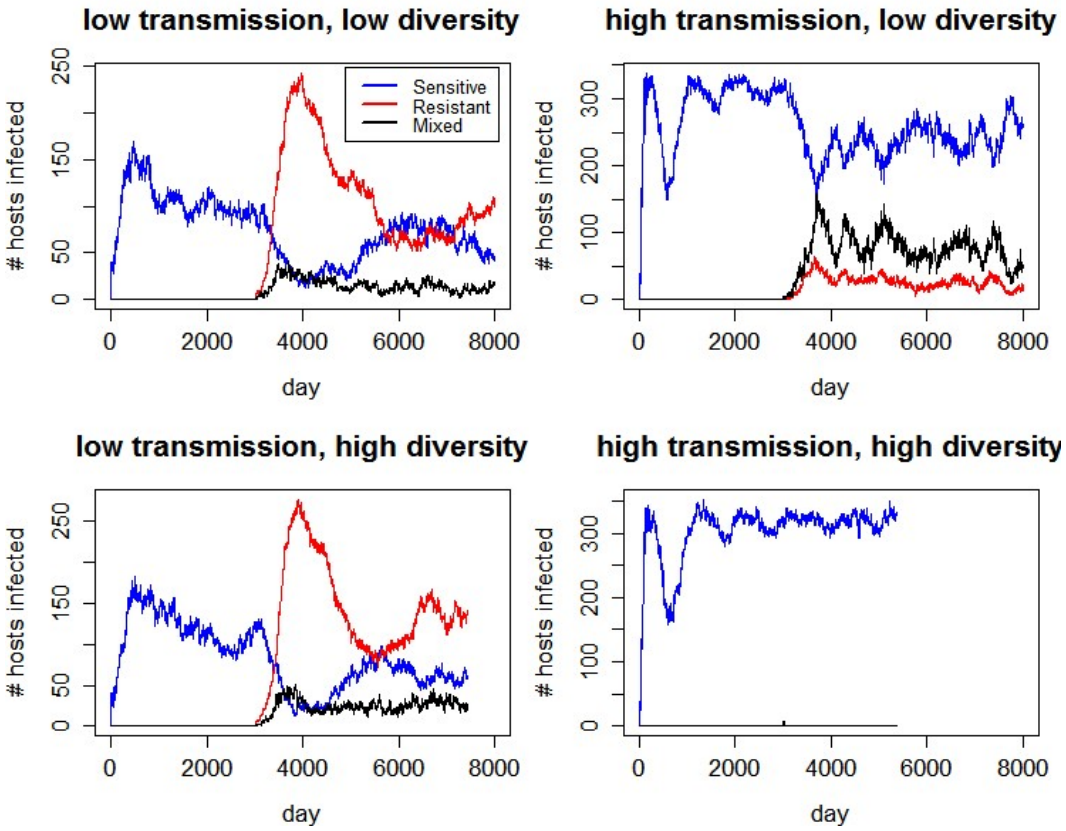

Figure A34. Simulation parameters: $\eta = 0.2, \nu = 0.05, Y_{TR} = 10, p_{TR}$=0.025, $\varphi_2 = 0.1$.

Simulation numbers: 24 (top left), 52 (bottom left), 80 (top right), 108 (bottom right).

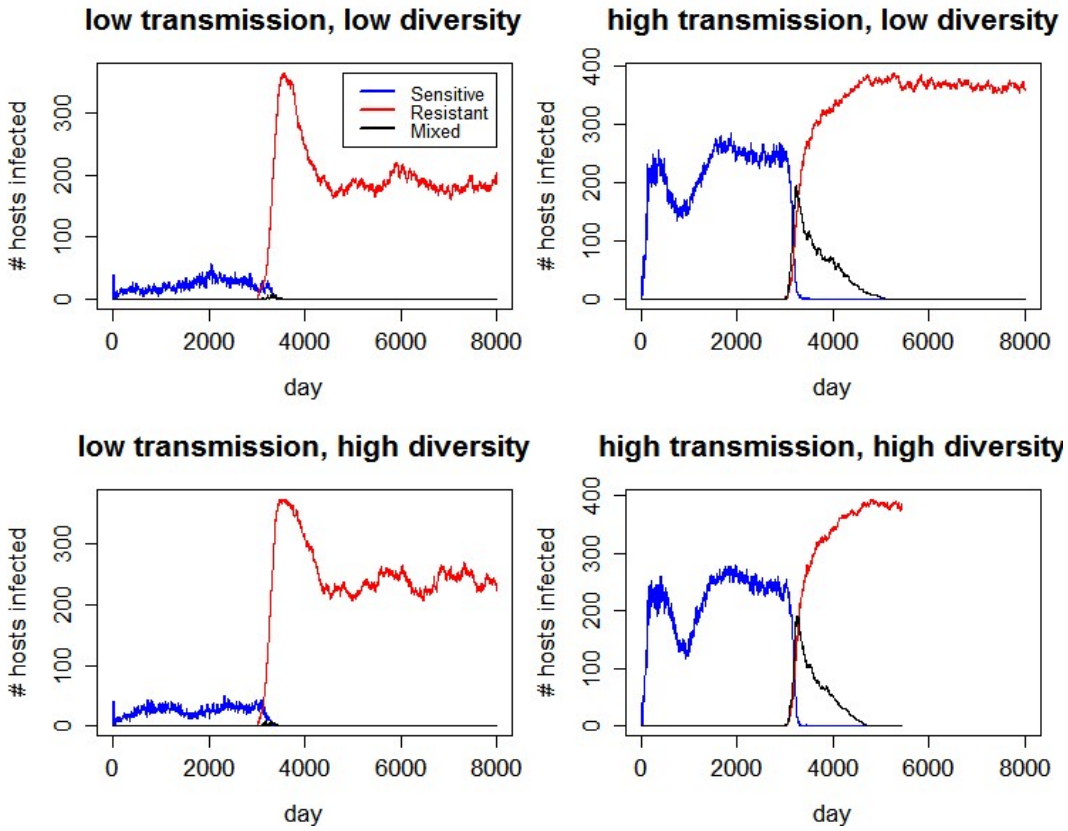

Figure A35. Simulation parameters: $\eta = 0.2, \nu = 0.05, Y_{TR} = 10, p_{TR}$=0.1, $\varphi_2 = 0$.

Simulation numbers: 25 (top left), 53 (bottom left), 81 (top right), 109 (bottom right).

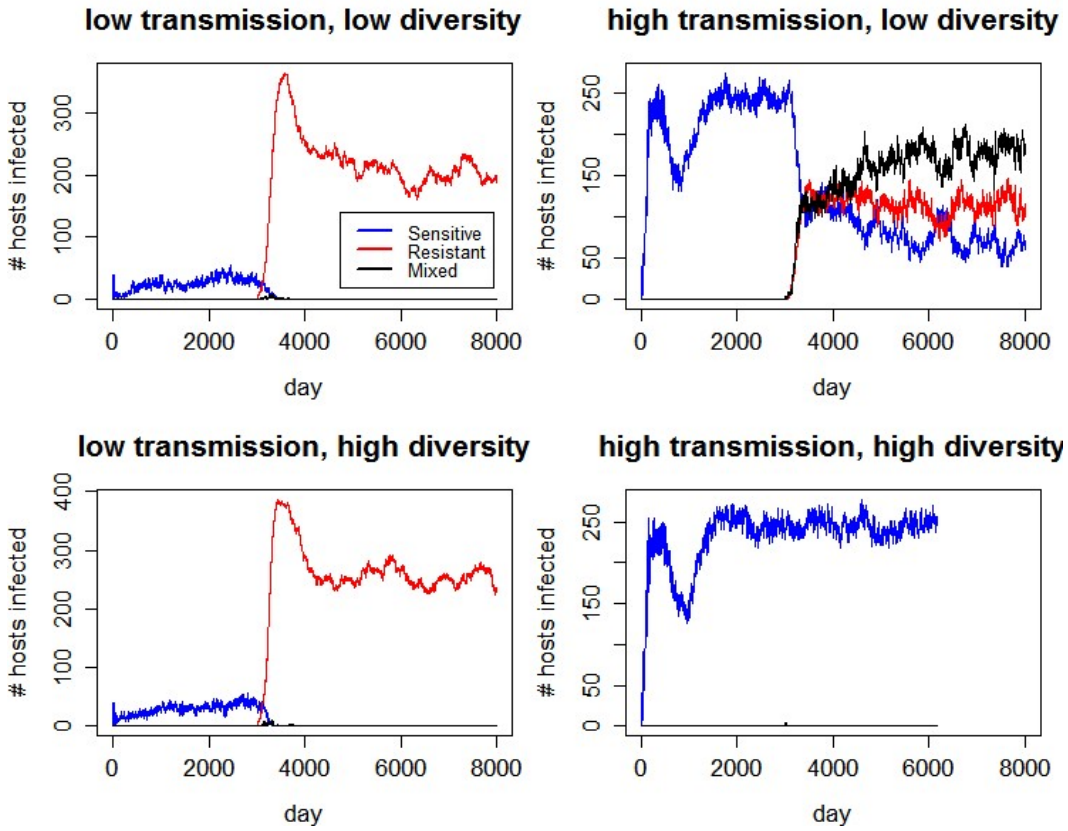

Figure A36. Simulation parameters: $\eta = 0.2, \nu = 0.05, Y_{TR} = 10, p_{TR}$=0.1, $\varphi_2 = 0.1$.

Simulation numbers: 26 (top left), 54 (bottom left), 82 (top right), 110 (bottom right).

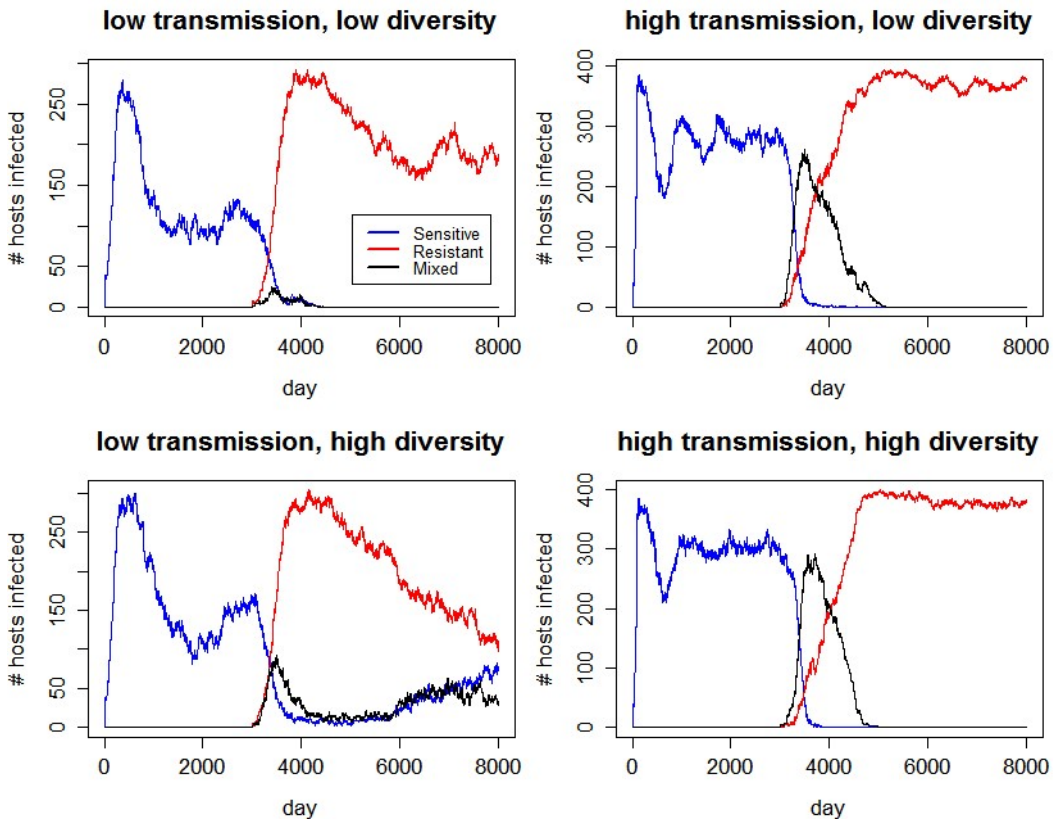

Figure A37. Simulation parameters: $\eta = 0.2, \nu = 0.05, Y_{TR} = 0, p_{TR}$=0.005, $\varphi_2 = 0$.

Simulation numbers: 27 (top left), 55 (bottom left), 83 (top right), 111 (bottom right).

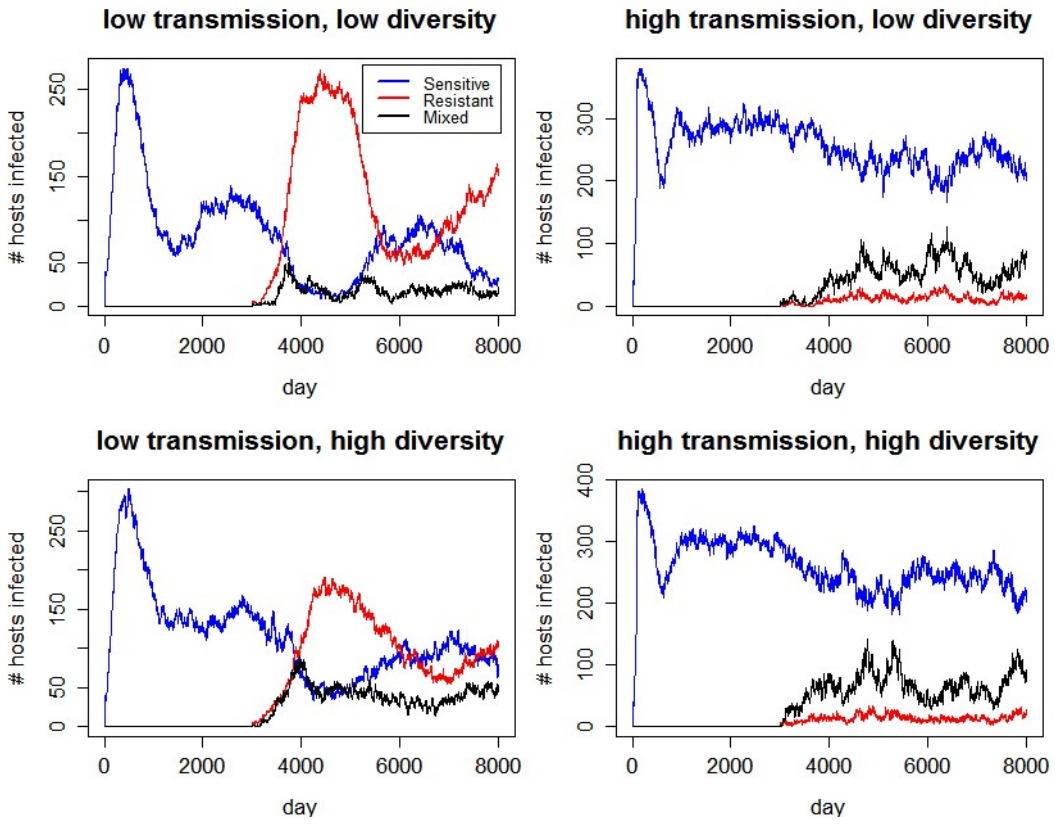

Figure A38. Simulation parameters: $\eta = 0.2, \nu = 0.05, Y_{TR} = 0, p_{TR}$=0.005, $\varphi_2 = 0.1$. Simulation numbers: 28 (top left), 56 (bottom left), 84 (top right), 112 (bottom right).

Model Code

The full model was run in RStudio version 1.0.136. The majority of simulations were run on Amazon Web Services EC2 instances (ami-94e26af4) with 16 to 64 cores. Simulations were run in parallel using *parLapplyLB* from the R package *parallel,* and results were uploaded directly to Dropbox.

```
fullmodel<-function(fmpars){
  with(as.list(fmpars),{
    if((b*N_H)>N_M){stop('b*N_H is greater than N_M')}
    ###################################
    library(deSolve)
```

```
    ###################################
    #Within-host model parameters
    B<-(5/12)*1e5 #red blood cell production (per uL per day)
    alpha_X<-(1/120) #red blood cell death (per capita per day)
    beta<-2.4e-6 #transmission parameter (mass action merozoites +
uninfected red blood cells)
    epsilon_1<-0.95 #treatment efficacy strain 1 (e_1=epsilon_1 when
host treated)
    epsilon_2<-0 #treatment efficacy strain 2 (e_2=epsilon_2 when host
treated)
    alpha_Y<-0.5 #infected red blood cell death rate (average
lifespan=2 days)
    gamma<-0.02 #gametocyte production rate (per capita per day)
    delta_IY<-4 #rate of killing of infected red blood cells by
adaptive immunity
    delta_ZY<-4 #rate of killing of infected red blood cells by innate
immunity
    R<-16 #burst size (merozoites produced per infected red blood cell)
    phi_1<-0 #fitness cost of strain 1
    #phi_2<-0 #fitness cost of strain 2
    alpha_S<-48 #merozoite death rate (average lifespan=30 minutes)
    delta_IS<-4 #rate of killing of merozoites by adaptive immunity
    delta_ZS<-4 #rate of killing of merozoites by innate immunity
    alpha_G<-0.0625 #gametocyte death rate (average lifespan=16 days)
    delta_ZG<-4 #rate of killing of gametocytes by innate immunity
    sigma<-1 #max growth rate (per capita per day) of adaptive immunity
    theta<-1e3 #merozoite density at which growth term of
dI/dt=0.5*sigma
    psi<-0.1 #initial decay rate of adaptive immunity due to antigenic
variation
    A<-120 #shape parameter for decay of immunity due to antigenic
variation
    k<-8 #shape parameter for decay of immunity due to antigenic
variation
    alpha_I<-0.001 #background decay rate of adaptive immunity (per
capita per day)
    zeta<-3e-5 #growth rate of innate immunity
    alpha_Z<-0.5 #innate immunity decay rate
    ###################################
    #Within-host ODE model
    withinhost<-function(t,start,pars){
      with(as.list(c(start,pars)),{
        #start=c(X,Y1,Y2,S1,S2,G1,G2,I1,I2,Z,C1,C2) at t=0

#pars=c(B,alpha_X,beta,e_1,e_2,alpha_Y,gamma,delta_IY,delta_ZY,R,phi_1,
phi_2,alpha_S,delta_IS,delta_ZS,alpha_G,delta_ZG,sigma,theta,psi,A,k,al
pha_I,zeta,alpha_Z,lambda,mu,eta,nu,H1,H2,J1,J2)
        dXdt<-B-alpha_X*X-beta*(S1+S2)*X #X=uninfected red blood cells
        dY1dt<-beta*S1*X-(1/(1-e_1))*alpha_Y*Y1-gamma*Y1-
delta_IY*(I1+omega2*I2)*Y1-delta_ZY*Z*Y1 #Y1=infected red blood cells
strain 1
        dY2dt<-beta*S2*X-(1/(1-e_2))*alpha_Y*Y2-gamma*Y2-
delta_IY*(I2+omega1*I1)*Y2-delta_ZY*Z*Y2 #Y2=infected red blood cells
strain 2
        dS1dt<-alpha_Y*R*(1-phi_1)*Y1-alpha_S*S1-beta*S1*X-
delta_IS*(I1+omega2*I2)*S1-delta_ZS*Z*S1 #S1=merozoites strain 1
```

```
        dS2dt<-alpha_Y*R*(1-phi_2)*Y2-alpha_S*S2-beta*S2*X-
delta_IS*(I2+omega1*I1)*S2-delta_ZS*Z*S2 #S2=merozoites strain 2
        dG1dt<-gamma*Y1-alpha_G*G1-delta_ZG*Z*G1 #G1=gametocytes strain
1
        dG2dt<-gamma*Y2-alpha_G*G2-delta_ZG*Z*G2 #G2=gametocytes strain
2
        dI1dt<-I1*((sigma*(S1+eta*S2))/(theta+S1+eta*S2))-
max(H1,H2)*psi*J1*I1*(1-(C1^k)/((C1^k)+(A^k)))-alpha_I*J1*(1-
max(H1,eta*H2))*I1 #I1=adaptive immunity to strain 1 #C1 is a time
"counter" that can be reset #H1=1 when host infected with strain 1, 0
otherwise #J1=0 when I1<I_N, 1 otherwise
        dI2dt<-I2*((sigma*(eta*S1+S2))/(theta+eta*S1+S2))-
max(H1,H2)*psi*J2*I2*(1-(C2^k)/((C2^k)+(A^k)))-alpha_I*J2*(1-
max(H2,eta*H1))*I2 #I2=adaptive immunity to strain 2
        dZdt<-zeta*(1-Z)*(S1+S2)-alpha_Z*Z #Z=innate immunity
        dC1dt<-H1+nu*H2
        dC2dt<-H2+nu*H1

return(list(c(dXdt,dY1dt,dY2dt,dS1dt,dS2dt,dG1dt,dG2dt,dI1dt,dI2dt,dZdt
,dC1dt,dC2dt)))
      })
    }
    ####################################
    #Mosquito infection probability function
    d<-0.0446
    f1<-0.181
    f2<-0.881
    f3<-0.0904
    g0<-0.0382
    g1<-0.165
    g2<-51.4
    g3<-0.0129
    #d,f1,f2,f3,g0,g1,g2,g3=parameters for infection prob. function
    P_infect<-function(G_total,par_total,age,d,f1,f2,f3,g0,g1,g2,g3){
#age=0 if child, 1 otherwise
      PHI<-1-((1+(G_total/(2*d)))^(d-1))
      PSI<-g0+(g1*exp(-g2*exp(-g3*G_total)))
      if(par_total<100){p<-0}else
if((par_total>=100)&(par_total<1000)){p<-f1}{else
if(par_total>=1000){p<-f2}else{}
      if(age==0){q<-0}else if(age==1){q<-f3}else{}
      Q<-PHI*PSI*(1+p+q)
      return(Q)
    } #P_infect gives probability mosquito infected by feeding on
infected host, based on gametocyte and parasite densities (and host
age)
    ####################################
    #Mosquito infection process component
    mosq.coords<-function(index){ #index=number between 1 and [total #
mosquitoes in population]
      quotient<-index%/%(z+1) #z=mosquito lifespan in days
      remainder<-index%%(z+1)
      if(remainder==0){coords<-c(z+1,quotient)}else{coords<-
c(remainder,quotient+1)}
      return(coords)
    }
    ####################################
```

```
    #Model constants
    DELTA<-0.2 #DELTA=ODE step size (steps per day=1/DELTA)
    L<-14 #L=duration of treatment (days)
    OMEGA<-1e-4 #OMEGA=extinction threshold (infected red blood cells
per uL)
    I_N<-1e-3 #I_N=baseline adaptive immunity (naive host)
    z<-14 #z=mosquito lifespan (days)
    y<-10 #y=latent period in mosquito
    w<-12 #w=latent period in human (liver stage)
    V<-2 #V=blood meal volume (uL)
    n<-12 #n=number of sporozoites transferred from one mosquito to
human
    M<-1e4 #number of merozoites produced by each sporozoite
    a<-3000 #host lifespan in days
    D_int<-D/n_int #length of each interval
    N_MZ<-floor(N_M/(z+1))
    allmosq<-1:((z+1)*(N_MZ))
    ###################################
    #Treatment determination parameters
    #Y_TR<-10 #threshold parasitemia (inf. red blood cells per uL) for
treatment
    #start.day<-1 #first day on which treatment administered
    #tau<-1 #number of days between treatment administration days
    treatdays<-seq(start.day,D,by=tau)
    ###################################
    human.pop<-array(NA,dim=c(D_int,13,N_H))
    mosq.pop<-array(NA,dim=c(z+1,N_MZ,z+1))
    latent<-array(0,dim=c(N_H,w+1,2))
    TR<-matrix(0,nrow=(D_int+L-1),ncol=N_H)
    strain.freq<-matrix(NA,nrow=D_int,ncol=3)
    track.inf<-array(0,dim=c(D_int+w,N_H,2))
    inf.count<-array(0,dim=c(D_int,N_H,2))
    age.matrix<-matrix(NA,nrow=D_int,ncol=N_H)
    ###################################
    age.matrix[1,]<-runif(N_H,min=0,max=a)
    start.conditions<-
array(rep(c(0,5e6,0,0,0,0,0,0,I_N,I_N,0,0,0),rep(N_H,13)),dim=c(N_H,13)
)
    ###################################
    for(h in 1:n_int){ #h=interval number
      for(i in 1:D_int){ #i=day of interval h
        day<-((h-1)*D_int)+i
        if(day==intr.day_1){
          start1<-sample(1:N_H,round(iota_1*N_H,digits=0))
          latent[start1,1,1]<-n
          track.inf[i+w,start1,1]<-1
        }else{}
        if(day==intr.day_2){
          start2<-sample(1:N_H,round(iota_2*N_H,digits=0))
          latent[start2,1,2]<-n
          track.inf[i+w,start2,2]<-1
        }else{}
        if(day==1){}else{  #ifelse statement 1
          inf.count[i,,]<-inf.count.prev+track.inf[i,,] # ***
          extinct.1<-
which((start.conditions[,3]<OMEGA)&(start.conditions[,3]<penultimate[,3
]))
```

```
          extinct.2<-
which((start.conditions[,4]<OMEGA)&(start.conditions[,4]<penultimate[,4
]))
          start.conditions[extinct.1,c(3,5)]<-0
          start.conditions[extinct.2,c(4,6)]<-0
          start.conditions[,5:6]<-
start.conditions[,5:6]+(M*latent[,w+1,]/(5e6))
          age.matrix[i,]<-age.prev+1
          dead<-which(age.matrix[i,]>a)
          age.matrix[i,dead]<-0
          inf.count[i,dead,]<-0
          latent[dead,,]<-0
          for(j in dead){ #j loop 1
            start.conditions[j,2:13]<-c(5e6,0,0,0,0,0,0,I_N,I_N,0,0,0)
          } #end j loop 1
          newinf.1<-which((track.inf[i,,1]!=0)&(inf.count.prev[,1]!=0))
          newinf.2<-which((track.inf[i,,2]!=0)&(inf.count.prev[,2]!=0))
          n.1<-inf.count.prev[,1]
          n.2<-inf.count.prev[,2]
          for(j in newinf.1){ #j loop 2
            start.conditions[j,9]<-max(start.conditions[j,9]*(1-((1-
lambda)^(n.1[j]))),I_N)
            start.conditions[j,12]<-start.conditions[j,12]*(1-((1-
mu)^(n.1[j]))*((1-nu)^(n.2[j])))
          } #end j loop 2
          for(j in newinf.2){ #j loop 3
            start.conditions[j,10]<-max(start.conditions[j,10]*(1-((1-
lambda)^(n.2[j]))),I_N)
            start.conditions[j,13]<-start.conditions[j,13]*(1-((1-
mu)^(n.2[j]))*((1-nu)^(n.1[j])))
          } #end j loop 3
        } #end ifelse statement 1
        omega.1<-(1-((1-eta))^inf.count[i,,1])
        omega.2<-(1-((1-eta)^inf.count[i,,2]))
        HJ<-matrix(0,nrow=N_H,ncol=4) #HJ[j,]=H1,H2,J1,J2 for host j
        E<-matrix(0,nrow=N_H,ncol=2) #E[j,]=e_1,e_2 for host j
        HJ[which(start.conditions[,5]!=0),1]<-1
        HJ[which(start.conditions[,6]!=0),2]<-1
        HJ[which(start.conditions[,9]>I_N),3]<-1
        HJ[which(start.conditions[,10]>I_N),4]<-1
        if(day%in%treatdays){ #ifelse statement 2
          Ytotal<-rowSums(start.conditions[,3:4])
          r.treat<-runif(N_H)
          start.treat<-which((TR[i,]==0)&(Ytotal>Y_TR)&(r.treat<=p_TR))
          TR[i:(i+L-1),start.treat]<-1
        }else{} #end ifelse statement 2
        E[which(TR[i,]==1),1]<-epsilon_1
        E[which(TR[i,]==1),2]<-epsilon_2
        ################################################
        human.pop[i,,]<-t(start.conditions)
        ################################################
        start.list<-vector("list",N_H)
        times.list<-vector("list",N_H)
        pars.list<-vector("list",N_H)
        func.list<-vector("list",N_H)
        for(j in 1:N_H){ #j loop 4
```

```
          start.list[[j]]<-
c(X=start.conditions[j,2],Y1=start.conditions[j,3],Y2=start.conditions[
j,4],S1=start.conditions[j,5],S2=start.conditions[j,6],G1=start.conditi
ons[j,7],G2=start.conditions[j,8],I1=start.conditions[j,9],I2=start.con
ditions[j,10],Z=start.conditions[j,11],C1=start.conditions[j,12],C2=sta
rt.conditions[j,13])
          times.list[[j]]<-seq(day-1,day,by=DELTA)
          pars.list[[j]]<-
c(B=B,alpha_X=alpha_X,beta=beta,e_1=E[j,1],e_2=E[j,2],alpha_Y=alpha_Y,g
amma=gamma,delta_IY=delta_IY,delta_ZY=delta_ZY,R=R,phi_1=phi_1,phi_2=ph
i_2,alpha_S=alpha_S,delta_IS=delta_IS,delta_ZS=delta_ZS,alpha_G=alpha_G
,delta_ZG=delta_ZG,sigma=sigma,theta=theta,psi=psi,A=A,k=k,alpha_I=alph
a_I,zeta=zeta,lambda=lambda,mu=mu,eta=eta,nu=nu,alpha_Z=alpha_Z,H1=HJ[j
,1],H2=HJ[j,2],J1=HJ[j,3],J2=HJ[j,4],omega1=omega.1[j],omega2=omega.2[j
])
          func.list[[j]]<-withinhost
        } #end j loop 4
        result<-mapply(ode,start.list,times.list,func.list,pars.list)
        result.reformat<-array(NA,dim=c((1/DELTA)+1,13,N_H))
        result.reformat[1:((1/DELTA)+1),,]<-unlist(result)
        start.conditions<-t(result.reformat[(1/DELTA)+1,,])
        penultimate<-t(result.reformat[1/DELTA,,])
        ################################################
        infected1<-
length(which((start.conditions[,5]!=0)&(start.conditions[,6]==0)))
        infected2<-
length(which((start.conditions[,5]==0)&(start.conditions[,6]!=0)))
        infected12<-
length(which((start.conditions[,5]!=0)&(start.conditions[,6]!=0)))
        strain.freq[i,]<-c(infected1,infected2,infected12)
        G<-cbind(start.conditions[,7],start.conditions[,8])
        G[which(G[,1]<0),1]<-0
        G[which(G[,2]<0),2]<-0
        totalG<-rowSums(G)
        totalpar<-start.conditions[,3]+start.conditions[,4]
        nonzeroprobs<-1-dpois(0,V*G[,1])*dpois(0,V*G[,2])
        infection.probs<-rep(0,N_H)
        age.indic<-rep(0,N_H)
        age.indic[which(age.matrix[i,]>=1825)]<-1
        nonzeroNZP<-which(nonzeroprobs!=0)
        for(j in nonzeroNZP){ #j loop 5
          infection.probs[j]<-
P_infect(totalG[j],totalpar[j],age.indic[j],d,f1,f2,f3,g0,g1,g2,g3)
        } #end j loop 5
        bites<-rpois(N_H,b)
        mosq.bite<-sample(allmosq,sum(bites))
        biterep<-rep(1:N_H,bites)
        mosq.infected<-rbinom(N_H,bites,infection.probs)
        infectmosq<-which(mosq.infected!=0)
        ntrials<-rep(NA,N_H)
        ntrials[infectmosq]<-
bites[infectmosq]+qnbinom(0.9999,mosq.infected[infectmosq],nonzeroprobs
[infectmosq])
        for(j in infectmosq){ #j loop 6
          m1<-rpois(ntrials[j],V*G[j,1])
          m2<-rpois(ntrials[j],V*G[j,2])
          successes<-which((m1+m2)>0)
```

```
          draws<-successes[1:mosq.infected[j]]
          propstrain1<-m1[draws]/(m1[draws]+m2[draws])
          infectedbyj<-
sample(mosq.bite[which(biterep==j)],mosq.infected[j])
          infcoords<-t(sapply(infectedbyj,mosq.coords))
          update.coords<-cbind(infcoords,rep(1,nrow(infcoords)))
          mosq.pop[update.coords]<-propstrain1
        } #end j loop 6
        for(j in 1:N_H){ #j loop 7
          if(bites[j]==0){}else{ #ifelse statement 3
            add<-matrix(0,nrow=bites[j],ncol=2)
            strainencounters<-matrix(0,nrow=bites[j],ncol=2)
            jmosq<-mosq.bite[which(biterep==j)]
            for(s in 1:bites[j]){ #s loop
              s.coord<-mosq.coords(jmosq[s])
              mosq.s<-c(mosq.pop[s.coord[1],s.coord[2],(y+1):(z+1)])
              notNA<-which(!is.na(mosq.s))
              if(length(notNA)==0){}else{ #ifelse statement 4
                frac1<-mosq.s[notNA]
                frac2<-1-frac1
                frac.all<-c(frac1,frac2)/length(notNA)
                sporz<-
matrix(tabulate(sample(1:length(frac.all),n,replace=T,prob=frac.all),nb
ins=length(frac.all)),ncol=2,byrow=F)
                add[s,]<-colSums(sporz)
                strainencounters[s,]<-
c(length(which(sporz[,1]!=0)),length(which(sporz[,2]!=0)))
              } #end ifelse statement 4
            } #end s loop
            add.rowtotals<-rowSums(add)
            infectious<-which(add.rowtotals!=0)
            nmtransmit<-rbinom(1,length(infectious),f)
            if(nmtransmit==0){}else{ #ifelse statement 5
              transmit<-sample(infectious,nmtransmit)
              addfinal<-matrix(add[transmit,],ncol=2)
              strainencountersfinal<-
matrix(strainencounters[transmit,],ncol=2)
              latent[j,1,]<-colSums(addfinal)
              track.inf[i+w,j,]<-colSums(strainencountersfinal)
            } #end ifelse statement 5
          } #end ifelse statement 3
        } #end j loop 7
        new.mosq.pop<-array(NA,dim=dim(mosq.pop))
        new.mosq.pop[2:(z+1),,2:(z+1)]<-mosq.pop[1:z,,1:z]
        mosq.pop<-new.mosq.pop
        new.latent<-array(0,dim=dim(latent))
        new.latent[,2:(w+1),]<-latent[,1:w,]
        latent<-new.latent
        inf.count.prev<-inf.count[i,,]
        age.prev<-age.matrix[i,]
        ########################################################
        if(i==D_int){ #ifelse statement 6
          outputs<-
list("human.pop"=human.pop,"TR"=TR,"strain.freq"=strain.freq,"track.inf
"=track.inf,"inf.count"=inf.count,"age.matrix"=age.matrix,"mosq.pop"=mo
sq.pop,"latent"=latent,"start.conditions"=start.conditions,"penultimate
"=penultimate)
```

```
          outputname<-paste("output","_",h,sep="")
          save(outputs,file=paste(path,"/",outputname,sep=""))
          rm(outputs)
          human.pop<-array(NA,dim=c(D_int,13,N_H))
          TR.new<-matrix(0,nrow=(D_int+L-1),ncol=N_H)
          TR.new[1:(L-1),]<-TR[(D_int+1):(D_int+L-1),]
          TR<-TR.new
          rm(TR.new)
          track.inf.new<-array(0,dim=c(D_int+w,N_H,2))
          track.inf.new[1:w,,]<-track.inf[(D_int+1):(D_int+w),,]
          track.inf<-track.inf.new
          rm(track.inf.new)
          age.matrix<-matrix(NA,nrow=D_int,ncol=N_H)
          strain.freq<-matrix(NA,nrow=D_int,ncol=3)
          inf.count<-array(0,dim=c(D_int,N_H,2))
        }else{} #end ifelse statement 6
      } #end i loop
    } #end h loop
  }) #end 'with' statement
} #end function
```

References

1. World Malaria Report. World Health Organization, 2016.

2. Meshnick SR, Dobson MJ. The History of Antimalarial Drugs. 2001. In: Antimalarial Chemotherapy: Mechanisms of Action, Resistance, and New Directions in Drug Discovery [Internet]. Humana Press; [15-25].

3. Talisuna AO, Bloland P, D'Alessandro U. History, dynamics, and public health importance of malaria parasite resistance. Clinical microbiology reviews. 2004;17(1):235-54. PubMed PMID: 14726463; PubMed Central PMCID: PMCPMC321461.

4. Global Report on Antimalarial Drug Efficacy and Drug Resistance: 2000-2010. World Health Organization, 2010.

5. Imwong M, Suwannasin K, Kunasol C, Sutawong K, Mayxay M, Rekol H, et al. The spread of artemisinin-resistant Plasmodium falciparum in the Greater Mekong subregion: a molecular epidemiology observational study. Lancet Infect Dis. 2017;17(5):491-7. doi: 10.1016/S1473-3099(17)30048-8. PubMed PMID: 28161569; PubMed Central PMCID: PMCPMC5406483.

6. Ecker A, Lehane AM, Clain J, Fidock DA. PfCRT and its role in antimalarial drug resistance. Trends Parasitol. 2012;28(11):504-14. doi: 10.1016/j.pt.2012.08.002. PubMed PMID: 23020971; PubMed Central PMCID: PMC3478492.

7. Le Bras J, Durand R. The mechanisms of resistance to antimalarial drugs in Plasmodium falciparum. Fundam Clin Pharmacol. 2003;17(2):147-53. PubMed PMID: 12667224.

8. Sidhu AB, Verdier-Pinard D, Fidock DA. Chloroquine resistance in Plasmodium falciparum malaria parasites conferred by pfcrt mutations. Science. 2002;298(5591):210-3. Epub 2002/10/05. doi: 10.1126/science.1074045. PubMed PMID: 12364805; PubMed Central PMCID: PMC2954758.

9. Lakshmanan V, Bray PG, Verdier-Pinard D, Johnson DJ, Horrocks P, Muhle RA, et al. A critical role for PfCRT K76T in Plasmodium falciparum verapamil-reversible chloroquine resistance. EMBO J. 2005;24(13):2294-305. doi: 10.1038/sj.emboj.7600681. PubMed PMID: 15944738; PubMed Central PMCID: PMCPMC1173140.

10. Mita T, Tanabe K, Kita K. Spread and evolution of Plasmodium falciparum drug resistance. Parasitol Int. 2009;58(3):201-9. doi: 10.1016/j.parint.2009.04.004. PubMed PMID: 19393762.

11. Anderson TJ, Haubold B, Williams JT, Estrada-Franco JG, Richardson L, Mollinedo R, et al. Microsatellite markers reveal a spectrum of population structures in the malaria parasite Plasmodium falciparum. Mol Biol Evol. 2000;17(10):1467-82. PubMed PMID: 11018154.

12. Triglia T, Cowman AF. Primary structure and expression of the dihydropteroate synthetase gene of Plasmodium falciparum. Proc Natl Acad Sci U S A. 1994;91(15):7149-53. PubMed PMID: 8041761; PubMed Central PMCID: PMCPMC44356.

13. Snewin VA, England SM, Sims PF, Hyde JE. Characterisation of the dihydrofolate reductase-thymidylate synthetase gene from human malaria parasites highly resistant to pyrimethamine. Gene. 1989;76(1):41-52. PubMed PMID: 2663650.

14. Klein EY, Smith DL, Boni MF, Laxminarayan R. Clinically immune hosts as a refuge for drug-sensitive malaria parasites. Malar J. 2008;7:67. Epub 2008/04/29. doi: 10.1186/1475-2875-7-67. PubMed PMID: 18439283; PubMed Central PMCID: PMC2409364.

15. Lindblade KA, Steinhardt L, Samuels A, Kachur SP, Slutsker L. The silent threat: asymptomatic parasitemia and malaria transmission. Expert Rev Anti-Infect Ther. 2013;11(6):623-39. Epub 2013/06/12. doi: 10.1586/eri.13.45. PubMed PMID: 23750733.

16. Guidelines for the Treatment of Malaria. World Health Organization, 2006.

17. Guidelines for the Treatment of Malaria. World Health Organization, 2010.

18. Arnot D. Unstable malaria in Sudan: the influence of the dry season. Clone multiplicity of Plasmodium falciparum infections in individuals exposed to variable levels of disease transmission. Trans R Soc Trop Med Hyg. 1998;92(6):580-5. Epub 1999/05/18. PubMed PMID: 10326095.

19. de Roode JC, Culleton R, Bell AS, Read AF. Competitive release of drug resistance following drug treatment of mixed Plasmodium chabaudi infections. Malar J. 2004;3:33. doi: 33

10.1186/1475-2875-3-33. PubMed PMID: WOS:000224997100002.

20. Hastings IM. A model for the origins and spread of drug-resistant malaria. Parasitology. 1997;115 (Pt 2):133-41. Epub 1997/08/01. PubMed PMID: 10190169.

21. Hastings IM, D'Alessandro U. Modelling a predictable disaster: the rise and spread of drug-resistant malaria. Parasitol Today. 2000;16(8):340-7. Epub 2000/07/20. PubMed PMID: 10900482.

22. Klein EY, Smith DL, Laxminarayan R, Levin S. Superinfection and the evolution of resistance to antimalarial drugs. Proc Biol Sci. 2012;279(1743):3834-42. Epub 2012/07/13. doi: 10.1098/rspb.2012.1064. PubMed PMID: 22787024; PubMed Central PMCID: PMC3415915.

23. De Roode JC, Read AF, Chan BHK, Mackinnon MJ. Rodent malaria parasites suffer from the presence of conspecific clones in three-clone Plasmodium chabaudi infections. Parasitology. 2003;127:411-8. doi: 10.1017/s0031182003004001. PubMed PMID: WOS:000187030600001.

24. Bell AS, de Roode JC, Sim D, Read AF. Within-host competition in genetically diverse malaria infections: parasite virulence and competitive success. Evolution. 2006;60(7):1358-71. Epub 2006/08/26. PubMed PMID: 16929653.

25. Taylor LH, Walliker D, Read AF. Mixed-genotype infections of malaria parasites: within-host dynamics and transmission success of competing clones. Proc Biol Sci. 1997;264(1383):927-35. Epub 1997/06/22. doi: 10.1098/rspb.1997.0128. PubMed PMID: 9225482; PubMed Central PMCID: PMC1688430.

26. de Roode JC, Culleton R, Cheesman SJ, Carter R, Read AF. Host heterogeneity is a determinant of competitive exclusion or coexistence in genetically diverse malaria infections. Proc Biol Sci. 2004;271(1543):1073-80. Epub 2004/08/06. doi: 10.1098/rspb.2004.2695. PubMed PMID: 15293862; PubMed Central PMCID: PMC1691691.

27. de Roode JC, Helinski MEH, Anwar MA, Read AF. Dynamics of multiple infection and within-host competition in genetically diverse malaria infections. Am Nat. 2005;166(5):531-42. doi: 10.1086/491659. PubMed PMID: WOS:000232832700005.

28. Read AF, Day T, Huijben S. The evolution of drug resistance and the curious orthodoxy of aggressive chemotherapy. Proc Natl Acad Sci U S A. 2011;108 Suppl 2:10871-7. Epub 2011/06/22. doi: 10.1073/pnas.1100299108. PubMed PMID: 21690376; PubMed Central PMCID: PMC3131826.

29. Legros M, Bonhoeffer S. A combined within-host and between-hosts modelling framework for the evolution of resistance to antimalarial drugs. J R Soc Interface. 2016;13(117). doi: 10.1098/rsif.2016.0148. PubMed PMID: 27075004; PubMed Central PMCID: PMCPMC4874437.

30. Mideo N, Alizon S, Day T. Linking within- and between-host dynamics in the evolutionary epidemiology of infectious diseases. Trends Ecol Evol. 2008;23(9):511-7. Epub 2008/07/29. doi: 10.1016/j.tree.2008.05.009. PubMed PMID: 18657880.

31. Cohen ML. Changing patterns of infectious disease. Nature. 2000;406(6797):762-7. Epub 2000/08/30. doi: 10.1038/35021206. PubMed PMID: 10963605.

32. Wootton JC, Feng X, Ferdig MT, Cooper RA, Mu J, Baruch DI, et al. Genetic diversity and chloroquine selective sweeps in Plasmodium falciparum. Nature. 2002;418(6895):320-3. Epub 2002/07/19. doi: 10.1038/nature00813. PubMed PMID: 12124623.

33. Roper C, Pearce R, Nair S, Sharp B, Nosten F, Anderson T. Intercontinental spread of pyrimethamine-resistant malaria. Science. 2004;305(5687):1124. Epub 2004/08/25. doi: 10.1126/science.1098876. PubMed PMID: 15326348.

34. Ashley EA, Dhorda M, Fairhurst RM, Amaratunga C, Lim P, Suon S, et al. Spread of artemisinin resistance in Plasmodium falciparum malaria. N Engl J Med. 2014;371(5):411-23. Epub 2014/07/31. doi: 10.1056/NEJMoa1314981. PubMed PMID: 25075834; PubMed Central PMCID: PMC4143591.

35. Dondorp AM, Nosten F, Yi P, Das D, Phyo AP, Tarning J, et al. Artemisinin resistance in Plasmodium falciparum malaria. N Engl J Med. 2009;361(5):455-67. Epub 2009/07/31. doi: 10.1056/NEJMoa0808859. PubMed PMID: 19641202; PubMed Central PMCID: PMC3495232.

36. Birger RB, Kouyos RD, Cohen T, Griffiths EC, Huijben S, Mina M, et al. The potential impact of coinfection on antimicrobial chemotherapy and drug resistance. Trends in microbiology. 2015;23(9):537-44. doi: 10.1016/j.tim.2015.05.002. PubMed PMID: 26028590.

37. Read AF, Taylor LH. The ecology of genetically diverse infections. Science. 2001;292(5519):1099-102. PubMed PMID: 11352063.

38. Juliano JJ, Porter K, Mwapasa V, Sem R, Rogers WO, Ariey F, et al. Exposing malaria in-host diversity and estimating population diversity by capture-recapture using massively parallel pyrosequencing. Proc Natl Acad Sci U S A. 2010;107(46):20138-43. Epub 2010/11/03. doi: 10.1073/pnas.1007068107. PubMed PMID: 21041629; PubMed Central PMCID: PMC2993407.

39. Day T, Huijben S, Read AF. Is selection relevant in the evolutionary emergence of drug resistance? Trends in microbiology. 2015;23(3):126-33. doi: 10.1016/j.tim.2015.01.005. PubMed PMID: 25680587; PubMed Central PMCID: PMC4494118.

40. Hansen J, Day T. Coinfection and the evolution of drug resistance. J Evol Biol. 2014. Epub 2014/11/25. doi: 10.1111/jeb.12518. PubMed PMID: 25417787.

41. Wargo AR, Huijben S, de Roode JC, Shepherd J, Read AF. Competitive release and facilitation of drug-resistant parasites after therapeutic chemotherapy in a rodent malaria model. Proc Natl Acad Sci U S A. 2007;104(50):19914-9. Epub 2007/12/07. doi: 10.1073/pnas.0707766104. PubMed PMID: 18056635; PubMed Central PMCID: PMC2148397.

42. Bell AS, Huijben S, Paaijmans KP, Sim DG, Chan BH, Nelson WA, et al. Enhanced transmission of drug-resistant parasites to mosquitoes following drug treatment in rodent malaria. PLoS One. 2012;7(6):e37172. Epub 2012/06/16. doi: 10.1371/journal.pone.0037172. PubMed PMID: 22701563; PubMed Central PMCID: PMC3368907.

43. Pollitt LC, Huijben S, Sim DG, Salathe RM, Jones MJ, Read AF. Rapid response to selection, competitive release and increased transmission potential of artesunate-selected Plasmodium chabaudi malaria parasites. PLoS Pathog. 2014;10(4):e1004019. doi: 10.1371/journal.ppat.1004019. PubMed PMID: 24763470; PubMed Central PMCID: PMC3999151.

44. Huijben S, Nelson WA, Wargo AR, Sim DG, Drew DR, Read AF. Chemotherapy, within-host ecology and the fitness of drug-resistant malaria parasites. Evolution. 2010;64(10):2952-68. Epub 2010/06/30. doi: 10.1111/j.1558-5646.2010.01068.x. PubMed PMID: 20584075; PubMed Central PMCID: PMC3066636.

45. Huijben S, Sim DG, Nelson WA, Read AF. The fitness of drug-resistant malaria parasites in a rodent model: multiplicity of infection. J Evol Biol. 2011;24(11):2410-22. Epub 2011/09/03. doi: 10.1111/j.1420-9101.2011.02369.x. PubMed PMID: 21883612.

46. Stephens R, Culleton RL, Lamb TJ. The contribution of Plasmodium chabaudi to our understanding of malaria. Trends Parasitol. 2012;28(2):73-82. Epub 2011/11/22. doi: 10.1016/j.pt.2011.10.006. PubMed PMID: 22100995.

47. Borrmann S, Matuschewski K. Protective immunity against malaria by 'natural immunization': a question of dose, parasite diversity, or both? Current opinion in immunology. 2011;23(4):500-8. doi: 10.1016/j.coi.2011.05.009. PubMed PMID: 21719266.

48. Bruce MC, Donnelly CA, Alpers MP, Galinski MR, Barnwell JW, Walliker D, et al. Cross-species interactions between malaria parasites in humans. Science. 2000;287(5454):845-8. doi: 10.1126/science.287.5454.845. PubMed PMID: WOS:000085136400043.

49. Harrington WE, Mutabingwa TK, Muehlenbachs A, Sorensen B, Bolla MC, Fried M, et al. Competitive facilitation of drug-resistant Plasmodium falciparum malaria parasites in pregnant women who receive preventive treatment. Proc Natl Acad Sci U S A. 2009;106(22):9027-32. Epub 2009/05/20. doi: 10.1073/pnas.0901415106. PubMed PMID: 19451638; PubMed Central PMCID: PMC2690058.

50. Naidoo I, Roper C. Mapping 'partially resistant', 'fully resistant', and 'super resistant' malaria. Trends Parasitol. 2013;29(10):505-15. doi: 10.1016/j.pt.2013.08.002. PubMed PMID: 24028889.

51. Methods for Surveillance of Antimalarial Drug Efficacy. World Health Organization, 2009.

52. Plucinski MM, Talundzic E, Morton L, Dimbu PR, Macaia AP, Fortes F, et al. Efficacy of artemether-lumefantrine and dihydroartemisinin-piperaquine for treatment of

uncomplicated malaria in children in Zaire and Uige Provinces, angola. Antimicrob Agents Chemother. 2015;59(1):437-43. doi: 10.1128/AAC.04181-14. PubMed PMID: 25367912; PubMed Central PMCID: PMC4291383.

53. Alam MT, de Souza DK, Vinayak S, Griffing SM, Poe AC, Duah NO, et al. Selective sweeps and genetic lineages of *Plasmodium falciparum* drug -resistant alleles in Ghana. J Infect Dis. 2011;203(2):220-7. Epub 2011/02/04. doi: 10.1093/infdis/jiq038. PubMed PMID: 21288822; PubMed Central PMCID: PMC3071065.

54. Alifrangis M, Dalgaard MB, Lusingu JP, Vestergaard LS, Staalsoe T, Jensen AT, et al. Occurrence of the Southeast Asian/South American SVMNT haplotype of the chloroquine-resistance transporter gene in *Plasmodium falciparum* in Tanzania. J Infect Dis. 2006;193(12):1738-41. Epub 2006/05/17. doi: 10.1086/504269. PubMed PMID: 16703518.

55. Fancony C, Gamboa D, Sebastiao Y, Hallett R, Sutherland C, Sousa-Figueiredo JC, et al. Various pfcrt and pfmdr1 genotypes of Plasmodium falciparum cocirculate with P. malariae, P. ovale spp., and P. vivax in northern Angola. Antimicrob Agents Chemother. 2012;56(10):5271-7. Epub 2012/08/02. doi: 10.1128/AAC.00559-12. PubMed PMID: 22850519; PubMed Central PMCID: PMC3457352.

56. Gama BE, Pereira-Carvalho GA, Lutucuta Kosi FJ, Almeida de Oliveira NK, Fortes F, Rosenthal PJ, et al. Plasmodium falciparum isolates from Angola show the StctVMNT haplotype in the pfcrt gene. Malar J. 2010;9:174. Epub 2010/06/23. doi: 10.1186/1475-2875-9-174. PubMed PMID: 20565881; PubMed Central PMCID: PMC2898790.

57. R Core Team. R: A language and environment for statistical computing. Vienna (Austria): R Foundation for Statistical Computing; 2012.

58. Crawley MJ. The R Book. 2nd Edition ed: John Wiley & Sons, Ltd; 2013.

59. Bates D, Maechler M, Bolker B. lme4: Linear mixed-effects models using S4 classes. version 0.999375-42 ed. p. R package.

60. Pinheiro J, Bates D, DebRoy S, Sarkar D, R Core Team. nlme: Linear and Nonlinear Mixed Effects Models. version 3.1-122 ed2015. p. R package.

61. Browne WJ, Subramanian SV, Jones K, Goldstein H. Variance partitioning in multilevel logistic models that exhibit overdispersion. J R Stat Soc Ser A-Stat Soc. 2005;168:599-613. doi: 10.1111/j.1467-985X.2004.00365.x. PubMed PMID: WOS:000230307700007.

62. Babiker HA, Hastings IM, Swedberg G. Impaired fitness of drug-resistant malaria parasites: evidence and implication on drug-deployment policies. Expert Rev Anti-Infect Ther. 2009;7(5):581-93. doi: 10.1586/eri.09.29. PubMed PMID: WOS:000267179400016.

63. Ord R, Alexander N, Dunyo S, Hallett R, Jawara M, Targett G, et al. Seasonal carriage of pfcrt and pfmdr1 alleles in Gambian Plasmodium falciparum imply reduced fitness of chloroquine-resistant parasites. J Infect Dis. 2007;196(11):1613-9. Epub 2007/11/17. doi: 10.1086/522154. PubMed PMID: 18008244.

64. Kublin JG, Cortese JF, Njunju EM, Mukadam RA, Wirima JJ, Kazembe PN, et al. Reemergence of chloroquine-sensitive Plasmodium falciparum malaria after cessation of chloroquine use in Malawi. J Infect Dis. 2003;187(12):1870-5. Epub 2003/06/07. doi: 10.1086/375419. PubMed PMID: 12792863.

65. Gething PW, Patil AP, Smith DL, Guerra CA, Elyazar IR, Johnston GL, et al. A new world malaria map: Plasmodium falciparum endemicity in 2010. Malar J. 2011;10:378. Epub 2011/12/22. doi: 10.1186/1475-2875-10-378. PubMed PMID: 22185615; PubMed Central PMCID: PMC3274487.

66. Bruce MC, Day KP. Cross-species regulation of malaria parasitaemia in the human host. Curr Opin Microbiol. 2002;5(4):431-7. Epub 2002/08/06. PubMed PMID: 12160865.

67. Metcalf CJ, Graham AL, Huijben S, Barclay VC, Long GH, Grenfell BT, et al. Partitioning regulatory mechanisms of within-host malaria dynamics using the effective propagation number. Science. 2011;333(6045):984-8. Epub 2011/08/20. doi: 10.1126/science.1204588. PubMed PMID: 21852493; PubMed Central PMCID: PMC3891600.

68. Raberg L, de Roode JC, Bell AS, Stamou P, Gray D, Read AF. The role of immune-mediated apparent competition in genetically diverse malaria infections. Am Nat. 2006;168(1):41-53. Epub 2006/07/29. doi: 10.1086/505160. PubMed PMID: 16874614.

69. Yap GS, Stevenson MM. Blood transfusion alters the course and outcome of Plasmodium chabaudi AS infection in mice. Infect Immun. 1994;62(9):3761-5. Epub 1994/09/01. PubMed PMID: 8063391; PubMed Central PMCID: PMC303028.

70. Mideo N, Kennedy DA, Carlton JM, Bailey JA, Juliano JJ, Read AF. Ahead of the curve: next generation estimators of drug resistance in malaria infections. Trends Parasitol. 2013;29(7):321-8. doi: 10.1016/j.pt.2013.05.004. PubMed PMID: 23746748; PubMed Central PMCID: PMC3694767.

71. Mackinnon MJ, Read AF. Virulence in malaria: an evolutionary viewpoint. Philos Trans R Soc Lond B Biol Sci. 2004;359(1446):965-86. Epub 2004/08/13. doi: 10.1098/rstb.2003.1414. PubMed PMID: 15306410; PubMed Central PMCID: PMC1693375.

72. Ross A, Killeen G, Smith T. Relationships between host infectivity to mosquitoes and asexual parasite density in Plasmodium falciparum. Am J Trop Med Hyg. 2006;75(2):32-7. PubMed PMID: WOS:000239781900005.

73. Kumpornsin K, Modchang C, Heinberg A, Ekland EH, Jirawatcharadech P, Chobson P, et al. Origin of robustness in generating drug-resistant malaria parasites. Mol Biol Evol. 2014;31(7):1649-60. doi: 10.1093/molbev/msu140. PubMed PMID: 24739308; PubMed Central PMCID: PMC4069624.

74. Hall AR, MacLean RC. Epistasis buffers the fitness effects of rifampicin- resistance mutations in Pseudomonas aeruginosa. Evolution. 2011;65(8):2370-9. doi: 10.1111/j.1558-5646.2011.01302.x. PubMed PMID: 21790582.

75. Lukens AK, Ross LS, Heidebrecht R, Javier Gamo F, Lafuente-Monasterio MJ, Booker ML, et al. Harnessing evolutionary fitness in Plasmodium falciparum for drug discovery and suppressing resistance. Proc Natl Acad Sci U S A. 2014;111(2):799-804. Epub 2014/01/02. doi: 10.1073/pnas.1320886110. PubMed PMID: 24381157; PubMed Central PMCID: PMC3896170.

76. Huijben S, Bell AS, Sim DG, Tomasello D, Mideo N, Day T, et al. Aggressive chemotherapy and the selection of drug resistant pathogens. PLoS Pathog. 2013;9(9):e1003578. Epub 2013/09/27. doi: 10.1371/journal.ppat.1003578. PubMed PMID: 24068922; PubMed Central PMCID: PMC3771897.

77. Kouyos RD, Metcalf CJ, Birger R, Klein EY, Abel zur Wiesch P, Ankomah P, et al. The path of least resistance: aggressive or moderate treatment? Proc Biol Sci. 2014;281(1794):20140566. Epub 2014/09/26. doi: 10.1098/rspb.2014.0566. PubMed PMID: 25253451; PubMed Central PMCID: PMC4211439.

78. Hastings IM. Why we should effectively treat malaria. Trends Parasitol. 2011;27(2):51-2. doi: 10.1016/j.pt.2010.10.003. PubMed PMID: 21281927.

79. Bushman M, Morton L, Duah N, Quashie N, Abuaku B, Koram KA, et al. Within-host competition and drug resistance in the human malaria parasite Plasmodium falciparum. Proc Biol Sci. 2016;283(1826):20153038. doi: 10.1098/rspb.2015.3038. PubMed PMID: 26984625; PubMed Central PMCID: PMCPMC4810865.

80. Talisuna AO, Langi P, Mutabingwa TK, Van Marck E, Speybroeck N, Egwang TG, et al. Intensity of transmission and spread of gene mutations linked to chloroquine and

sulphadoxine-pyrimethamine resistance in falciparum malaria. Int J Parasitol. 2003;33(10):1051-8. Epub 2003/09/18. PubMed PMID: 13129527.

81. Bloland PB, Ruebush TK, McCormick JB, Ayisi J, Boriga DA, Oloo AJ, et al. Longitudinal cohort study of the epidemiology of malaria infections in an area of intense malaria transmission I. Description of study site, general methodology, and study population. Am J Trop Med Hyg. 1999;60(4):635-40. Epub 1999/05/29. PubMed PMID: 10348240.

82. Lucchi NW, Narayanan J, Karell MA, Xayavong M, Kariuki S, DaSilva AJ, et al. Molecular diagnosis of malaria by photo-induced electron transfer fluorogenic primers: PET-PCR. PLoS One. 2013;8(2):e56677. doi: 10.1371/journal.pone.0056677. PubMed PMID: 23437209; PubMed Central PMCID: PMCPMC3577666.

83. Sridaran S, McClintock SK, Syphard LM, Herman KM, Barnwell JW, Udhayakumar V. Anti-folate drug resistance in Africa: meta-analysis of reported dihydrofolate reductase (dhfr) and dihydropteroate synthase (dhps) mutant genotype frequencies in African Plasmodium falciparum parasite populations. Malar J. 2010;9:247. Epub 2010/08/31. doi: 10.1186/1475-2875-9-247. PubMed PMID: 20799995; PubMed Central PMCID: PMC2940896.

84. Talundzic E, Ndiaye YD, Deme AB, Olsen C, Patel DS, Biliya S, et al. Molecular Epidemiology of Plasmodium falciparum kelch13 Mutations in Senegal Determined by Using Targeted Amplicon Deep Sequencing. Antimicrob Agents Chemother. 2017;61(3). doi: 10.1128/AAC.02116-16. PubMed PMID: 28069653; PubMed Central PMCID: PMCPMC5328579.

85. McCollum AM, Schneider KA, Griffing SM, Zhou Z, Kariuki S, Ter-Kuile F, et al. Differences in selective pressure on dhps and dhfr drug resistant mutations in western

Kenya. Malar J. 2012;11:77. Epub 2012/03/24. doi: 10.1186/1475-2875-11-77. PubMed PMID: 22439637; PubMed Central PMCID: PMC3338400.

86. Rogier C, Commenges D, Trape JF. Evidence for an age-dependent pyrogenic threshold of Plasmodium falciparum parasitemia in highly endemic populations. Am J Trop Med Hyg. 1996;54(6):613-9. PubMed PMID: 8686780.

87. Plucinski MM, Morton L, Bushman M, Dimbu PR, Udhayakumar V. Robust Algorithm for Systematic Classification of Malaria Late Treatment Failures as Recrudescence or Reinfection Using Microsatellite Genotyping. Antimicrob Agents Chemother. 2015;59(10):6096-100. doi: 10.1128/AAC.00072-15. PubMed PMID: 26195521; PubMed Central PMCID: PMCPMC4576024.

88. Read AF, Huijben S. PERSPECTIVE: Evolutionary biology and the avoidance of antimicrobial resistance. Evolutionary Applications. 2009;2(1):40-51. doi: 10.1111/j.1752-4571.2008.00066.x.

89. Trape JF. The public health impact of chloroquine resistance in Africa. Am J Trop Med Hyg. 2001;64(1-2 Suppl):12-7. PubMed PMID: 11425173.

90. Roper C, Pearce R, Bredenkamp B, Gumede J, Drakeley C, Mosha F, et al. Antifolate antimalarial resistance in southeast Africa: a population-based analysis. Lancet. 2003;361(9364):1174-81. Epub 2003/04/11. doi: 10.1016/S0140-6736(03)12951-0. PubMed PMID: 12686039.

91. Vinayak S, Alam MT, Mixson-Hayden T, McCollum AM, Sem R, Shah NK, et al. Origin and evolution of sulfadoxine resistant Plasmodium falciparum. PLoS Pathog. 2010;6(3):e1000830. Epub 2010/04/03. doi: 10.1371/journal.ppat.1000830. PubMed PMID: 20360965; PubMed Central PMCID: PMC2847944.

92. Beier JC, Killeen GF, Githure JI. Short report: entomologic inoculation rates and Plasmodium falciparum malaria prevalence in Africa. Am J Trop Med Hyg. 1999;61(1):109-13. Epub 1999/08/04. PubMed PMID: 10432066.

93. Hastings IM, Watkins WM. Intensity of malaria transmission and the evolution of drug resistance. Acta Trop. 2005;94(3):218-29. Epub 2005/04/26. doi: 10.1016/j.actatropica.2005.04.003. PubMed PMID: 15847846.

94. Doolan DL, Dobano C, Baird JK. Acquired immunity to malaria. Clinical microbiology reviews. 2009;22(1):13-36, Table of Contents. doi: 10.1128/CMR.00025-08. PubMed PMID: 19136431; PubMed Central PMCID: PMC2620631.

95. Geiger C, Agustar HK, Compaore G, Coulibaly B, Sie A, Becher H, et al. Declining malaria parasite prevalence and trends of asymptomatic parasitaemia in a seasonal transmission setting in North-Western Burkina Faso between 2000 and 2009-2012. Malar J. 2013;12:27. doi: 10.1186/1475-2875-12-27. PubMed PMID: 23339523; PubMed Central PMCID: PMCPMC3639197.

96. Douglas AD, Andrews L, Draper SJ, Bojang K, Milligan P, Gilbert SC, et al. Substantially reduced pre-patent parasite multiplication rates are associated with naturally acquired immunity to Plasmodium falciparum. J Infect Dis. 2011;203(9):1337-40. doi: 10.1093/infdis/jir033. PubMed PMID: 21459819; PubMed Central PMCID: PMC3398130.

97. Hviid L. Development of vaccines against Plasmodium falciparum malaria: taking lessons from naturally acquired protective immunity. Microbes Infect. 2007;9(6):772-6. doi: 10.1016/j.micinf.2007.02.008. PubMed PMID: 17398137.

98. Scherf A, Lopez-Rubio JJ, Riviere L. Antigenic variation in Plasmodium falciparum. Annu Rev Microbiol. 2008;62:445-70. doi: 10.1146/annurev.micro.61.080706.093134. PubMed PMID: 18785843.

99. Churcher TS, Bousema T, Walker M, Drakeley C, Schneider P, Ouedraogo AL, et al. Predicting mosquito infection from Plasmodium falciparum gametocyte density and estimating the reservoir of infection. Elife. 2013;2:e00626. doi: 10.7554/eLife.00626. PubMed PMID: 23705071; PubMed Central PMCID: PMCPMC3660740.

100. Childs LM, Buckee CO. Dissecting the determinants of malaria chronicity: why within-host models struggle to reproduce infection dynamics. J R Soc Interface. 2015;12(104):20141379. doi: 10.1098/rsif.2014.1379. PubMed PMID: 25673299; PubMed Central PMCID: PMCPMC4345506.

101. Mohammed A, Ndaro A, Kalinga A, Manjurano A, Mosha JF, Mosha DF, et al. Trends in chloroquine resistance marker, Pfcrt-K76T mutation ten years after chloroquine withdrawal in Tanzania. Malar J. 2013;12:415. doi: 10.1186/1475-2875-12-415. PubMed PMID: 24225406; PubMed Central PMCID: PMC3830541.

102. Zhou Z, Griffing SM, de Oliveira AM, McCollum AM, Quezada WM, Arrospide N, et al. Decline in sulfadoxine-pyrimethamine-resistant alleles after change in drug policy in the Amazon region of Peru. Antimicrob Agents Chemother. 2008;52(2):739-41. Epub 2007/11/21. doi: 10.1128/AAC.00975-07. PubMed PMID: 18025120; PubMed Central PMCID: PMC2224716.

103. Takala SL, Smith DL, Stine OC, Coulibaly D, Thera MA, Doumbo OK, et al. A high-throughput method for quantifying alleles and haplotypes of the malaria vaccine candidate Plasmodium falciparum merozoite surface protein-1 19 kDa. Malar J. 2006;5:31. doi: 10.1186/1475-2875-5-31. PubMed PMID: 16626494; PubMed Central PMCID: PMCPMC1459863.

104. Methods Manual for Product Testing of Malaria Rapid Diagnostic Tests (v. 5) Foundation for Innovative New Diagnostics, World Health Organization (Global Malaria

Programme), Centers for Disease Control and Prevention (Division of Parasitic Diseases, Malaria Branch), 2012.

105. Anderson TJ, Su XZ, Bockarie M, Lagog M, Day KP. Twelve microsatellite markers for characterization of Plasmodium falciparum from finger-prick blood samples. Parasitology. 1999;119 (Pt 2):113-25. Epub 1999/08/31. PubMed PMID: 10466118.

106. McCollum AM, Mueller K, Villegas L, Udhayakumar V, Escalante AA. Common origin and fixation of Plasmodium falciparum dhfr and dhps mutations associated with sulfadoxine-pyrimethamine resistance in a low-transmission area in South America. Antimicrob Agents Chemother. 2007;51(6):2085-91. Epub 2007/02/07. doi: 10.1128/AAC.01228-06. PubMed PMID: 17283199; PubMed Central PMCID: PMC1891388.

107. Nair S, Williams JT, Brockman A, Paiphun L, Mayxay M, Newton PN, et al. A selective sweep driven by pyrimethamine treatment in southeast asian malaria parasites. Mol Biol Evol. 2003;20(9):1526-36. Epub 2003/07/02. doi: 10.1093/molbev/msg162. PubMed PMID: 12832643.

108. Carlsson AM, Ngasala BE, Dahlstrom S, Membi C, Veiga IM, Rombo L, et al. Plasmodium falciparum population dynamics during the early phase of anti-malarial drug treatment in Tanzanian children with acute uncomplicated malaria. Malar J. 2011;10:380. Epub 2011/12/22. doi: 10.1186/1475-2875-10-380. PubMed PMID: 22185672; PubMed Central PMCID: PMC3280947.

109. Rao PN, Uplekar S, Kayal S, Mallick PK, Bandyopadhyay N, Kale S, et al. A Method for Amplicon Deep Sequencing of Drug Resistance Genes in Plasmodium falciparum Clinical Isolates from India. J Clin Microbiol. 2016;54(6):1500-11. doi: 10.1128/JCM.00235-16. PubMed PMID: 27008882; PubMed Central PMCID: PMCPMC4879288.